

METABOLISM OF ALPHA-SYNUCLEIN BY THE 20S PROTEASOME

APPROVED BY SUPERVISORY COMMITTEE

Josep Rizo, Ph.D., Chair

Elizabeth J. Goldsmith, Ph.D.

George N. DeMartino, Ph.D.

Philip J. Thomas, Ph.D.

For my family.

METABOLISM OF ALPHA-SYNUCLEIN BY THE 20S PROTEASOME

by

KAREN ADELL LEWIS

DISSERTATION

Presented to the Faculty of the Graduate School of Biomedical Sciences

The University of Texas Southwestern Medical Center at Dallas

In Partial Fulfillment of the Requirements

For the Degree of

DOCTOR OF PHILOSOPHY

The University of Texas Southwestern Medical Center at Dallas

Dallas, Texas

March, 2009

Copyright

by

KAREN ADELL LEWIS, 2009

All Rights Reserved

ACKNOWLEDGMENTS

Contrary to the popular image of a solitary scientist working steadily away at a lonely bench, science is always performed by a team of people working closely together. My mentor, Philip Thomas, continually assembles an impressive team that performs excellent science and works well together. It is this environment in which I have been blessed to learn and grow as a scientist and as a person. Thank you, Phil, for your mentorship, your leadership, your encouragement, and the freedom to make mistakes and learn from them without ever going too far afield.

I owe a great deal to those in the Thomas lab who have worked on the α Syn/proteasome project. Changwei Liu, the post-doctoral fellow who began the project, helped shape my specific aims, taught me experimental techniques, and had many productive conversations with me. Arynn Yaeger contributed to this work in many ways, from making α Syn proteins to developing a variety of assays to probe the physiological function of α Syn truncations. She also helped me learn a lot about shaping projects and mentoring, for which I am most grateful. I also very much appreciate Caroline Ritchie's contributions to understanding the mechanism of interaction between the 20S and α Syn. The stimulating discussion, alternative perspectives, and essential collaborations that these labmates provided enriched my experience in the lab and strengthened the project.

Our lab manager, Linda Millen, keeps the lab running smoothly while also expertly juggling her own experiments. Her expertise, including many patient lessons on the HPLC, has helped me significantly and often, and I am thankful for the professional and personal friendship offered me.

I am grateful to the post-doctoral fellows and senior scientists whose time in the Thomas lab overlapped with mine. Likewise, my fellow students in the lab, both former and present, never hesitated to share their experience and insight. Their willingness to share their knowledge and experience made the lab a stimulating place to learn and a fun place to work. Thank you all. I am also grateful to the technicians and lab helpers who kept the lab well-stocked and clean, often while also pursuing their own projects. Special

thanks to Anita Contreras and Jocelyn Wrighting, whose administrative support was essential in so many ways.

George DeMartino has been in many ways a co-mentor to me, from including me in his group meetings to assisting with experimental design and sharing his extensive knowledge of the proteasome field. It has been a privilege to be a close collaborator with him and with his group, and I am deeply appreciative of their technical and scientific assistance as well as their collegiality. In particular, David Thompson taught me how to purify proteasomes from bovine blood, and he shared his unique sense of humor along the way. I also thank Tom Gillette for many helpful discussions about various experimental efforts, particularly chemical crosslinking and reversed-phase chromatography of the proteasome.

I was extremely fortunate to have an excellent dissertation committee, who helped guide me toward the central questions of my project. Thank you to Jose Rizo-Rey and Betsy Goldsmith, who were always available for a discussion or experimental assistance. Their insights and recommendations were always helpful and encouraging.

My project involved multiple fields, and I benefited from collaborations with individuals with diverse sets of interests. Rakez Kayed, of UTMB-Galveston, was very generous with his time, resources, and reagents, to the extent of hosting me in his lab for four days to troubleshoot some issues with the oligomerization assay. I am grateful for the on-campus collaboration with Kimmo Hatanpaa, Chan Foong, and Charles White, III, on the immunohistochemistry project. Virginia Lee of the University of Pennsylvania provided a panel of anti- α Syn antibodies, without which many of my experiments would not have been possible. Communications with Remco Sprangers and Lewis Kay at the University of Toronto concerning activation of the 20S proteasome contributed to our understanding of possible activation mechanisms. I am also appreciative of Thomas Kodadek, Chase Archer, and Lyle Burdine at UT-Southwestern for the collaborative efforts to use chemical crosslinking to identify the site of α Syn interaction on 20S.

The Molecular Biophysics program provided excellent training, with many opportunities to be challenged and taught in journal clubs, WIPs, retreats, and discussion groups. The entire MB faculty deserves thanks, with particular gratitude to Kevin

Gardner and Stephen Sprang for their leadership of the program during my tenure at UT-Southwestern. The program would not have run as smoothly nor as successfully as it has without the support and hands-on work of the program administrative assistants Jo Appleton and Aurora del Rosario.

I had the exceptional opportunity to be supported by the NIH training grant Mechanisms of Drug Action and Disposition (GM07062) and participate in the weekly journal club helmed by David Mangelsdorf and Rama Ranganathan. The alternate perspectives demanded by this program, through courses and journal club, significantly enhanced my experience and training at UT-Southwestern by challenging me to always consider the bigger picture. I am indebted to my fellow students for their challenging presentations and engaging discussions. I also deeply appreciate the constant support and encouragement of the grant's administrative assistant, Carla Childers.

In addition to the training grant, multiple agencies provided funding for the work described here. A grant from the Parkinson's Disease Foundation to P.J.T. was central to starting this project, and continued funding from the Welch Foundation to P.J.T. and from the NIH to both P.J.T. (DK49835) and G.N.D. (DK46181) supported the majority of the experiments described in this dissertation. Additionally, a grant from the NIH to the UT-Southwestern Alzheimer's Disease Center (P30AG-12300) provided the resources for the brain tissue bank, from which the patient samples were obtained for the terminus-specific antibody studies.

The opportunity to pursue scientific research is a privilege, of which I am constantly aware and for which I am constantly thankful. My graduate education would not have been possible without the support and encouragement of many people before I joined the Thomas lab. I owe much to my first mentors, Thomas D. Schneider (National Cancer Institute at Frederick) and Valerie M. Kish (University of Richmond), whose high expectations challenged me first as a high school student and then as an undergraduate student to perform to the science, rather than being limited by my experience. During my time in Dallas, many people have provided invaluable friendship and support. I am grateful for their presences in my life.

Throughout all of my schooling, my family has been steadfast supporters of my efforts, celebrating the successes and commiserating the failures (or rather, the times when I discovered ways that things didn't work). I will never be able to fully express my gratitude to them for all the ways in which they supported me. From the moment in high school that I decided to pursue science, my parents, Don and Nancy Lewis, have been fully on board. Thank you for constantly encouraging me, affording me opportunities to learn, and always being there to help me no matter what the task.

My brother, Todd, and my sister-in-law, Sara, were a reliable source of laughter and support when I needed it. My grandmother, Grace Wickline, is a wonderful pen-pal; seeing an envelope in the mail from her always brightened my day, and her letters never failed to make me smile. My parents-in-law, Craig and Trudy Emerick, have been rock-steady in their encouragement and support throughout all the highs and lows, and my sister-in-law, Shannon, always had a word of encouragement or reassurance.

To my husband, Barrett Emerick, I give unending thanks for encouraging, listening, waiting, celebrating, understanding, and loving.

METABOLISM OF ALPHA-SYNUCLEIN BY THE 20S PROTEASOME

KAREN ADELL LEWIS, Ph.D.

The University of Texas Southwestern Medical Center at Dallas, 2009

PHILIP JORDAN THOMAS, Ph.D.

Parkinson's disease is one of several common neurodegenerative disorders that are related by the intracellular aggregation of the neuronal protein α -synuclein (α Syn) that normally associates with synaptic vesicles. Within the aggregates, a fraction of α Syn is truncated at the C-termini, and these truncations are hypothesized to participate in disease pathogenesis. The prevailing model for cytotoxicity of the aggregated protein proposes that oligomeric forms cause dysfunction of the ubiquitin-proteasome pathway of protein degradation, thereby enhancing an alternative pathway that involves ubiquitin-independent degradation by the 20S core particle of the proteasome. The 20S proteasome is known to degrade proteins with regions of intrinsic disorder, which figure prominently in a wide range of neurodegenerative disorders, including α Syn in Parkinson's disease. Importantly, some forms of 20S exert an endoproteolytic activity that

produces highly amyloidogenic truncations of α Syn. An *in vitro* system containing liposomes and the 20S proteasome was developed to identify the mechanism by which the three point mutations in α Syn associated with familial Parkinson's disease exert cytotoxicity. The proteasome produced truncations from all three mutants in the presence of liposomes, but not wildtype α Syn. Additionally, the putative cytotoxic oligomer was formed most rapidly in the presence of both 20S proteasome and liposomes. Polyclonal antibodies specific for the C-termini of a set of truncated α Syn proteins were successfully developed to detect cleavage products of α Syn *in vitro* and *in vivo*. To better understand the physiological role of 20S-mediated degradation of intrinsically disordered proteins, the mechanism of recognition and interaction between substrate and enzyme was studied. While the presence of disorder appears to be necessary for 20S degradation, it was found to be insufficient to define a protein as a 20S substrate. Furthermore, a novel correlation was identified between the endoproteolytic activity of 20S and a modification of the α 6 subunit. The data support a role for the 20S proteasome in Lewy body disease pathogenesis, where it accelerates the formation of cytotoxic species by endoproteolysis of an intrinsically disordered protein. In that regard, a form of the 20S proteasome was identified that may be responsible for the endoproteolytic cleavage of intrinsically disordered proteins *in vivo*.

TABLE OF CONTENTS

Dedication	i
Acknowledgments	iv
Abstract	ix
Table of Contents	xi
Prior Publications	xii
List of Figures	xiii
List of Tables	xv
List of Appendices	xvi
List of Definitions	xvii
Chapter One: Introduction	1
Chapter Two: α-synuclein and Lewy Body Disorders	5
Physiological function of α -synuclein	6
Structure of lipid-bound α -synuclein	9
Structure of free α -synuclein	14
Self-association of α -synuclein	16
Molecular genetics of Parkinson disease	19
C-terminal truncation of α -synuclein	21
Pathology of the Lewy body disorders	23
Chapter Three: The Proteasome and Intrinsically Disordered Proteins	26
Alpha subunits and gating	28
Beta subunits and proteolysis	32
Mechanisms of proteasomal degradation	33
20S-mediated degradation	36
Endoproteolysis by 20S	37
Intrinsically disordered proteins	40
Role of intrinsically disordered proteins in neurodegeneration	43
The proteasome and neurodegeneration	44
Chapter Four: Degradation of α-synuclein mutants by the 20S proteasome	48
Results	53
Discussion	68
Chapter Five: Immunodetection of Truncated α-synuclein	74
Results	78
Discussion	93
Chapter Six: Degradation of disordered substrates by the 20S proteasome	99
Results	104
Discussion	120
Chapter Seven: Prospectus for Future Work	127
Appendix A: Materials and Methods	132
Appendix B: Chapter Collaborations	146
References	148

PRIOR PUBLICATIONS

Chen Z*, Lewis KA*, Shultzaberger RK, Lyakhov IG, Zheng M, Doan B, Storz G, Schneider TD. (2007) “Discovery of Fur binding site clusters in Escherichia coli by information theory models.” *Nucleic Acids Res.* 35(20):6762-77. *denotes equal authorship

Shultzaberger RK, Chen Z, Lewis KA, Schneider TD. (2007) “Anatomy of Escherichia coli sigma70 promoters.” *Nucleic Acids Res.* 35(3):771-88.

Liu CW, Giasson BI, Lewis KA, Lee VM, DeMartino GN, Thomas PJ. (2005) “A precipitating role for truncated alpha-synuclein and the proteasome in alpha-synuclein aggregation: implications for pathogenesis of Parkinson disease.” *J Biol. Chem.* 280(24):22670-8.

Zheng M, Wang X, Doan B, Lewis KA, Schneider TD, Storz G. (2001) “Computation-directed identification of OxyR DNA binding sites in Escherichia coli.” *J Bacteriol.* 183(15):4571-9.

LIST OF FIGURES

Figure 2-1.	Lewy body.....	5
Figure 2-2.	Sequence alignment of <i>Homo sapiens</i> synucleins.....	8
Figure 2-3.	Structural architecture of α -synuclein	9
Figure 2-4.	Structure of phospholipid-bound α Syn	13
Figure 2-5.	Schematic representations of therapeutic strategies to prevent α Syn misfolding	18
Figure 2-6.	C-terminal truncations of α Syn are present in PD patient brains.....	22
Figure 3-1.	Crystal structure of the archaeal and mammalian proteasomes	27
Figure 3-2.	Cutaway view of the bovine 20S proteasome	28
Figure 3-3.	CLUSTAL-W2 alignment of bovine alpha sequences.....	29
Figure 3-4.	The bovine α -ring	30
Figure 3-5.	Alpha rings of three species	31
Figure 3-6.	20S degradation of bilaterally protected disordered proteins.....	39
Figure 3-7.	Three kinds of functional polypeptide conformations	41
Figure 4-1.	Potential reactions of α Syn.....	52
Figure 4-2.	Helix formation of α Syn proteins when bound to liposomes.....	54
Figure 4-3.	Helix formation by α Syn-A30P induced by TFE.....	55
Figure 4-4.	20S proteasomal degradation of α Syn mutants associated with PD	56
Figure 4-5.	Degradation of wildtype and mutant α Syn by the 20S proteasome in the presence of liposomes	57
Figure 4-6.	Amyloid fibril formation of α Syn proteins	59
Figure 4-7.	Amyloid fibril formation of α Syn proteins in the presence of liposomes	60
Figure 4-8.	Truncations produced by the 20S proteasome under conditions of the fibrillization assay	61
Figure 4-9.	Average lag times to fibril nucleation of α Syn proteins.....	62
Figure 4-10.	Oligomer formation of mutant α Syn proteins	63
Figure 4-11.	Quantitation of oligomer formation of mutant α Syn proteins.....	64
Figure 4-12.	Time-dependent appearance of immunoreactive species in liposome samples.....	65
Figure 4-13.	Oligomerization of truncated α Syn proteins	66
Figure 4-14.	A dynamic model of Parkinson disease pathogenesis.....	69

Figure 5-1.	Slot blots of recombinant truncated α Syn proteins	79
Figure 5-2.	ELISAs of polyclonal antibodies against α Syn110 and α Syn119 with 2.5 μ g of capture antigen.....	80
Figure 5-3.	ELISAs of polyclonal antibodies against α Syn122 and α Syn123 with 2.5 μ g of capture antigen.....	81
Figure 5-4.	ELISAs of antibodies against α Syn122 with lower amounts of capture antigen	82
Figure 5-5.	ELISAs of antibodies against α Syn123 with lower amounts of capture antigen	83
Figure 5-6.	The polyclonal antibodies recognize products of proteasomal degradation of α Syn	84
Figure 5-7.	Sequential fractionation of human cortex samples.....	88
Figure 5-8.	Blot for α Syn110 in cortex samples with the 1976-2 antibody.....	89
Figure 5-9.	Detection of α Syn119 in cortex samples by the 1977-1 and 1977-2 antibodies	90
Figure 5-10.	Immunohistochemical detection of α Syn in a cingulate cortex sample from a patient with LBVAD.....	91
Figure 5-11.	Control IHC stains for the 1976-2 serum	92
Figure 5-12.	Sensitivity of 1976-2 against α Syn110 in Western blotting.....	96
Figure 6-1.	Rate of RNase Sa degradation by 20S is correlated with thermodynamic stability	104
Figure 6-2.	C-terminal truncations of α Syn are selectively degraded by 20S	106
Figure 6-3.	N-terminal truncations of α Syn are also selectively degraded by 20S	107
Figure 6-4.	α Syn is not degraded by all 20S proteasome preparations.....	108
Figure 6-5.	The endoproteolytic activity of 20S is reproducible	109
Figure 6-6.	PA28 activation inhibits the 20S proteasome against α Syn.....	110
Figure 6-7.	Native gel electrophoresis of M57 and M58 proteasomes	111
Figure 6-8.	Overlay of M57 and M58 proteasomes.....	112
Figure 6-9.	Mass spectrometric identification of $\alpha 6(\alpha 1)$	113
Figure 6-10.	Confirmation of the M57-unique spots as $\alpha 6(\alpha 1)$	114
Figure 6-11.	Confirmation of the M58-unique spots as $\alpha 6(\alpha 1)$	115
Figure 6-12.	All four endoproteolytic 20S proteasomes contain the same $\alpha 6(\alpha 1)$ modified subunits	116
Figure 6-13.	λ phosphatase treatment of M57 and M58 proteasomes	117
Figure 6-14.	Substrates of the 20S proteasome in a fraction from rodent liver	119

LIST OF TABLES

Table 2-1.	Proteins found in Lewy bodies.....	6
Table 2-2.	Molecular genetics of Parkinson disease	20
Table 3-1.	Some substrates for 20S-dependent degradation.....	37
Table 5-1.	Peptide antigens for polyclonal antibodies.....	78
Table 5-2.	Polyclonal sera raised against α Syn peptide antigens	78
Table 5-3.	Human cortex samples and clinical diagnoses	86
Table 6-1.	Identified post-translational modifications of α 6(α 1).....	122
Table A-1.	Bacterial expression constructs of α -synuclein	133
Table A-2.	Fluorogenic peptide substrates for the proteasome	134

LIST OF APPENDICES

Appendix A: Materials and Methods	132
Recombinant expression and purification of α -synuclein	132
Circular dichroism measurement of α -synuclein.....	134
Bovine 20S proteasome purification	
Endoproteolytic 20S	134
Latent 20S	135
Proteasome peptidase activity assay.....	136
Native gel electrophoresis of the proteasome.....	137
Two-dimensional electrophoresis of proteasome.....	137
<i>In vitro</i> RNase Sa degradation assay	138
<i>In vitro</i> α -synuclein degradation assay.....	138
Liposome preparation.....	139
α -synuclein fibrillization assay.....	139
α -synuclein oligomerization assay	140
Polyclonal antibody development	140
Enzyme-linked immunosorbent assay	141
Dissection and storage of human brain tissue	142
Sequential fractionation of human brain tissue	142
Immunohistochemistry of human brain tissue	143
Fractionation of mouse liver tissue.....	144
20S degradation assay with mouse liver fractions.....	145
Appendix B: Chapter Collaborations	146

LIST OF DEFINITIONS

- 11S – an activator complex of the proteasome (see PA28/PA26)
- 2D – two-dimensional
- 20S – the core catalytic particle of the proteasome (also called CP)
- 26S – the core particle complexed with one or two PA700 activator complexes
- AD – Alzheimer’s disease
- AMC – 4-aminomethyl coumarin, a fluorophore used as a hydrolysis reporter when fused to peptide substrates
- ATP – adenosine triphosphate
- α Syn – the alpha-synuclein protein, the protein product of the SNCA gene at the PARK1 locus
- A β – a highly amyloidogenic peptide that is the primary protein component of plaques found in Alzheimer’s disease
- ALS – amyotrophic lateral sclerosis, a neurodegenerative disease affecting motor neurons
- β -ME – beta-mercaptoethanol
- β NA – beta-naphthyl-amine, a fluorophore
- CD – circular dichroism
- CLUSTAL-W2 – a general purpose multiple sequence alignment program for DNA or proteins
- CP – the core catalytic particle of the proteasome (also called 20S)
- CSP α – cysteine string protein α , an abundant presynaptic protein, the deletion of which causes a neurodegeneration phenotype
- DLB – Dementia with Lewy bodies
- DLBD – Diffuse Lewy body disease
- DJ-1 – a mitochondrion-associated kinase that is genetically linked to familial PD; product of PARK7 gene locus
- DNA – deoxyribonucleic acid
- DTT – dithiothreitol, a reducing agent

EDTA – ethylenediaminetetraacetic acid, a divalent cation chelator

ELISA – enzyme-linked immunosorbent assay

EPR – electron paramagnetic resonance spectroscopy

ER – endoplasmic reticulum

ERAD – endoplasmic reticulum-associated protein degradation, a proteasome-dependent process

FTIR – Fourier-transform infrared spectroscopy

GAPDH – glyceraldehyde-3-phosphate dehydrogenase

GFP – green fluorescent protein

GTP – guanosine nucleotide triphosphate

HM – homogenizing media, used for tissue fractionation experiments

HSQC – heteronuclear quantum coherence, an NMR experiment

IDP – intrinsically disordered protein

IgG – immunoglobulin isotype G

IHC – immunohistochemistry

IEF – isoelectric focusing

kDa – kilodalton, a measure of molecular mass. One Dalton = 1 g/mol.

LBD – Lewy body disorder

LBVAD – Lewy body variant of Alzheimer’s disease

LB – Lewy body

LN – Lewy neurite

LRRK2 – Leucine-rich repeat kinase 2, a protein genetically implicated in familial PD

LUV – large unilamellar vesicles

MG132 – N-benzoyloxycarbonyl Z-Leu-Leu-leucinal, a reversible aldehyde inhibitor of the proteasome

MHC – major histocompatibility complex

MLV – multilamellar vesicles

MWCO – molecular weight cutoff

NAC – non-amyloid component, a peptide within α Syn that is found in A β plaques

NCBI – National Center for Biotechnology Information

NMR – nuclear magnetic resonance spectroscopy

Ntn – N-terminal nucleophile, a class of hydrolases

OD – optical density

OPD – ortho-phenylenediamine, a chromogenic substrate used in ELISAs

PA28 or PA26 – a proteasome activator complex that enables protein degradation in a ubiquitin- and ATP-independent manner

PA200 – a 200 kDa molecule that activates the proteasome

PA700 – a proteasome activator complex that mediates ubiquitin-dependent degradation in an ATP-dependent manner (also called RP)

PAN – the archaeobacterial homologue of PA28/PA26

PBS – phosphate-buffered saline

PD – Parkinson's disease

PDI – protein disulfide isomerase

PDB – Protein Data Bank, used in conjunction with a catalog number for structure information

PDD – Parkinson's disease with dementia

PGPH – post-glutamyl peptide hydrolysis

pI – isoelectric point

PSI – carbobenzoxy-Ile-Glu(O-t-butyl)-Ala-leucinal, a reversible aldehyde proteasome inhibitor

POPA – 1-palmitoyl-2-oleoyl-*sn*-glycero-3-phosphate

POPC – 1-palmitoyl-2-oleoyl-*sn*-glycero-3-phosphocholine

RP – the ATPase activating complex of the proteasome (also called PA700)

SDS – sodium dodecyl sulfate, a detergent

SDS-PAGE – SDS-polyacrylamide gel electrophoresis

SNARE – soluble NSF attachment protein receptors, a family of proteins involved in vesicle fusion to larger membrane

SOD1 – superoxide dismutase 1, a protein involved in free radical scavenging; the misfolding of this protein is associated with ALS

SUV – small unilamellar vesicles

ThioT – thioflavin T, a fluorescent dye that binds specifically to amyloid

TFE – 2,2,2-trifluoroethanol

TMA – tissue microarray, a slide with several slices of brain tissue used for IHC

UCH-L1 – ubiquitin carboxy terminal esterase L1, a dual-function enzyme with ubiquitin ligase and hydrolase activities that is genetically implicated in familial PD; product of PARK5 gene locus

UPS – ubiquitin-proteasome system

Chapter One

General Introduction

A human disease can have its genesis in a variety of errors within the complex system that is the body. Disease-related dysfunctions may occur in the expression of a gene, the translation of the gene into a protein product, or the ability of that protein to properly carry out its cellular function. One way that a protein is prevented from properly functioning is by the failure of the linear protein sequence to fold into its functional three-dimensional structure (Luheshi et al., 2008). Many human diseases are caused by such misfolding events. These diseases are particularly good candidates for drug therapies, as a correction of the misfolding event by a small molecule would alleviate the primary cause of the disease (Rochet, 2007). The set of protein-misfolding diseases can be divided into two subsets: those that are caused by the loss of a functional protein (loss-of-function) and those that are caused by the creation of a toxic misfolded conformation (gain-of-function) (Gregersen, 2006; Thomas et al., 1995).

The majority of neurodegenerative disorders are gain-of-function protein misfolding diseases, in which a protein accumulates and aggregates into a cytotoxic conformation that is often associated with the formation of amyloid fibrils (Soto and Estrada, 2008). Alzheimer's disease is characterized by aggregates of the A β peptide and the tau protein; the protein huntingtin aggregates in Huntington's disease; the SOD1 protein is implicated in amyotrophic lateral sclerosis (ALS, also known as Lou Gehrig's disease). The presence of protein aggregates is associated with the death of neurons, which is the cause of well-known symptoms such as memory loss or loss of muscle control (Soto and Estrada, 2008).

Parkinson's disease is one of several common neurodegenerative disorders that are marked by the intracellular aggregation of the neuronal protein α -synuclein (α Syn). In addition to Parkinson's (PD), this spectrum of movement and dementia disorders includes diffuse Lewy body disease (DLBD), dementia with Lewy bodies (DLB), and Parkinson's with dementia (PDD). Additionally, Lewy body variant of Alzheimer's disease (LBVAD) presents similar histopathology to this spectrum in addition to typical Alzheimer's pathology. In all of these disorders, the presence of intracellular inclusion bodies of aggregated proteins is a major pathologic hallmark (Lippa et al., 2007).

By far, α Syn is the predominant protein in the inclusions, leading to the collective designation of the diseases as "synucleinopathies". It is a 140-amino acid, 14.4 kDa protein of unknown function that is enriched in the presynaptic termini of neurons. In addition to its intracellular accumulation and aggregation, there is substantial genetic evidence that implicates α Syn in PD pathogenesis. Early-onset familial PD has been associated with gene duplication, triplication, and three single point mutations (Yang et al., 2009). Within the inclusions, α Syn has been found to have multiple post-translational modifications to its primary sequence, including phosphorylation, *o*-nitrosylation, ubiquitination, and truncation (Beyer, 2006). Any or all of these modifications may play a role in pathogenesis, but they could also be a consequence of the cell trying to handle the potentially toxic misfolded protein.

Because protein misfolding can be damaging through either loss-of-function or gain-of-function mechanisms, the cell has evolved multiple systems to promote folding and removal of misfolded proteins. If proper folding cannot be aided or restored by the chaperone proteins, the misfolded protein may be metabolized by either the lysosome or the ubiquitin-proteasome system (Tai and

Schuman, 2008). These two systems have distinct mechanisms. The lysosome is a distinct organelle within the cytoplasm, wherein pH-sensitive proteases are sequestered from the rest of the cell by a phospholipid bilayer. Protein turnover in the lysosome occurs through microautophagy, a process that engulfs a volume of the cytosol along with the intended targets for degradation. In contrast, the proteolytic machine of the ubiquitin-proteasome system, the proteasome, is a large multisubunit protein complex that is present throughout the cytosol and nucleus (Wolf and Hilt, 2004). The proteasome is comprised of the core complex, termed “20S”, a hollow cylinder formed from 28 separate subunits and contains the active sites for proteolysis. The 20S can bind to a multisubunit activator complex, termed “PA700”, which has multiple enzymatic activities but no protease activity. Together, they form the “26S” proteasome. Substrates for proteasomal degradation are identified by the covalent addition of a chain of ubiquitin protein molecules, which are ultimately recognized and degraded by the 26S proteasome in a reaction that requires the hydrolysis of ATP (Wolf and Hilt, 2004).

Dysfunction of the ubiquitin-proteasome system (UPS) has been implicated in neurodegenerative diseases, including the synucleinopathies (Tai and Schuman, 2008). In addition to α Syn, the synucleinopathy intracellular inclusions also contain the protein ubiquitin, leading to a hypothesis that proteasomal dysfunction contributes to pathogenesis. Further supporting this hypothesis is genetic evidence that other components of the UPS, including a putative ubiquitin ligase (parkin) and ubiquitin hydrolase (UCH-L1), are associated with familial early-onset PD (Yang et al., 2009). As noted above, some of the α Syn present in intracellular inclusions is ubiquitinated, while a fraction has also been found to be truncated. As one might predict, *in vitro* studies revealed that polyubiquitinated α Syn is a substrate for the 26S

proteasome. Much more surprising was the discovery that non-ubiquitinated α Syn is also a substrate for the 20S core particle *in vitro* (Liu et al., 2003; Tofaris et al., 2001). The 20S proteasome endoproteolytically cleaves α Syn *in vitro*, creating cleavage products that are highly similar to those observed in the insoluble aggregates of brain tissue from both synucleinopathy patients and mouse models of PD (Liu et al., 2005). This cleavage occurs independently of both polyubiquitin tags and ATP, underscoring that the 20S – not the 26S – is the form of the proteasome that is responsible for this particular activity.

This dissertation will describe several distinct but related studies of the protein α Syn and its interactions with the 20S proteasome. Chapter II will present a review of the α -synuclein literature, including the pathology of the synucleinopathies. Chapter III will continue the literature review with a focus on the function and dysfunction of the proteasome with regard to neurodegeneration and intrinsically disordered proteins. Chapter IV describes the study of the three point mutants of α Syn that are associated with early-onset familial PD within an *in vitro* reconstituted system. Chapter V details the development and characterization of polyclonal antibodies that specifically recognize C-terminal truncations of α Syn, which is an extension of the work in Chapter IV as well as of work performed in the Thomas lab by Chang-wei Liu. All of these studies are predicated on the cleavage of intrinsically disordered α Syn by the 20S proteasome, which was first described by Liu *et al.* in 2003. The work described in Chapter VI continues that investigation by identifying the elements of the 20S proteasome and of the potential disordered substrate that are necessary for the observed protease activity, using proteasomes from multiple sources and multiple disordered or destabilized proteins as substrates. Chapter VII is presented as a prospectus for future work, to build upon the discoveries and reagents described in the previous chapters.

Chapter Two

α -Synuclein and the Lewy Body Disorders

Parkinson's disease is the best-known of several disorders that are characterized by the formation of intracellular protein inclusions called Lewy bodies. These inclusions are characterized by a distinct morphology of a dense nucleus with a surrounding fibrillar halo (Figure 2-1). Lewy bodies stain positive for the small modifying protein ubiquitin, and contain a variety of cellular proteins (Table 2-1). The predominant protein within the Lewy bodies is α -synuclein, a 140-residue protein of unknown function. In the inclusions, α -synuclein is present in an amyloid fibril conformation, as detected by Thioflavin S and Thioflavin T fluorescence and Congo Red birefringence. Only a small fraction of the α Syn is polyubiquitinated (Sampathu et al., 2003). In mature neurons, the protein is enriched in presynaptic terminals, both excitatory and inhibitory (Murphy et al., 2000). It has been demonstrated to associate with microtubules and with presynaptic vesicles (Alim et al., 2004; Kahle et al., 2000). The avian homolog of α Syn has been shown to be involved in synaptic plasticity in songbirds (Davidson et al., 1998).

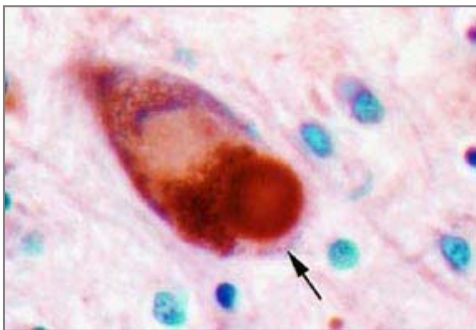


Figure 2-1. Lewy body. A magnified view of a tissue section stained with an anti-ubiquitin antibody (brown) and counterstained with hematoxylin (blue). The Lewy body is identified by the arrow, and is characterized by a dense core surrounded by a fuzzy halo. Reprinted by permission from MacMillan Publishers

Table 2-1. Proteins found in Lewy bodies.

Protein	Original Reference
α -synuclein	Spillantini et al., 1998
ubiquitin	Lowe et al., 1988
synphilin-1	Schmidt et al., 1991
septin-4	Ihara et al., 2003
14-3-3 proteins	Kawamoto et al., 2002
tubulin polymerization promoting protein	Olah et al., 2006
glyceraldehyde-3-phosphate dehydrogenase	Olah et al., 2006
parkin	Shimura et al., 2001
ring-finger protein 11	Anderson et al., 2007
NEDD8 (ubiquitin-like protein)	Mori et al., 2005
ubiquitin C-terminal hydrolase-1	Lowe et al., 1990

Physiological function of α Syn

Several cellular functions have been proposed for α Syn that are consistent with these observations. A murine knockout of α Syn exhibits no physiological phenotype, but electron microscopy of synapses reveals a significant decrease in the number of distal presynaptic vesicles, which are those that are awaiting docking to the synaptic membrane (Murphy et al., 2000). Overexpression of wildtype α Syn has been shown to rescue a mouse model of neurodegeneration. Cysteine-string protein α (CSP α) is a vesicle-bound chaperone, and the knockout of this gene induces a neurodegenerative phenotype (Fernandez-Chacon et al., 2004). However, overexpression of α Syn on the CSP α ^{-/-} background rescues the neurodegeneration (Chandra et al., 2005). Notably, the overexpression of a mutant form of α Syn associated with familial Parkinson disease does not rescue the CSP α -deficient phenotype (Chandra et al., 2005). Because CSP α is a vesicle-associated chaperone, the rescue suggests that α Syn may directly compensate by acting as a chaperone itself, perhaps by aiding in the formation of SNARE complexes at the vesicle-membrane docking site. A chaperone-like activity of α Syn was demonstrated *in vivo* against bacterial esterases (Ahn et al., 2006).

Additionally, α Syn has been convincingly implicated in pathways of Rab1-mediated vesicle trafficking. Yeast cells that overexpressed α Syn developed endoplasmic reticulum (ER) stress and early deficiencies in ER-to-Golgi trafficking (Cooper et al., 2006). The concurrent overexpression of a Rab1 GTPase rescued these deficiencies in an α Syn-specific manner, and similar results were obtained in *Drosophila* and rat primary neuronal cell model systems. The mechanism of action of α Syn-mediated toxicity was suggested to be an inhibition of vesicle docking, beginning with the docking and fusion of vesicles to the Golgi membrane (Gitler et al., 2008). In all, the current evidence suggests that α Syn is a mediator of vesicle transport, but the precise roles by which α Syn participates remain to be elucidated.

α -synuclein is one of three members of the synuclein family found in mammals. The products of the SNCA, SNCB, and SNCG genes are, respectively, α -synuclein, β -synuclein, and γ -synuclein. The N-termini of the three human synucleins is highly homologous, with >65% identity in the first 100 residues. Within this region, which mediates interactions with lipid surfaces, the synucleins have seven imperfect hexameric repeats of the conserved sequence KTKEGV. In contrast, significant differences are found in the C-termini. Comparing α -synuclein to the others in the C-terminus, β -synuclein has only 31% similarity to α -synuclein, while γ -synuclein has a much shorter tail with only minimal sequence similarity. Additionally, while all three proteins are intrinsically disordered in aqueous solution, neither β -synuclein nor γ -synuclein is amyloidogenic. This characteristic can be attributed to a highly hydrophobic region that is unique to α -synuclein, termed the non-A β component, as it was first identified as a peptide in the plaques of Alzheimer's patients (Xia et al., 1996).

```

alpha MDVFMKGLSKAKEGVVAAAETKQGVAAEAAKTKKEGVLYVGSKTKEGVVHGVATVAEKTKEQVITNVGGAVVTG 70
beta MDVFMKGLSMAKEGVVAAAETKQGVTEAAEKTKEGVLYVGSKTREGVVQCVASVAEKTKEQASHLGGAVFES- 69
gamma MDVFMKGLSMAKEGVVGAVEKTKQGVTEAAEKTKEGVVYVGAKTKENVVQSVTSVAEKTKEQANAVSEAVVSS 70

alpha VTAVAQKTVEGAGSIAAATCFVKKDQLG---KNEEGAPQ--EGILEDMPVDPDNEAYEMPSEEGYQDYEPPEA- 140
beta -----CAGNIAAATGLVKREDFPTDLKPEEVAQEAAEPELIEPLMEPEGESYEDPPQEEFYQEYEPPEA- 134
gamma VNTVAIKTVEEAEENIAVTSGVVRKEDLR-----PSAPQ-----QEGEASKK-KEEVAEEAQSGLD 127

```

Figure 2-2. Sequence alignment of *Homo sapiens* synucleins. This alignment shows the high degree of similarity between the human synuclein proteins, with near-identity between the three in the first 69 residues. Identical residues are shaded in black and similar residues are shaded gray. The NAC region of α Syn is marked by a red bar above the sequence (residues 61-95).

Structurally, α -synuclein is classified as an intrinsically unstructured protein, as it has no ordered secondary structure in aqueous solution (Weinreb et al., 1996). However, upon association with a negatively charged lipid surface or detergent, the first 98 amino acids form a discontinuous alpha-helix (Bisaglia et al., 2005; Cole et al., 2002; Davidson et al., 1998; Eliezer et al., 2001). This helix is amphipathic, and contains the NAC, a part of the protein that is necessary for amyloid fibril formation (Han et al., 1995). The C-terminal 40 residues are highly acidic, and do not acquire helical structure in either an aqueous or a lipidic environment (Chandra et al., 2003). The disorder of the C-terminal tail has been proposed to enable interactions with other proteins (Eliezer et al., 2001). This region also contributes to α Syn solubility, as deletion of the C-terminal acidic region makes the protein more susceptible to aggregation and the formation of amyloid fibrils (Hoyer et al., 2004; Li et al., 2005; Liu et al., 2005). Substantial work has been done to understand the structures of α Syn in both its vesicle-bound and free states, and to understand the relationship between the monomeric structures and multimeric forms of α Syn.

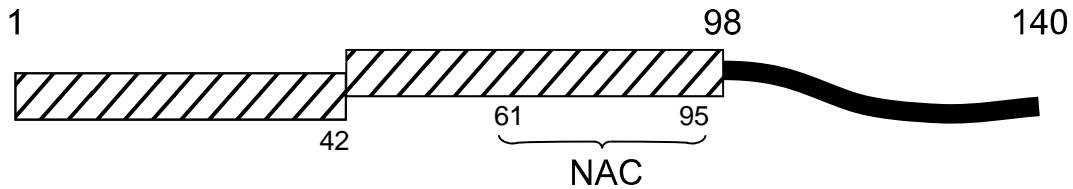


Figure 2-3. Structural architecture of α -synuclein. Upon interaction with phospholipid surfaces, the N-terminus of α Syn forms two amphipathic helices split by a turn after residue 42, while the C-terminus remains unstructured. Within the second helix formed by the N-terminus, residues 61-95 comprise the hydrophobic NAC region (residues 61-95) that is required for amyloid fibril formation.

Structure of lipid-bound α Syn

The N-terminus of α Syn interacts with both lipid vesicle surfaces and detergent micelles through an amphipathic helical domain (Chandra et al., 2003; Davidson et al., 1998; Eliezer et al., 2001). Multiple assays have been performed using a variety of vesicles, including multilamellar vesicles (MLVs), large unilamellar vesicles (LUVs, 100-200 nm in diameter), and small unilamellar vesicles (SUVs, 15-30 nm in diameter). SUVs best approximate the size and structure of presynaptic vesicles (Drescher et al., 2008a). Despite the formation of an amphipathic helix upon vesicle association, the role of ionic forces as the primary governor of the interaction between α Syn and the vesicle surface has been debated. Two studies used circular dichroism measurements of the helical content of α Syn to report on the amount of vesicle binding under increased ionic conditions (Davidson et al., 1998; Zhu et al., 2003). Both studies used SUVs containing a mixture of palmitoyl-oleoyl anionic and zwitterionic phospholipids (phosphatidic acid (POPA) and phosphocholine (POPC), respectively). The inclusion of anionic phospholipids as well as the smaller size of these vesicles is preferred by α Syn for binding (Davidson et al., 1998; Jo et al., 2000; Zhu et al., 2003). Davidson and colleagues used vesicles with a PC:PA ratio of 1:1, and

found that 200 mM NaCl reduced α Syn binding by approximately 30%. Zhu and colleagues used vesicles with less anionic character, composed of a 5:1 ratio of PC:PA, and observed a significant reduction in α Syn helicity at 200 mM NaCl, indicating that less α Syn was bound to the vesicle. While both groups found that strong ionic conditions (750 mM and 1.5 M NaCl, respectively) reduced the binding of α Syn to vesicles, these conditions were not sufficient to completely ablate binding. This indicated that other forces contribute to the α Syn-vesicle association. A third study also used CD to report on helical content as a marker of α Syn binding to the vesicle, although this group used MLVs containing brain-derived palmitoyl-oleoyl zwitterionic and anionic phospholipids (Jo et al., 2000), and determined that only 15% of α Syn remained bound at 800 mM NaCl. Finally, a contemporaneous experiment by yet another group using electron paramagnetic resonance and dimyristoylated phosphatidylglycerol membranes also found that only 15% of α Syn remained bound to the surface at 500 mM NaCl (Ramakrishnan et al., 2003). Even less α Syn, ~10%, was found to be bound to anionic LUVs at 400 mM NaCl by fluorescence correlation spectroscopy (Rhoades et al., 2006). Most recently, an evaluation of fluorescently-labeled α Syn binding to giant unilamellar vesicles, which eliminated the effect of vesicle curvature, provided additional evidence that electrostatic interactions were required, as 105 mM NaCl significantly reduced binding (Stockl et al., 2008). The discrepancy between the two sets of results may be attributable to several factors. First, the use of MLVs and LUVs to bind α Syn has been shown to be inferior compared to SUVs (Davidson et al., 1998; Jo et al., 2000), empirically supporting the fact that SUVs are more similar to the physiologically relevant presynaptic vesicles. Furthermore, the absence of anionic phospholipids in the latter study is questionable, as endogenous membranes in the brain are known to contain 15% anionic phospholipids (Mitchell et al., 2007). A study that compared α Syn binding to synthetic liposomes to α Syn association with membranes *in vivo*

concluded that the two systems were distinct (Kim et al., 2006). These data suggested that α Syn binds stably to synthetic vesicles via electrostatic interactions, whereas the binding of the protein to cellular membranes is more transient and unaffected by ionic forces. The existence of the amphipathic helix is certain, but its role remains unclear. Significant work has been done to develop a structural model of α Syn binding to phospholipid surfaces, with the focus on the N-terminal 100 residues of the protein.

Fits of the primary sequence into a helical net showed that a nonconventional $11/3$ α -helix is required to create a true amphipathic helix (Bussell and Eliezer, 2003; Jao et al., 2004). However, because the difference between an $11/3$ and the conventional $10.8/3$ helix is small (Segrest JBC 1999), subsequent experimental evidence has supported but not been able to confirm the pitch of the helices formed by α Syn (Bussell and Eliezer, 2003; Drescher et al., 2008a). Full-length α Syn discriminates between phospholipid headgroups, preferentially binding negatively charged phospholipids (Davidson et al., 1998; Jo et al., 2000; Zhu et al., 2003). While biochemical studies have used MLVs, LUVs, and SUVs, all these vesicles are large compared to α Syn and make the tumbling time of vesicle-bound α Syn slow. This resulted in overly broad peaks and therefore undetectable signals by NMR.

The NMR resolution problem was initially solved using detergent micelles, which are much smaller (~ 50 Å in diameter), and also bind α Syn as measured by an increase in the α -helical structure of the protein (Eliezer et al., 2001). Using the micelles as mimetics of phospholipid surfaces, NMR and EPR experiments determined that α Syn formed a discontinuous helix on the surface. Two models then evolved for the structure of the discontinuous helix. The first model was an extended helix with a break or kink in the middle, supported by

prediction algorithms and data from NMR and EPR experiments (Bisaglia et al., 2005; Chandra et al., 2003; Davidson et al., 1998; Jao et al., 2004; Ramakrishnan et al., 2003). Subsequent NMR experiments using α Syn bound to SDS micelles produced a horseshoe-shaped structure of two antiparallel helices on vesicle surfaces (Ulmer et al., 2005). However, as noted above, micelles are smaller than SUVs, and therefore have greater surface curvature. The more extreme curvature could artificially induce an antiparallel arrangement of the helices, producing a stable but physiologically irrelevant structure. Recently, two-frequency EPR was used to study the arrangement of α Syn helices on SUVs, which can accommodate both extended helices and the antiparallel structure (Drescher et al., 2008b). The authors placed spin-labels in the N-terminus of helix 1 and the C-terminus of helix 2 and evaluated signal broadening, which would indicate close proximity of the labels. Upon incubation with SUVs containing anionic phospholipids, they observed signal broadening of the spin-labeled α Syn. This provided additional support for the model of lipid-bound α Syn is an antiparallel arrangement of two helices in the N-terminus, separated by a turn at amino acid 42 (Figure 2-4).

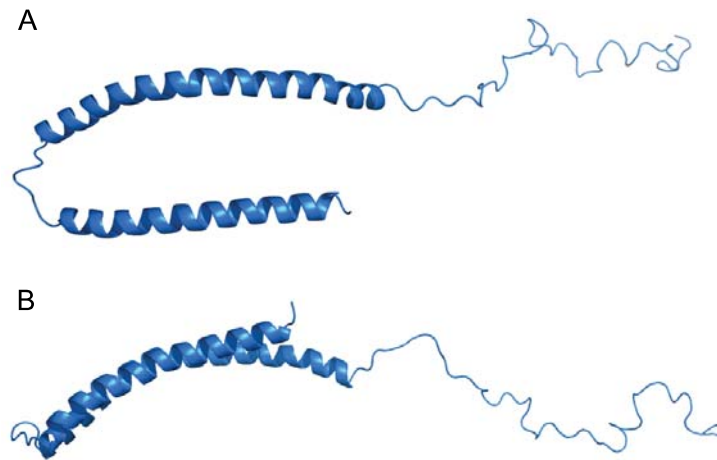


Figure 2-4. Structure of phospholipid-bound α Syn. The antiparallel arrangement of N-terminal helices on the phospholipid surface that form a horseshoe-shaped structure that was first identified by NMR and which was supported by subsequent EPR experiments. **A:** View looking down onto the phospholipid surface. **B:** Side view from within the curved plane of the phospholipid surface. Note the curved nature of the N-terminal helices. PDB 1XQ8 (Ulmer et al., 2005). Image rendered with PyMol.

Regarding the structure of the C-terminal tail (residues 95-140), most studies have concluded that it remains disordered upon association with vesicles (Chandra et al., 2003; Eliezer et al., 2001). However, one report of limited proteolysis of the C-terminal tail suggested that the C-terminal tail becomes ordered when α Syn binds to the vesicle, allowing for a single endoproteolytic event by three proteases: thermolysin (after residue 111), proteinase K (after residue 113), and the glutamate-specific V8 protease (after residue 123) (de Lauroto et al., 2006).

Several studies have investigated the topology of α Syn when bound to a lipid vesicle. As mentioned above, two reports argue that forces other than ionic interactions contribute to α Syn binding (Davidson et al., 1998; Zhu et al., 2003).

This hypothesis was supported by salt washes (up to 800 mM NaCl) of membrane fractions from rat brains, which did not disrupt endogenous α Syn interaction with the membranes (Lee et al., 2002). A potential source of this non-ionic interaction has been suggested by several groups to be the insertion or partial insertion of α Syn into the lipid bilayer. Consistent with that hypothesis, disruption of planar lipid bilayers by full-length, wildtype α Syn has been detected using atomic force microscopy (Jo et al., 2000; Zhu et al., 2003). α Syn-mediated disruption of bilayers that contain negatively-charged phospholipids was also observed by proton NMR (Madine et al., 2006). A more detailed model of insertion by α Syn into the lipid bilayer was provided by paramagnetic relaxation experiments, where spin-labeled probes within the micelle specifically broadened signals corresponding to residues of the NAC region of α Syn, using both full-length and N-terminally truncated forms of the protein (Bisaglia et al., 2006; Bisaglia et al., 2005). However, that model is disputed by evidence suggesting that the first helix of the N-terminus binds to lipid vesicles more strongly than the second helix, which contains the NAC (Drescher et al., 2008a). In summary, the current consensus structure of vesicle-bound α Syn is that it forms an antiparallel arrangement of helices on the vesicle surface, although the details of the interaction between the helices and the phospholipid headgroups are still controversial.

Free structure of α Syn

While α Syn is classified as an “intrinsically disordered protein”, the solution structure is well-accepted to be an ensemble of dynamic and transient conformations. To identify the conformations adopted by α -synuclein in solution, researchers have used a variety of techniques, including Raman spectroscopy and NMR-based techniques. Raman spectroscopy produced spectra that indicated an ensemble of conformations (Maiti et al., 2004). Soon after, spin-labeled α Syn

was subjected to paramagnetic relaxation experiments and then analyzed by molecular dynamics simulations led to a model in which α -synuclein was modeled to fold back on itself via long-range interactions (Dedmon et al., 2005). At about the same time, another group published similar paramagnetic relaxation studies as well as residual dipolar coupling experiments that revealed three distinct long-range interactions within the protein: residues 85-95 and 110-130, residues 105-115 and 120-130, and between residues 20 and 120 (Bertoncini et al., 2005). Using these interactions as restrictions, the authors developed models that showed the α Syn polypeptide in various conformations. Five of the seven most populated conformations show α Syn forming a loop, with the other two conformations appear to be a more compact, molten-globule tertiary structure. Simulations of the residual dipolar couplings that were used to create those models were used to propose that modeling α Syn in solution requires two features: (1) local conformational flexibility based on phi/psi angles and (2) long-range contacts between sequences distant in the primary sequence (Bernado et al., 2005). Independent evidence for long-range interactions came from fluorescence resonance energy transfer experiments using the triplet excited state of tryptophan as the donor (Lee et al., 2005; Lee et al., 2007). Based on the locations of the donor and acceptor moieties and the kinetics of energy transfer, these studies concluded that α Syn was not a random polymer.

These studies have established that “disordered” α -synuclein, while lacking in regular secondary structure, is not an extended polypeptide but is in fact an ensemble of globular structures with transient long-range interactions between the N- and C-termini. This conclusion is consistent with the elution of the 14.4-kDa monomeric α Syn protein from a gel filtration column at an elution volume corresponding to a ~40 kDa protein (Liu et al., 2005). Additional supporting evidence was obtained from paramagnetic relaxation enhancement

experiments, which confirmed two sets of long-range interactions within α Syn: between the C-terminus and NAC and between the C- and N-termini (Sung and Eliezer, 2007). Interestingly, there is a report of monomeric α Syn in the living *Escherichia coli* cytoplasm existing in an “unfolded” conformation as measured by hydrogen-deuterium exchange and ^1H - ^{15}N HSQC (Croke et al., 2008), suggesting that even *in vivo* and in a crowded macromolecular milieu, the ensemble of non-helical structures may exist. A physiological function for the ability of α Syn to form an ensemble of structures in solution remains unknown, but as discussed above, its high degree of conformational flexibility may enable multiple protein-protein interactions.

Self-association of α Syn

The ability of α Syn to form amyloid fibrils has been repeatedly demonstrated *in vitro* (Conway et al., 2000a; Kim et al., 2007; Marsh et al., 2006; Munishkina et al., 2003; Shtilerman et al., 2002). Amyloid formation by α Syn is a nucleation-dependent process, and can be accelerated by an increase in concentration, agitation, and temperature. As with other amyloidogenic proteins like A β , the conformational changes that precede (and/or compete with) amyloid fiber formation have been controversial. Pre-amyloid conformations of α -synuclein have been given various names, including protofibril, oligomer, and pre-amyloid. The relationship of these species to amyloid fibrils, and to one another, remains uncertain. The protofibrils are often identified as “annular” conformations, as a result of atomic force microscopy images (Apetri et al., 2006; Yu et al., 2008). One model holds that the pre-amyloid conformations are on-pathway, and are necessarily formed as the protein forms amyloid. An alternative model proposes that they are off-pathway, and that amyloid fibril formation can occur without the formation of any intermediate species. Within the discussion of these two models is also an active debate about the nature of the cytotoxic

species. Because inclusion bodies and amyloid fibrils are observed in diseased tissue, an early hypothesis was developed that the amyloid fibrils are toxic to the neurons. However, subsequent work has strongly implicated a pre-amyloid conformation (the “oligomer” or “protofibril”) as the cytotoxic species, with the amyloid fibrils initially being a protective conformation as the cell attempts to cope with the cytotoxicity of the oligomer. Supporting this latter model was the observation that pharmacological inhibition of the sirtuin Sir2, a nicotinamide adenine dinucleotide-dependent histone deacetylase, alleviates α Syn-mediated cytotoxicity while simultaneously altering the cellular distribution of α Syn inclusions from multiple aggregates to large inclusions (Outeiro et al., 2007). The authors postulated that the correlation between these two phenotypes indicated that the large fibrillar inclusions may be cytoprotective, and that cytotoxicity could be mediated by smaller oligomers.

Regardless of which conformation is the toxic species, the self-association of α Syn is a kinetic process, and any therapeutic treatment directed at α Syn aggregation will have to manipulate the kinetics in some way. Identification of the toxic species is essential, however, to identify the target reaction within the self-association scheme (Figure 2-5). Because the formation of oligomers and fibrils is a kinetic process, targeting the production of one species may affect the production or stability of another. For example, if a small molecule inhibits amyloid fibril formation but does not affect the conversion of monomer to oligomer, there is the potential for oligomers to build up (whether the oligomer is an on-pathway intermediate or an off-pathway alternate conformation). If the oligomer is the cytotoxic species, then amyloid inhibition would actually be more damaging to the cell by promoting the formation of the toxic oligomer.

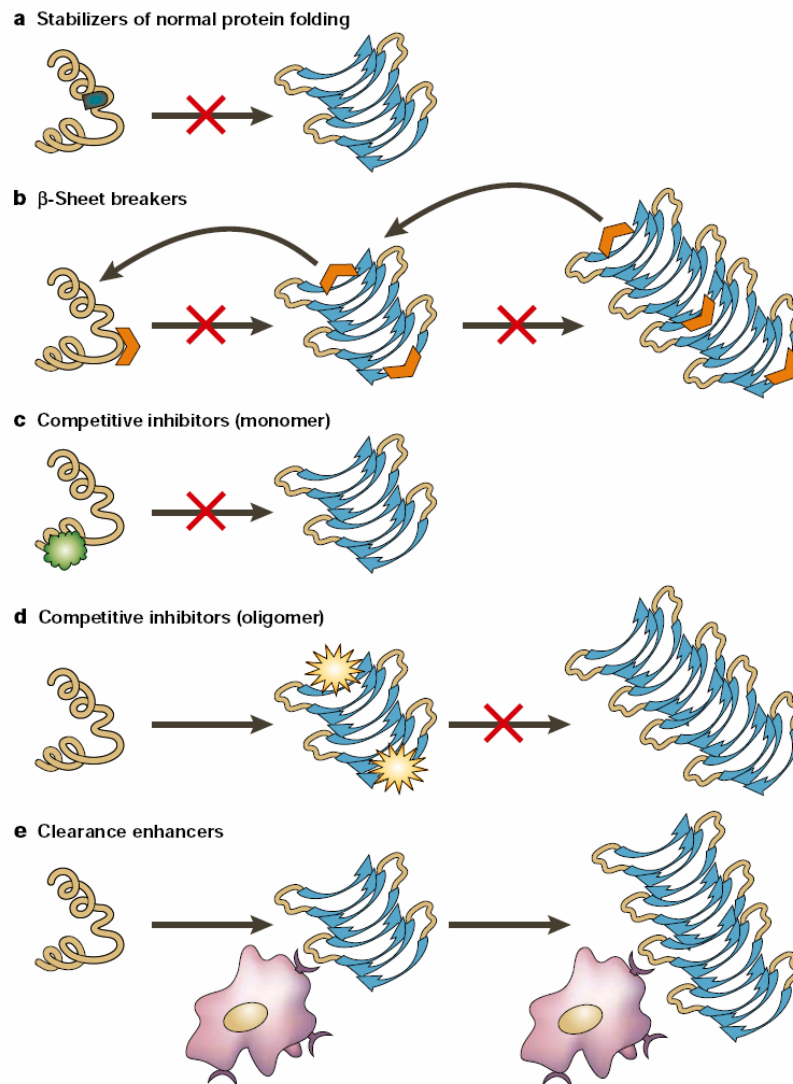


Figure 2-5. Schematic representations of therapeutic strategies to prevent α Syn misfolding. A: stabilization of the folding of the native protein. B: Inhibition and reversal of β -sheet formation. C: Competitive inhibition of oligomerization by binding to the native state. D: Competitive inhibition of fibrillization by binding to the oligomeric state. E: Increased clearance of protein aggregates, by upregulating clearance pathways and/or destabilizing the aggregated state(s). Reprinted by permission from Macmillan Publishers Ltd: Nature Reviews Neuroscience (Soto, 2003), copyright 2003.

In vitro, conditions have been found that manipulate the kinetics of the α Syn self-association reactions. In addition to protein concentration and temperature, fibrillization can be accelerated by pesticides (Manning-Bog et al., 2002; Uversky et al., 2002a; Uversky et al., 2001c), metals (Uversky et al., 2001b), and low pH (Uversky et al., 2001a), among others. Fibrillization has also been inhibited by the stabilization of the monomeric unfolded state via oxidation of methionines (Uversky et al., 2002b). Notably, even though the oligomeric state appears to be a transient species, it can be trapped by nitration of α Syn, which prevents fibrillization by stabilizing the oligomer (Yamin et al., 2003). Therefore, an understanding of the kinetics of aggregate formation and the conclusive identification of the cytotoxic species is essential to the development of effective anti- α Syn therapies.

Molecular genetics of Parkinson's disease

Several pieces of genetic evidence have linked α -synuclein with Parkinson's disease. Gene duplication and triplication events have been correlated with early-onset inherited forms of PD in multiple kindred (Chartier-Harlin et al., 2004; Ibanez et al., 2004; Ikeuchi et al., 2008; Singleton et al., 2003). In these cases, the gene dosage was found to be inversely correlated with the age of onset. The average onset of disease in the family that carries the gene triplication is 34 years old (Singleton et al., 2003). Notably, a patient homozygous for SNCA gene duplication – therefore carrying four copies of the gene – presented with motor symptoms at age 28 and developed significant cognitive impairment by age 35 (Ikeuchi et al., 2008).

Table 2-2. Molecular genetics of Parkinson disease.

Protein	Function	Mutation in PD
α Syn	unknown	GOF
Parkin	E3 ligase	LOF
UCH-L1	Ubiquitin ligase/hydrolase	LOF/GOF
LRRK2	Kinase, GTPase	GOF
DJ-1	Mitochondrion-associated kinase	LOF
PINK1	Mitochondrion-associated kinase	LOF

Three missense mutations associated with early-onset familial PD have been found in multiple families: A30P, E46K, and A53T (Kruger et al., 1998; Polymeropoulos et al., 1997; Zarranz et al., 2004). The discovery of point mutations within α Syn associated with disease rapidly led to studies attempting to establish a biochemical connection between the mutations and pathology. The primary aims of these studies were to evaluate the changes exerted by the mutations on amyloid fibril formation, protofibril formation, and/or lipid vesicle binding. A variety of techniques have been used to assess these biochemical processes. In addition to analysis by the structural methods described above, biochemical assays have been developed for rapid and straightforward analysis of the known biochemical characteristics of α Syn. Amyloid fibril formation was evaluated by electron microscopy, Thioflavin T fluorescence, FTIR, and turbidity and light scattering assays. Formation of pre-amyloid oligomers or protofibrils was assessed by electron microscopy, atomic force microscopy, and light scattering. Other assays used small-angle x-ray scattering to evaluate a self-association events, not distinguishing between amyloid and high-molecular weight oligomers or amorphous aggregates (Li et al., 2001). The mutation A53T significantly increased the amyloidogenicity of α -synuclein (Choi et al., 2004; Conway et al., 1998; El-Agnaf et al., 1998a; El-Agnaf et al., 1998b; Greenbaum et al., 2005; Li et al., 2001; Narhi et al., 1999). Similarly, the E46K mutation

increased amyloidogenicity *in vitro* (Choi et al., 2004; Fredenburg et al., 2007) and *in vivo* (cell culture) (Pandey et al., 2006). In contrast, the A30P mutation appeared to increase the formation of a pre-amyloid oligomer but not amyloid fibrils (Conway et al., 2000b; Conway et al., 2000c; Li et al., 2001).

Evaluations of the effect of the mutations on lipid vesicle binding employed flotation assays, pulldown assays, assessment of helical structure by CD, and vesicle permeabilization assays. Of the three mutations, A30P has been shown to reduce the affinity of α Syn for the lipid vesicle surface (Bussell and Eliezer, 2004; Choi et al., 2004; Cole et al., 2002; Jo et al., 2002; Stockl et al., 2008; Ulmer and Bax, 2005). By contrast, the E46K substitution enhances binding to vesicles, perhaps by strengthening the ionic interaction with the phospholipid headgroups (Choi et al., 2004; Stockl et al., 2008). Additionally, the pre-amyloid protofibrils formed by E46K-syn exhibited reduced vesicle permeability in an *in vitro* assay relative to wildtype α Syn (Fredenburg et al., 2007). Data for lipid binding by A53T have suggested that it does not differ from wildtype (Choi et al., 2004; Cole et al., 2002). This is supported by NMR data that showed no difference between A53T-syn and wildtype α Syn upon association with SDS micelles (Bussell and Eliezer, 2004), although anisotropy studies suggest that the A53T mutant protein may have a different topology on the vesicle surface (Jo et al., 2004).

C-terminal truncation of α Syn

The aggregation of α Syn is closely associated with the development of Parkinson's disease in both human patients and in mouse models. Recent data from the Thomas lab indicated that critical proteolytic events produce specific N-terminal fragments of α Syn that dramatically accelerate the misfolding process and the development of cytotoxicity (Liu et al., 2005). In that study, N-terminal

fragments of α Syn were found in the insoluble fractions of substantia nigra neurons from Parkinson's disease patients but not Alzheimer's disease patients (Figure 2-6). Similar fragments were found in the insoluble fractions of mouse brain lysates, and the appearance of the fragments strongly correlated with the onset of pathological symptoms. Others have also demonstrated a tight correlation between these fragments and disease (Li et al., 2005). Moreover, removal of the C-terminal tail, whether by recombinant expression of a truncated form or by endoproteolysis of full-length α Syn, accelerates amyloid fibril formation *in vitro* (Hoyer et al., 2004; Li et al., 2005; Liu et al., 2005).

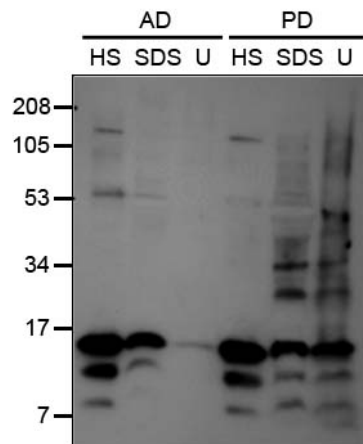


Figure 2-6. C-terminal truncations of α Syn are present in PD patient brains. Samples of PD and an age-matched AD patient were subjected to sequential fractionation (HS, high salt soluble fraction; SDS, SDS-soluble fraction; U, urea-soluble fraction). Full-length α Syn was observed in all fractions of both tissues. C-terminal truncations were only observed in the solubilized aggregates of the PD patient. The three truncations were found to contain residues 1-110, 1-100, and 60-100 by epitope mapping with a panel of anti- α Syn antibodies. Reprint permission granted by the American Society for Biochemistry and Molecular Biology from (Liu et al., 2005), copyright 2005.

Underscoring the potential role for C-terminal truncations of α Syn in pathogenesis, two transgenic mouse models of PD have been developed that express C-terminally truncated forms of human α Syn (Tofaris et al., 2006; Wakamatsu et al., 2006). The first mouse was transgenic for human α Syn(1-120) on a murine α Syn null background. The expression of the α Syn(1-120) was under control of the rat tyrosine hydroxylase promoter, which directed expression to dopaminergic neurons (Tofaris et al., 2006). These mice displayed progressive accumulation of α Syn-positive inclusions, selective degeneration of dopaminergic neurons, and age-dependent motor deficits. Furthermore, the substantia nigra experienced increased microglial invasion, indicative of an inflammatory response that has been implicated as an element in the early pathology of PD. The second mouse model was transgenic for the human α Syn truncation 1-130 with the disease-associated A53T mutation on a murine wildtype α Syn background (Wakamatsu et al., 2006). As in the previous model, the transgenic expression was driven by the rat tyrosine hydroxylase promoter. These mice also displayed selective degeneration of dopaminergic neurons, a subsequent decrease in striatal dopamine content, and behavioral abnormalities that were rescued by the administration of levo-DOPA, which is processed into dopamine in the brain. Because of these traits, these mouse models recapitulate some of the critical symptoms and pathophysiology of human PD, and therefore provide tantalizing evidence that C-terminal truncation of α Syn may be a precipitating event in Lewy body disease pathology.

Clinical and molecular pathology of the Lewy body disorders

As noted above, Parkinson disease is only one of several disorders that are collectively referred to as “the Lewy body disorders” (LBD) (Lippa et al., 2007). The protein aggregates can be found throughout the postmortem brain tissue of LBD patients, and may be found in the neuronal cell body (where they are termed

Lewy bodies), neurites (Lewy neurites), the presynaptic terminal, or the glia (reviewed in Jellinger, 2007; Lippa et al., 2007; Tarawneh and Galvin, 2007).

In the clinic, the presentation of symptoms dictates the diagnosis. A diagnosis of PD is given to patients who initially present with the well-known motor symptoms of tremor, bradykinesia, and rigidity of movement. There are six stages of PD: stages 1 and 2 are presymptomatic, but contain α Syn lesions in the medullary and olfactory regions of the brain; stages 3 and 4 present with motor symptoms and significant reduction of neurons in the substantia nigra; and stages 5 and 6 have cognitive impairment that has been correlated with the appearance of α Syn pathology in the cortex (Aarsland et al., 2005a; Hurtig et al., 2000; Jellinger, 2008). If the cognitive deficits appear more than 12 months after a PD diagnosis, the patient is considered to have Parkinson's disease with dementia (PDD).

Dementia with Lewy bodies (DLB) was originally intended to distinguish cognitive impairment from other dementias (McKeith et al., 1996), and includes patients who develop parkinsonism-like movement disorders within a 12 months of the onset of cognitive symptoms. DLB and AD have many common clinical and pathological features, including a coincidence of both A β plaques and α Syn pathology in later-stage DLB (Jellinger, 2008; Tarawneh and Galvin, 2007) and concurrent A β and α Syn pathology in AD patients (Ranginwala et al., 2008). It has been suggested that Lewy body pathology is affected by AD pathology (Iseki et al., 2003; Marui et al., 2002), and indeed α Syn was first identified by the deposition of the NAC fragment in A β plaques in Alzheimer's patients. Although the relationship between α Syn, tau, and A β aggregates is still murky, progress is being made in distinguishing between these dementias in the clinic with vitally

important consequences. DLB patients have more profound psychiatric symptoms than AD patients, including hallucinations and psychoses (Aarsland et al., 2001), and they appear to be more sensitive than AD patients to antipsychotic medications, which can cause life-threatening reactions (McKeith et al., 1992). Notably, PDD patients appear to be tolerant of antipsychotics, which enables a wider spectrum of treatment with antiparkinsonism medications that are also potentially psychotogenic (Aarsland et al., 2005b). Additionally, DLB patients may respond better than AD patients to cholinesterase inhibitors, even though both diseases involve dysfunction of the neurotransmitting cholinergic system (Tarawneh and Galvin, 2007). Therefore, the clinical distinction between PD/PDD, DLB, and AD has direct consequences for treatment. Additional work to further define clinical, pathological, and molecular distinctions between the various Lewy body disorders is an active project of the DLB/PDD Working Group (Lippa et al., 2007).

Chapter Three

The Proteasome and Intrinsically Disordered Proteins

The ubiquitin-proteasome system is responsible for the majority of cytosolic protein turnover within the cell. The enzyme responsible for the turnover, the proteasome, is a complex macromolecular machine that exists in multiple forms. It is one of many self-compartmentalizing proteases that are known to exist, as the proteolytic activity is structurally sequestered from the cytosol. All forms of the proteasome contain the catalytic core, which was originally termed the “20S” proteasome for its sedimentation coefficient, and is also referred to as the “core particle” or “CP”. It is approximately 700 kDa and is a multimeric complex of two related subunits, α and β , arranged into four stacked heptameric rings to form a hollow cylinder (Figure 3-1). Alpha subunits form each of two outer rings, while beta subunits form each of two inner rings (Groll et al., 1997; Lowe et al., 1995). Proteasomes are found in archaea, mammals, and eubacteria, and the quaternary configuration of $\alpha_7\text{-}\beta_7\text{-}\beta_7\text{-}\alpha_7$ is conserved throughout.

Comparison of proteasomes from these evolutionarily diverse organisms reveals an evolved complexity in higher organisms. In archaea, the 20S is composed of a single alpha and a single beta subunit, with 7 of each subunit forming homoheptameric rings that assemble to form a single proteasome macromolecule (Figure 3-1, panel A). Similarly, the actinobacteria proteasomes appear to contain a single alpha and a single beta, although the genomes contain two distinct operons that each code for an alpha and a beta subunit (Tamura et al., 1995). Yeast express seven alpha and seven beta subunits that form heteroheptameric rings (Lowe et al., 1995; Monaco and Nandi, 1995). Yet more complex are the mammalian proteasomes, for which the genome encodes seven

alpha and ten beta subunit genes, although only seven of each are present at any time within one ring of the proteasome to form a symmetrical structure of $\alpha_{(1-7)}-\beta_{(1-7)}-\beta_{(1-7)}-\alpha_{(1-7)}$ (Figure 3-1, panel B).

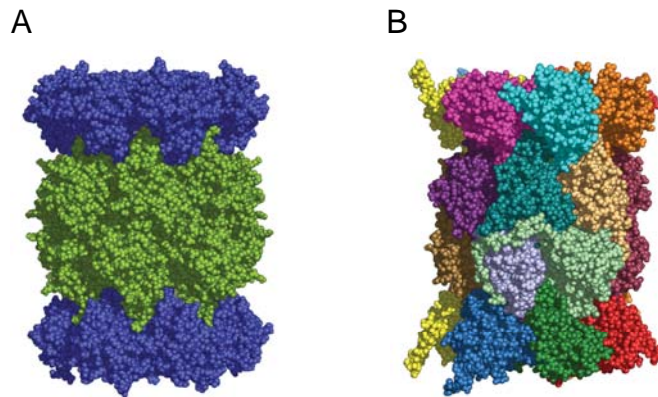


Figure 3-1. Crystal structure of the archaeal and mammalian proteasomes. (A) Structure of 20S from *Thermoplasma acidophilum* (PDB 1PMA) (Lowe et al., 1995). α subunits, blue; β subunits, green. (B) Structure of 20S from *Bos taurus* (PDB 1IRU) (Unno et al., 2002). Each subunit is colored according to the Baumeister/Groll subunit nomenclature as discussed below: α 1, red; α 2, dark green; α 3, blue; α 4, yellow; α 5, magenta; α 6, cyan; α 7, orange; β 1, burgundy; β 2, pale green; β 3, lavender; β 4, dark tan; β 5, purple; β 6, teal; β 7, light tan. Images rendered with PyMol.

In all proteasomes, polypeptides enter and exit the lumen through annuli controlled by the α rings on either end of the proteasome. Once within the 20S cylinder, the polypeptide chain enters into chambers that are formed by the interfaces between the heptameric rings: two antechambers between the α and β rings, and a catalytic chamber between the two β rings (Figure 3-2).

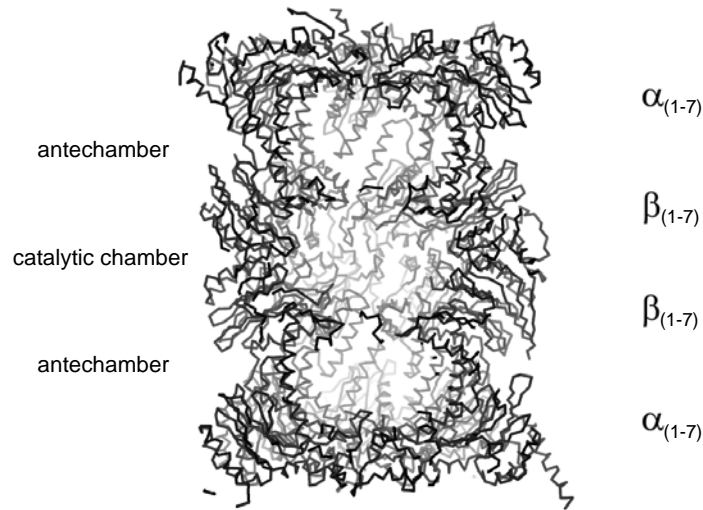


Figure 3-2. Cutaway view of the bovine 20S proteasome. A side-view cutaway of the 20S proteasome shows the three internal chambers (two antechambers and central catalytic chamber) formed by the stacked α - β - β - α rings. PDB 1IRU (Unno et al., 2002); image was rendered with PyMol.

Alpha subunits and structure

Both the alpha and beta families of proteasomal subunits share the same general fold of a central five-stranded beta sheet sandwich flanked by alpha helices on either side (Groll et al., 1997; Lowe et al., 1995). This fold is prototypical of the N-terminal nucleophile (Ntn) hydrolase family, of which the proteasome subunits were the first identified members (Brannigan et al., 1995). The alpha subunits are more conserved than the beta subunits (Coux et al., 1994), and are further distinguished from the beta family by a highly conserved N-terminal extension that sits across the beta sheet (Baumeister et al., 1998; Groll et al., 1997). An alignment of the alpha subunits from *Bos taurus*, the proteasome used throughout this dissertation work, shows the conservation of all seven subunits (Figure 3-3). During proteasome assembly, the alpha subunits form rings independently of other factors, which then serve as scaffolds on which the beta subunits can assemble (Zwickl et al., 1994).

```

gi | 77735717 | Bt_a4  ----MSRRYDSRTTIFSPGRLYQVEYAMEAIG-HAGTCLGILANDGVLLAAERRNIHKLLEDEVFFSEKIYKLNEDMACS
gi | 62751982 | Bt_a5  -MFLTRSEYDRGVNTFSPGRLFQVEYAEATK-LGSTATGIQTSEGVCLAVEKR-ITSPLEMPSSIEKIVEIDAHIGCA
gi | 77736269 | Bt_a2  MAER---GYFSLTTTFSPCKLVLQIEYALAAVA-GGAPSVGIKAANGVVLATEKK-QKSILYDERSVHKVEPITKHIGLV
gi | 114053135 | Bt_a6  MSRGSSAGDRHITIFSPGRLYQVEYAFKALNQGLTSSAVVRGKDCAVLVTQKK-VDPKLLDSSTVTHLFKITENIGCV
gi | 77735425 | Bt_a7  -----MSYDRAITVTFSPDGHLFQVEYAEAVK-KGSTAVGVRGKDTVVLGVVEKK-SVAKLQDERTVTKCALDDNVCA
gi | 78369458 | Bt_a1  ---MFRNQYDNDVTVVSPQGRTHQIEYAMEAVK-QGSATVGLKSKTHAVLVALKR---AQSELAAHQKKILHVDNHIGIS
gi | 77735429 | Bt_a3  -MSSIGTGYDLSASTFSPDGRVVFQVEYAKKAVE-NSSTATGIRCKDGVVFGVEKL-VLSKLYEEGSNKRLFNVDHRVGM

gi | 77735717 | Bt_a4  VAGITSDANVLTNELRLIAQRVLLQYQEPICEQLVTAICDIKQAYTQFCGK-----RPFVSVLLYIGWDXHYGFQLYQS
gi | 62751982 | Bt_a5  MSGLIADAKTLIDKARVETONHWFTYNETMTVESVTQAVSNLALQFGEEDADPGAMSRPFGVALLFGGVDEK-GPOLPHM
gi | 77736269 | Bt_a2  YSGMGPDYRVLVHRARKLAQQYLLVYQEPPTAQLVQRVASVMQEYTOQSGV-----RPFVSVLLICGNNRGR-PYLEQS
gi | 114053135 | Bt_a6  MTGMTADSRSQVQRARYEAAWKKYKYGYEIPVDMLCRRLADISOVYTONAEM-----RPLGCCMILIGHDFEQGPQVYKC
gi | 77735425 | Bt_a7  FAGLTADARIVINRARVECSHRLTVEDEPVTVEYITRYIASLQRYTQSNR-----RPFGISALIVGFDFDGTPLRYQT
gi | 78369458 | Bt_a1  IAGLTADARLLCNFMROECLDSRFVFDRLPVSRLVSLICSKTOIPTORYGR-----RPVGVGLLIAGYDDMG-PHIFQT
gi | 77735429 | Bt_a3  VAGLLADARSLADIAREEASNFRSNFGYNLPIKHLADRVAWYVHAYTLYSAV-----RPFVSVFMIIGSVNDGAQLYMI

gi | 77735717 | Bt_a4  DPSGNYGKWKATCIGNNSAAAVSMLKQDYKE-GEMTLKSAALALAKVFNKTMDSV-KLSAEKVEIATLTRENGKTVIRVL
gi | 62751982 | Bt_a5  DSPGTFVQCDARAIGSASEGAQSSLOEVYHK-S-MTLKEATKSSLIILKQVMEE--KLNATNIELATVQPGQN---FHMV
gi | 77736269 | Bt_a2  DSPGAYFAWKATAMGKNYVNGKTFLEKRYNE--DLELEDAIHTAILTLKESFEG--QMTEDNIEVVICNEAG----FRRL
gi | 114053135 | Bt_a6  DPAGYCYCGFKATAAGVKQTESTSFLEKKVKKKFDWTFEQTVETAITCLSTVLSI--DFKPSIEVGVVTVENPK--FRIL
gi | 77735425 | Bt_a7  DSPGTYHAWKANAIGRGAKSVREFLEKNYIDEAIEITDDLTKLVIKALLEVVQS----GCKNIELAVMRRDQP---LKLIL
gi | 78369458 | Bt_a1  CPSANYFDCRAMSIGARSQSARTYLERHMSFMECNLELVKHLRALRETLPAEQDITTKNVSIGIVGKLE---FTIY
gi | 77735429 | Bt_a3  DPSGVSYGYWCCAIGKARQAAKTEIEKLQMK--EMTCRQVVKVAKIITYIVHDEV-KDKAFELELSWVGEITNG--RHEI

gi | 77735717 | Bt_a4  KQKEVEQLKKEHEEEAKAEREKKEKEQKEKDK-----
gi | 62751982 | Bt_a5  TKEELEEVTKDI-----
gi | 77736269 | Bt_a2  TPTEVKDYLAATA-----
gi | 114053135 | Bt_a6  TEAEIDAHLVAAERD-----
gi | 77735425 | Bt_a7  NPEEIEKYVAEIEKEKEENEKQKAS-----
gi | 78369458 | Bt_a1  DDDDVSPFLEGLEERPQRKAQPTQPADEPAEKADPEMEH
gi | 77735429 | Bt_a3  VPKDVRREEAEKYAKESLKEEDESDDDNM-----

```

Figure 3-3. CLUSTAL-W2 alignment of bovine alpha sequences. GenBank accession numbers are included in the sequence labels. Conserved residues are in black; similar residues are gray. The sequences and nomenclature are identical to the human alpha subunit sequences, although multiple isoforms have been identified for some human sequences that are not documented for the bovine sequences.

Access to the lumen is restricted by the N-termini of the alpha subunits, which overlay one another to form a “gate” (Figure 3-4). The function of the antechambers is unknown, but they have been postulated to prime the polypeptide chain prior to entry into the catalytic chamber for cleavage (Pickart and Cohen, 2004).

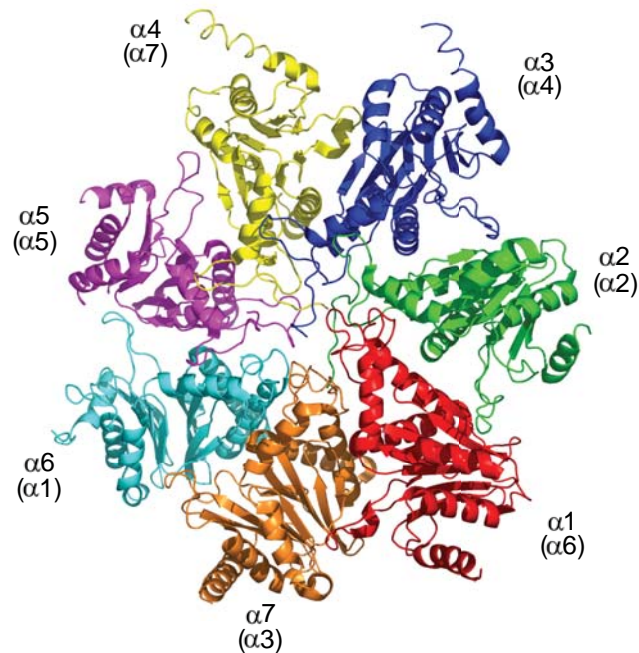


Figure 3-4. The bovine α -ring. Individual subunits are colored differently and labeled by two nomenclatures: the primary annotation follows the Baumeister/Groll nomenclature and the parenthetical annotation is the nomenclature used by Coux/NCBI/GenBank, which corresponds to the gene names. PDB 1IRU (Unno et al., 2002); image rendered with PyMol.

The ordered N-termini form a pore, the size of which varies in structures from different species (Figure 3-5). NMR studies of the archaeal *Thermoplasma acidophilum* 20S have shown that the N-terminal 13 amino acids are highly flexible, as the residues are not observed in the NMR spectra (Sprangers and Kay, 2007). The alpha ring is responsible for interactions with activator complexes

(Gray et al., 1994; Peters et al., 1993; Yoshimura et al., 1993), which reorder the gate to enlarge the pore, thereby providing access to the catalytic lumen (Whitby et al., 2000). Low concentrations of SDS have also been shown to increase 20S peptidase activity against fluorogenic peptides, presumably by also changing the conformation of the gate (Tanaka et al., 1988).

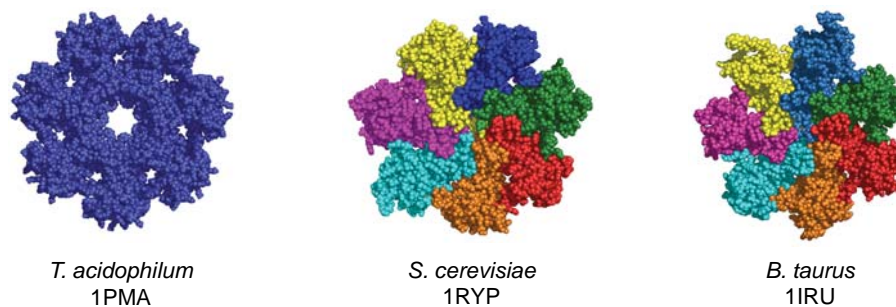


Figure 3-5. Alpha rings of three species. The structures of the 20S proteasome from *Thermoplasma acidophilum*, *Saccharomyces cerevisiae*, and *Bos taurus* were solved by x-ray crystallography (Unno et al., 2002). Shown here is a top-down view of only the alpha rings from each species. The mammalian subunits are colored according to subunit using the Baumeister/Groll nomenclature: $\alpha 1$, red; $\alpha 2$, green; $\alpha 3$, blue; $\alpha 4$, yellow; $\alpha 5$, magenta; $\alpha 6$, cyan; $\alpha 7$, orange. All images rendered with PyMol.

The regulatory function of the gate was conclusively shown using mutants of the yeast 20S. N-terminal deletion mutants of the $\alpha 3$ and $\alpha 7$ subunits were expressed in *Saccharomyces cerevisiae*, and the intact 20S proteasomes formed with these mutant subunits were purified (Groll et al., 2000). The single deletion mutants $\alpha 3\Delta N$ significantly increased the rate at which the yeast 20S hydrolyzed small peptide substrates over 10-fold compared to the wildtype 20S, while the single mutant $\alpha 7\Delta N$ only slightly increased peptidase activity (Bajorek et al., 2003; Groll et al., 2000). The double mutant, $\alpha 3\alpha 7\Delta N$, was found to increase peptidase activity similarly to the $\alpha 3\Delta N$ single mutant. However, unlike the

single mutants, $\alpha 3\alpha 7\Delta N$ hydrolyzed carboxymethylated casein at a rate tenfold greater than the wildtype 20S (Bajorek et al., 2003).

Beta subunits and proteolysis

The 20S proteasome is a member of the N-terminal nucleophilic family of proteases. In this family, proteolysis is catalyzed by a nucleophilic attack by an amino-terminal residue. In the proteasome, the nucleophile is a threonine on the beta subunit, termed Thr10^γ (Fenteany et al., 1995). The threonine of each subunit is exposed following processing of a precursor form into the active form during 20S assembly. Archaeal and eubacterial proteasomes have fourteen active sites, one per β subunit, and exert a chymotrypsin-like cleavage activity. In eukaryotes, only the $\beta 1$, $\beta 2$, and $\beta 5$ subunits contain a catalytic threonine, yielding six sites of catalysis per proteasome. Unlike the proteasome of the other two kingdoms, each of these three subunits is associated with a particular kind of proteolytic activity, making the eukaryotic proteasome a multicatalytic enzyme: $\beta 1$ exerts trypsin-like activity, $\beta 2$ hydrolyzes bonds after acidic residues and so is termed peptidylglutamyl peptide hydrolase-like (PGPH-like), and $\beta 5$ has chymotrypsin-like activity. As mentioned above, eukaryotic genomes contain 10 genes for expression of β subunits, but only seven are assembled into the 20S core particle at any time. The additional three genes found in the mammalian genome are inducible by interferon- γ , as is the activator complex PA28. The inducible β subunits are termed $\beta 1i$, $\beta 2i$, and $\beta 5i$, as they replace the constitutively expressed catalytic subunits $\beta 1$, $\beta 2$, and $\beta 5$ within the 20S. This “immunoproteasome” associates with PA28 to facilitate the processing of cytosolic proteins for MHC class I antigen presentation.

A variety of pharmacological inhibitors of the 20S proteasome are available, and have been useful for elucidating the catalytic mechanisms of the proteasome as well as for *in vitro* and *in vivo* studies of the physiological function of the enzyme (Lee and Goldberg, 1998). MG132 and PSI are reversible aldehyde inhibitors that target all three activities of the eukaryotic proteasome. The small molecule lactacystin is a natural product discovered in the bacterium *Streptomyces*. In its active form, clasto-lactacystin β -lactone, it irreversibly and selectively inhibits the proteasome but does not affect cellular cysteine or serine proteases (Fenteany et al., 1995). In contrast, inhibitors that selectively target each of the three active sites are also available. Leupeptin targets the trypsin-like activity of β 1; the PGPH-like activity of β 2 can be quenched by the small molecule YU102 (Myung et al., 2001); and low levels of lactacystin can be used to selectively inhibit the β 5 chymotrypsin-like activity. Because the proteasome has a central role in healthy cell growth and regulation, it is a difficult target for therapeutic small molecules. However, the proteasome-specific inhibitor Velcade (bortezomib) was approved by the United States Food and Drug Administration in 2003 for treatment of human multiple myeloma, which was shown to be more sensitive to proteasomal inhibition than noncancerous cells (LeBlanc et al., 2002).

Mechanisms of proteasomal activation

Entry of a substrate into the lumen of the 20S is often regulated by the binding of one or two multisubunit regulatory complexes. The PA700, or 19S, complex binds to the 20S core to form a holoenzyme termed the 26S proteasome that conducts ATP-dependent ubiquitin-mediated degradation. The PA700 contains ubiquitin-binding, ubiquitin hydrolase, unfoldase, and ATPase activities, and can bind at either or both ends of the 20S cylinder. In addition to its functions as part of the 26S, PA700 has activities independent of the 26S proteasome

(Ferdous et al., 2002; Liu et al., 2002a). In the ubiquitin-proteasome system (UPS) (Tanahashi et al., 2000), proteins targeted for degradation by the addition of a polyubiquitin tag via an isopeptide bond to a lysine residue. This tag is recognized by the PA700 molecule, which then removes the ubiquitin moiety as part of the translocation of the target protein into the lumen for degradation. Due to the primary importance of the UPS in a variety of cellular activities, including the cell cycle and misfolded protein response, extensive research has been done to understand its mechanisms and regulatory elements as part of the 26S proteasome. PA700 associates with the alpha ring of 20S in manner which requires ATP binding, but not ATP hydrolysis (Liu et al., 2006). The interaction is mediated by the C-terminal tails of two of its ATPase subunits, Rpt2 and Rpt5, as demonstrated by the ability of short peptides of the same sequence to activate the 20S proteasome against fluorogenic peptide substrates (Gillette et al., 2008). The interaction between the archaeal activator complex PAN and the archaeal 20S was found to be similar to the eukaryotic activator and 20S in ATP-dependence and activation by the C-terminal tails (Smith et al., 2007; Smith et al., 2005). Rpt2 may have an additional conformational role that enables access to the pore of the 20S (Kohler et al., 2001). Furthermore, the non-ATPase subunits Rpn1 and Rpn2 may also participate in the gating of the alpha ring (Rosenzweig et al., 2008). These recent advances have enhanced the understanding of degradation by the 26S proteasome, but the precise mechanisms and relationships between substrate recognition, deubiquitination, unfolding, and translocation remain to be elucidated.

Other activating complexes stimulate proteasome activity without ATP. PA28, or 11S, is a heteromeric complex composed of alpha and beta subunits, each approximately 28 kDa (Gray et al., 1994; Ma et al., 1992; Mott et al., 1994). Individual recombinant alpha and gamma subunits form homoheptamers that are

also capable of 20S activation, although the mixed α/β heteroheptamer has the greatest affinity for the 20S proteasome (Realini et al., 1997). A PA28 α homolog, PA26, exists in *Trypanosoma brucei* that shares 24.2% identity and 35% similarity with human PA28 α . *In vivo*, PA28 expression is induced by interferon- γ , as are the alternative 20S β i catalytic subunits, and functions in concert with the β i subunits to produce ligands for MHC class I antigen presentation on T-cells (Groettrup et al., 1996; Tanahashi et al., 2000). *In vitro*, the addition of PA28 stimulates the peptidase activity of 20S, but not protease activity (Ma et al., 1992). This family of activator complexes is capable of cross-species activation, as evidenced by a variety of combinations. Those complexes include *T. brucei* PA26 + yeast (Whitby et al., 2000), human PA28 α + bovine 20S, and human PA28 α + yeast 20S (Forster et al., 2005), among several others (Forster et al., 2005; Mykles, 1996; Yao et al., 1999). A 3.2 Å crystal structure of the *T. brucei* PA26 bound to the yeast 20S (Forster et al., 2003; Whitby et al., 2000), confirmed experimental evidence that the activator complex bound directly to the 20S alpha ring via the C-termini and adjacent “activation loops”, formed by the turn between helices 2 and 3 of each subunit (Forster et al., 2003; Gray et al., 1994; Ma et al., 1993; Whitby et al., 2000). The same structure revealed that binding of PA26 created a 13 Å-diameter pore in the center of the alpha ring (Whitby et al., 2000), in contrast to a closed gate in the unactivated proteasome (Tanaka et al., 1988). This opening of the gate was caused by the reorientation of the N-terminal tails of subunits α 2, α 3, α 4, and α 5 upward into the channel of the PA26.

Another activating complex, PA200, was recently discovered that also stimulates peptidase activity. Unlike the other two known multisubunit activators, PA200 is a single polypeptide chain of molecular weight 200 kDa that appears to

be involved in DNA repair (Ustrell et al., 2002). Electron microscopy showed that forms an asymmetrical, hollow dome that binds to all but one alpha subunit (perhaps $\alpha 7$), and appears to similarly open the gate to enable substrate access to the lumen (Ortega et al., 2005).

20S-mediated degradation

In contrast to the canonical ubiquitin-proteasome system, there is considerable evidence for proteasome-dependent degradation that is ATP- and ubiquitin-independent. That is, the proteasome degrades substrates without the involvement of 19S or 11S activator complexes. Studies of the cellular distribution of the proteasome have shown that the 20S core particle is present within the cell independent of any activator complex (Brooks et al., 2000; Peters et al., 1994). 20S molecules have also been shown to localize to the endoplasmic reticulum, whereas 26S molecules are primarily cytosolic (Yang et al., 1995). The biological presence of free 20S particles suggests that the 20S proteasome may have activity independently of an activator complex.

Several proteins have been found to be substrates in this manner (Table 3-1). Additionally, a role for ATP- and ubiquitin-independent proteasomal turnover has been postulated in the degradation of nascent polypeptide chains that are prematurely released by the ribosome (Qian et al., 2006).

Table 3-1. Some substrates for 20S-dependent degradation.

Substrate	20S source	Reference
NF- κ B1 p105	human cultured cells, rabbit reticulocyte, and bovine liver	Moorthy et al., 2006
I κ B α	rat liver	Alvarez-Castelao and Castano, 2005
GAP-43	rabbit reticulocyte	Denny, 2004
apo-SOD1	rat liver	Di Noto et al., 2005
oxidized ferritin and lysozyme	Chinese hamster lung fibroblasts (CH E36)	Shringarpure et al., 2003
α -synuclein	bovine erythrocyte human	Liu et al., 2003 Tofaris et al., 2001
DHFR	human	Amici et al., 2004

There are several reasons that the cell may have evolved and/or preserved 20S-mediated degradation independent of activator complexes. Evolutionarily, the 20S proteasome is conserved from archaea through mammals, indicating that a 20S-only mechanism may be an evolutionarily old mechanism of cellular protein turnover. The cell may have evolved to adapt regulatory complexes to work in concert with the 20S, as the use of more complex targeting systems became advantageous. Even with the onset of degradation mediated by the regulatory complexes, the 20S-mediated degradation may still be a useful or even vital mechanism within the cell. In addition to a possible role in the turnover of aborted ribosomal products, the 20S proteasome has been demonstrated *in vivo* to be capable of degrading proteins that contain regions of disorder.

Endoproteolysis by the 20S proteasome

The mechanism by which the 20S proteasome degrades proteins is unknown, although it is clear that the process is independent of ATP or ubiquitin conjugation. In 2003, a postdoctoral researcher in the Thomas lab, Chang-wei Liu, demonstrated that the purified 20S proteasome was capable of internally cleaving disordered substrates (Liu et al., 2003). This observation suggested a novel mechanism for proteasomal degradation, in contrast to the commonly-accepted mechanism of processive degradation from a free terminus. To conclusively demonstrate endoproteolysis by the 20S proteasome, Liu employed two methods. First, he created expression constructs for p21 and α Syn in which the substrate sequence was flanked by the coding sequence for green fluorescence protein (GFP) (Figure 3-6, top panels). GFP forms an extraordinarily stable beta-barrel structure, which was hypothesized to not be a substrate for the 20S proteasome. Incubation with 20S proteasome resulted in a degradation of the substrate sequence, as detected by Western blot (Figure 3-6, middle panels). However, a simultaneous measurement of the GFP fluorescence signal showed no change, indicating that the GFP was not being degraded (Figure 3-6, bottom panels). A Western blot for GFP showed a change in molecular weight, consistent with degradation of the disordered substrate but not the bilateral GFP domains (Figure 3-6, graph insets). Processive degradation from either of the termini would have required that one of the two GFPs be degraded, resulting in a loss of fluorescence. Since that was not observed, the method of degradation must involve an endoproteolytic event. Endoproteolysis by 20S was then confirmed by creating circular p21 and α Syn using an intein system, which eliminated both the N- and C-termini (Liu et al., 2003).

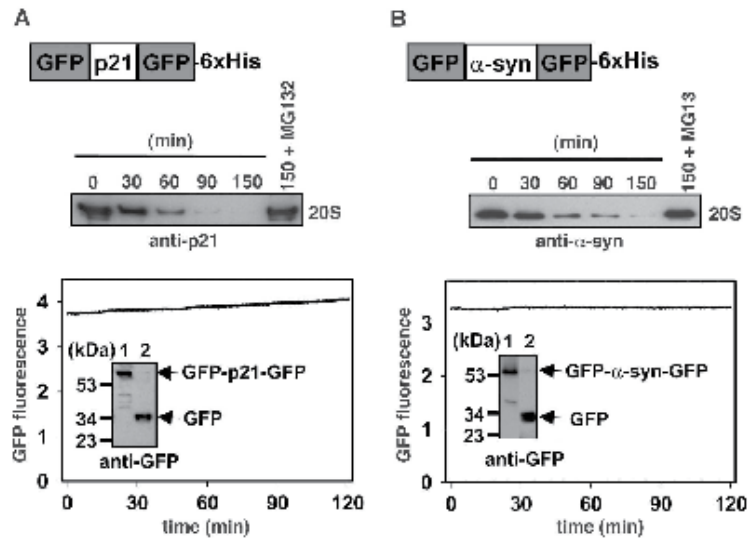


Figure 3-6. 20S degradation of bilaterally protected disordered proteins. Substrates were developed that had two GFP domains flanking either an internal p21 (A) or α Syn (B) domain (top panels). These substrates were analyzed for degradation by 20S by Western blot for the internal disordered substrate (middle panels). Coincident measurements of GFP stability using fluorescence showed that the GFP was not degraded by 20S (bottom panels). Pre- and post-degradation samples were Western blotted for GFP, and showed a shift in molecular weight of the substrates, which corresponded to the loss of the internal disordered substrate sequence while GFP remained intact (bottom panel, insets). From (Liu et al., 2003). Reprinted with permission from AAAS.

Intrinsically disordered proteins

The set of proteins that contain at least one region of structural disorder has gained recognition in recent years (Dunker et al., 2000; Radivojac et al., 2007; Uversky et al., 2000). The members of this set – variously described as intrinsically disordered, intrinsically unstructured, natively disordered, or natively unfolded – will be named here as intrinsically disordered proteins (IDPs). An IDP is as a protein (or protein region) that exists as a structural ensemble at either the secondary or tertiary structural level (Xie et al., 2007b). In more structural and biophysical terms, an intrinsically disordered polypeptide exists as a dynamic ensemble of conformations in which there are no equilibrium values for dihedral angles or backbone atom positions (Radivojac et al., 2007). This definition contrasts with a similar description of ordered protein structures, in which there are equilibrium values for both parameters. The equilibrium is reached between competing random thermal motion and local cooperative conformational changes, both of which are subject to the influence of packing interactions of nearby residues (Halle, 2002).

In 2001, Dunker and colleagues proposed that some functions of a protein may not require an ordered structure (Dunker et al., 2001; Dunker and Obradovic, 2001; Uversky, 2002). Instead, they argued that function can exist in a protein that adopts any one of three states (ordered, molten globule, or random coil) or a transition between any two of those states (Figure 3-7). A fourth state, pre-molten globule, has also been proposed (Uversky, 2002).

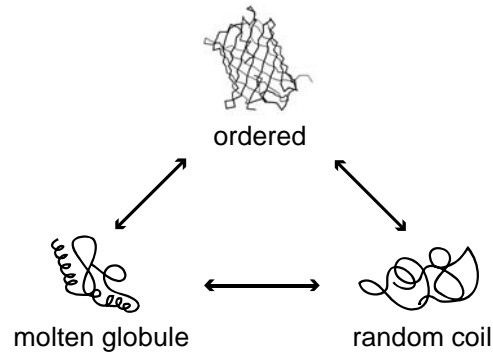


Figure 3-7. Three kinds of functional polypeptide conformations. A functional polypeptide sequence may have an ordered structure, a molten globule conformation(s) in which some elements of secondary and/or tertiary structure are retained, or a fully extended random coil conformation. Function may also exist within the transition between two of these states. Reprinted by permission from Macmillan Publishers Ltd: Nature Reviews Neuroscience, (Dunker and Obradovic, 2001), copyright 2001.

Two areas of research have provided support for this model of functional dynamic structure(s). First, computationally predicted disorder in genomes suggested that many, if not most, protein products contain some amount of intrinsic disorder (Dunker et al., 2001; Dunker et al., 2000). Multiple studies have justified that computational prediction by providing evidence for biological functions of disordered regions (Baker et al., 2007; Dunker et al., 2002; Uversky et al., 2000; Wright and Dyson, 1999), and whole-cell NMR studies have demonstrated that intrinsic disorder is present in proteins *in vivo* (Croke et al., 2008). Interestingly, IDPs have not been shown to have an appreciably higher rate of turnover *in vivo* (Tompa et al., 2008). This evidence that an intrinsically disordered region is not recognized as a misfolding event to be engaged by the protein quality control machinery suggested that intrinsic protein disorder has evolutionary – and therefore functional – significance.

A variety of experimental methods have been employed in the identification and analysis of IDPs, including NMR, near- and far-UV CD, fluorescence, and hydrogen-deuterium exchange (Bracken et al., 2004; Mittag and Forman-Kay, 2007; Radivojac et al., 2007). Experimentally characterized proteins that contain at least one region of disorder (>40 residues) are deposited in the DisProt database along with information about biological function (Sickmeier et al., 2007; Vucetic et al., 2005). Consistent with the growing literature and biological interest in IDPs, the DisProt database grew exponentially in the first three years of existence, from 190 regions in 2004 to 1114 regions in 2006. Currently, the database has 1195 disordered regions in 523 proteins (as of January 2009). An alternative operational definition of IDPs has been proposed, identifying an IDP as being susceptible to degradation by the 20S proteasome (Tsvetkov et al., 2008). However, an increased susceptibility to degradation is contrary to earlier findings that IDPs have similar halflives to proteins with well-ordered structure (Tompa et al., 2008). While this operational definition may have identified some IDPs *in vitro*, it does not identify all IDPs, nor can it explain the widespread physiological roles of IDPs *in vivo*.

Computational analysis has provided a more widespread analysis of disorder in genomes (Vucetic et al., 2007; Xie et al., 2007a; Xie et al., 2007b). A correlation analysis of SwissProt keywords and predicted disorder by VL3E predictor (Peng et al., 2005) revealed relationships between disorder and several key components of cellular biology, including signaling and cell regulation pathways and nucleic acid binding (Vucetic et al., 2007; Xie et al., 2007b). Consistent with those findings, correlations between predicted disorder and domains were identified, including SH3 protein-protein interaction domains, ligand-binding domains (*e.g.* DNA binding, RNA binding, and cyclic nucleotides), as well as relationships between disorder and post-translational

modifications that are often found within signaling and regulation pathways (*e.g.* phosphorylation, ubiquitin-like conjugation, and lipoproteins).

The diversity of functions ascribed to proteins with intrinsic disorder is a reflection of the functional flexibility afforded by such conformational flexibility. Recently, Radivojac and colleagues succinctly described several important capabilities that arise from intrinsic disorder in proteins:

1), decoupling of specificity and affinity due to the free energy penalty paid to fold the disordered state; 2), binding diversity in which one region folds differently to recognize differently shaped partners by different structural accommodations at the various binding interfaces; 3), binding commonality in which multiple, distinct sequences fold differently yet each recognize a common binding surface; 4), the formation of large interaction surfaces as the disordered region wraps-up or surrounds its partner; 5), faster rates of association by reducing dependence on orientation factors and by enlarging target sizes; and 6), faster rates of dissociation by unzipping mechanisms (Radivojac et al., 2007).

Therefore, intrinsic disorder is an essential biological feature of many proteins. Mechanisms of escaping the protein quality control machinery, for routine protein turnover, and for regulation of protein levels must therefore also be present for the proper function of these highly dynamic structures.

Role of intrinsically disordered proteins in neurodegeneration

IDPs have a close connection to several diseases, including cancer and neurodegeneration. The implication of IDPs in oncogenesis is due to the overwhelming presence of IDPs in cell regulation and signaling, as briefly described above (Xie et al., 2007b). The role of IDPs in neurodegeneration is primarily a gain-of-toxic function, as the proteins that form toxic conformations are all intrinsically disordered (*e.g.*, α Syn in Lewy body diseases, A β and tau in

Alzheimer's disease, and the prion protein in spongiform encephalopathies such as Creutzfeldt-Jakob).

Conformational states that are somewhat unfolded (*i.e.*, “pre-molten globule”) have been implicated as the species that precipitate the nucleation of toxic aggregates (Uversky and Fink, 2004). Because protein aggregation involves a significant structural rearrangement of the monomer (Fink, 1998), it is reasonable to expect that the intrinsic conformational flexibility of the monomer contributes to the propensity of a protein to aggregate. Supporting this hypothesis was a study in which a sequence that is conserved between three amyloidogenic proteins (α Syn, A β , and prion) was engineered into non-amyloidogenic proteins. When the sequence was inserted into IDPs, the resulting chimeras formed aggregates. Insertion of the same sequence into the well-folded proteins thioredoxin and protein G did not promote aggregation (Ji et al., 2005).

The proteasome and neurodegeneration

Because many neurodegenerative diseases are correlated with toxic gain-of-function conformational changes, the recognition and disposal of the misfolded forms may be important. As discussed above, the cell has many mechanisms by which damaged or toxic proteins can be disposed. However, the accumulation of misfolded proteins strongly implicates either a dysfunction in the protein metabolism machinery of the cell or that the machinery is overwhelmed by the amount of misfolded proteins to be processed.

In addition to this assessment of general cell biology, genetic studies have also pinpointed the ubiquitin-proteasome pathway of protein degradation as being involved in neurodegeneration. As discussed above, several components of the ubiquitin-ligase pathway have been identified in familial Parkinson's disease

(Table 2-2). Neurodegeneration has also been correlated with an increase in oxidative stress experienced by the affected neurons (Berlett and Stadtman, 1997; Smith et al., 2000). This has been attributed in part to an accumulation of oxidated proteins, which can be substrates for the 20S proteasome (Amici et al., 2004; Shringarpure et al., 2001; Shringarpure et al., 2003). Evidence that the activity of the proteasome decreases with age (Davies and Shringarpure, 2006) may account for the inability of the cell to properly turn over misfolded proteins by any pathway involving the proteasome. Such changes in proteasomal activity may be in part due to changes in the α subunit composition of the 20S proteasome, which was found to be reduced in the substantia nigra of PD patients (McNaught et al., 2002a).

To test the model of proteasomal dysfunction as an underlying cause of PD, several groups have treated animals with proteasomal inhibitors. An injection of the irreversible proteasomal inhibitor lactacystin into the substantia nigra of rats induced locomotor deficits reminiscent of PD patients, including bradykinesia and stooped posture (McNaught et al., 2002b). The brains of the treated animals also showed a loss of dopaminergic neurons, increased influx of glia into the substantia nigra, and accumulation of α Syn (McNaught et al., 2002b). Similarly, injection of the reversible proteasomal inhibitor MG-132 into the substantia nigra of mice resulted in a loss of dopaminergic neurons, although the effects of MG132 treatment on locomotion was not evaluated (Sun et al., 2006). Similarly, several studies have found that dysfunction of the ubiquitin-proteasome pathway increased the susceptibility of neurons to apoptosis (Sun et al., 2005; Sun et al., 2007). While these studies demonstrated that the loss of proteasomal function in the substantia nigra cause similar pathological changes as observed in PD, the results may not have been unexpected. The proteasome is a vital component of the cell, and so inhibition of the proteasome will result in eventual

cell death. Because the inhibitors were applied directly to the substantia nigra, the dopaminergic cells at the site of injection will be the cells most susceptible to the effects of proteasomal inhibition. A more convincing test of the hypothesis would be a systemic administration of proteasomal inhibitors. Such a study has been performed in rats (McNaught et al., 2004). Intraperitoneal injection of either the irreversible inhibitor epoxomicin or the reversible inhibitor PSI caused progressive locomotor deficits, nigral degeneration, and α Syn-positive inclusion body formation (Fitzgerald et al., 2008; McNaught et al., 2004). However, some attempts to replicate these results have been unsuccessful (Bove et al., 2006; Kordower et al., 2006). Furthermore, studies of chronic, chemically-induced animal models of PD that were treated with proteasomal inhibitors showed that proteasomal inhibition actually relieved some pathological symptoms of the animals (Inden et al., 2005). Together, these studies showed that the role of the proteasome in neurodegeneration is complex, and may have different roles in healthy animals compared to animals that are already showing pathology.

All of the aforementioned studies used pharmacological inhibition of the proteasomal active sites, which would block both 20S and 26S activities. However, since 20S exists in the cell independently of activator complexes, a dysfunction in the 26S-dependent UPS may not necessarily coincide with deficits in a 20S-dependent pathway. The contribution of deficits in the 26S-dependent pathway has been studied using a tissue-specific knockdown of a PA700 subunit in mice (Bedford et al., 2008). This knockout caused neuronal death and formation of inclusions that were positive for ubiquitin and α Syn, demonstrating that disruption of the 26S proteasome was sufficient for neurodegeneration (Bedford et al., 2008).

During pathogenesis *in vivo*, proteasomal activity may be inhibited by the cytotoxic forms of undegraded oligomers. Several groups have shown that aggregated forms of α Syn, particularly the oligomer/protofibril species, impair the activity of the 26S proteasome that is involved in the ubiquitin-proteasome pathway (Chen et al., 2005; Lindersson et al., 2004; Zhang et al., 2008). These discoveries led to a model in which the cytotoxicity of intracellular aggregates is at least partially due to the inhibition of the canonical 26S protein degradation pathway (Carrard et al., 2002; Liu et al., 2005). With the 26S pathway inhibited, some substrates may become more prone to interaction with the 20S proteasome, which could produce cleavage products via endoproteolysis that are more lethal than the full-length substrates (Liu et al., 2005). The work described in this dissertation was designed to test this hypothesis for neurodegeneration. First, the mechanism by which point mutations in α Syn associated with familial Parkinson's disease exert cytotoxicity were examined. The description of that work was followed by the development of antibodies to detect the aberrant cleavage products of degradation by the 20S proteasome *in vitro* and *in vivo*. Finally, the physiological role of 20S-mediated degradation was examined with respect to both potential substrates and the mechanism by which 20S is able to degrade proteins that contain regions of intrinsic disorder.

Chapter Four

Degradation of α -synuclein mutants by the 20S proteasome

Introduction

A hallmark of Parkinson disease is the formation of intracellular protein inclusions called Lewy bodies. α -Synuclein (α Syn) is the predominant protein in Lewy bodies, where it is in an amyloid conformation and is modified by phosphorylation, glycosylation, ubiquitinylation, and truncation. Previously, we demonstrated that the 20S proteasome cleaves α Syn *in vitro* to produce Lewy body-like truncations that accelerate the formation of amyloid fibrils from full-length α Syn. The three point mutations in α Syn that have been associated with early-onset familial PD, A30P, E46K, and A53T, have different effects on amyloidogenicity and vesicle-binding of α Syn. Here, we evaluate the effect of the mutations on the conformation and association reactions of α Syn in the presence of the 20S proteasome. When liposomes were also present, mutant α Syns were truncated more readily than wildtype. These truncations accelerated fibrillization of all α -synucleins, but there was no clear correlation between amyloid formation in the presence of liposomes and the PD-associated mutations. By contrast, formation of soluble oligomers was correlated with the mutations when both 20S proteasome and liposomes were present. Under these conditions, the wildtype protein also readily formed oligomeric structures, suggesting that 20S-mediated truncation of α Syn has a role in sporadic PD as well. Evaluation of the biochemical reactions of the PD-associated α -synuclein mutants in our *in vitro* system provides insight into the possible pathogenetic mechanism of both familial and sporadic PD.

α Syn forms amyloid fibrils in a nucleation-dependent manner, and differences in fibrillization profiles are observed among the familial mutations. A53T-syn both nucleates earlier and fibrillizes faster than wildtype α Syn (Choi et al., 2004; Conway et al., 1998; Conway et al., 2000b; Conway et al., 2000c; Greenbaum et al., 2005; Li et al., 2001; Li et al., 2002; Narhi et al., 1999). Data for A30P-syn are less conclusive. In general, A30P appears to form soluble higher molecular weight aggregates faster than wildtype α Syn (Conway et al., 1998; Li et al., 2002; Narhi et al., 1999), while the formation of amyloid structure is slower than wildtype (Choi et al., 2004; Conway et al., 2000c; Li et al., 2001). The relative timing of the A30P nucleation event varies, with some methods showing a longer lag phase than wildtype (Conway et al., 2000c; Li et al., 2001) and others showing a reduced lag phase (Li et al., 2001; Narhi et al., 1999). Studies of E46K-syn have shown that it nucleates and fibrillizes more rapidly than wildtype, similar to A53T-syn (Choi et al., 2004; Greenbaum et al., 2005).

Because α Syn appears to be associated with presynaptic membranes *in vivo* (Jensen et al., 1998), the lipid-binding characteristics of both wildtype and mutant α Syns have been studied. A30P-syn exhibits weaker binding to lipid vesicles both *in vivo* and *in vitro* (Choi et al., 2004; Cole et al., 2002; Jo et al., 2002; Nuscher et al., 2004). Data for A53T-syn have suggested both equal and lower affinity for binding lipid vesicles as wildtype α Syn (Choi et al., 2004; Cole et al., 2002). Moreover, A53T-syn has been suggested to interact with vesicles differently than the wildtype protein (Jo et al., 2004). Liposome pulldown assays suggest that E46K-syn may bind liposomes more strongly than wildtype (Choi et al., 2004).

In both patients and model systems, the levels of both soluble and insoluble α Syn levels increase with age as well as disease progression (Alvarez-

Garcia et al., 2006; Hishikawa et al., 2001; Kim et al., 2004; Klucken et al., 2006; Li et al., 2004; Liu et al., 2005; McFarlane et al., 2005), suggesting that the clearance of α Syn is compromised. However, the physiological clearance pathway(s) is controversial, since autophagy via the lysosome, the ubiquitin-proteasome system (UPS), and calcium-dependent proteases all degrade α Syn (Bennett et al., 1999; Cuervo et al., 2004; Iwata et al., 2003; Kim et al., 2003; Webb et al., 2003). The relevance of the UPS is highlighted by molecular genetics, implicating both a ubiquitin hydrolase and a putative ubiquitin ligase (UCH-L1/*park5* and parkin/*park2*, respectively) (Kitada et al., 1998; Liu et al., 2002b). As evidence continues to mount for multiple pathways (Ancolio et al., 2000; Li et al., 2004), a model has emerged in which the lysosome is responsible for the turnover of membrane-bound α Syn, the proteasome degrades unfolded and/or misfolded α Syn, and calpain acts on fibrillar protein. It remains unknown which of these systems, if any, act on the nucleating and/or toxic species.

Recently, N-terminal fragments of α Syn were identified in both PD patient brain samples and mouse models (Li et al., 2005; Liu et al., 2005). Fragments of α Syn similar to those observed in PD patients are produced by calpain I (Greenbaum et al., 2005; Mishizen-Eberz et al., 2003; Mishizen-Eberz et al., 2005) and by the 20S core particle of the proteasome (Liu et al., 2005). *In vitro*, these N-terminal fragments of α Syn form amyloid fibrils earlier and faster than wildtype and are able to seed the fibrillization of the full-length protein at sub-stoichiometric concentrations (Liu et al., 2005; Murray et al., 2003). The importance of the fragments to disease is further highlighted by the fact that transgenic mice expressing N-terminal fragments of human α Syn display the characteristics of PD, including selective loss of substantia nigral neurons and progressive behavioral deficits (Tofaris et al., 2006; Wakamatsu et al., 2006).

These data led to a model in which N-terminal fragments of α Syn contribute to early steps in PD pathology. The protease responsible for cleavage remains elusive, although several enzymes have been proposed to cleave α Syn *in vivo*. Previous work from our lab showed that the 20S proteasome endoproteolytically cleaves α Syn *in vitro* to form truncations that are similar to those observed in tissue (Liu et al., 2003). It is well-established that the 20S proteasome is capable of degrading proteins in a ubiquitin- and ATP-independent manner. In addition to α Syn (Bennett et al., 1999; Liu et al., 2003; Liu et al., 2005; Tofaris et al., 2001), identified substrates for this activity include DHFR (Amici et al., 2004), I κ B α (Alvarez-Castelao and Castano, 2005), GAP-43 (Denny, 2004), SOD1 (Di Noto et al., 2005), tau (David et al., 2002), moderately oxidized proteins (Shringarpure et al., 2001; Shringarpure et al., 2003) and reviewed in (Davies and Shringarpure, 2006)), p21^{WAF1/CIP1} (Liu et al., 2003; Touitou et al., 2001), and the Epstein-Barr viral proteins EBNA1-3 (Touitou et al., 2005). Previous studies have suggested that 20S particles outnumber both 26S and free regulatory particles *in vivo*, suggesting an independent role for 20S (Brooks et al., 2000; Tanahashi et al., 2000). This hypothesis has been further supported by recent work implicating the 20S in the turnover of nascent polypeptides (Qian et al., 2006).

We set out to test the hypothesis that the action of the 20S proteasome on α Syn produces N-terminal fragments that enhance the formation of the presumptive toxic species. To do this, we evaluated all known reactions of α Syn as well as the three familial PD mutations in the presence of the 20S proteasome. Individual assessments of α Syn amyloidogenicity and lipid vesicle binding have not provided a cohesive model for the role of α Syn in PD pathogenesis. Inside the cell, monomeric α Syn is able to undergo several reactions, including the self-association that is correlated with disease (Figure 4-1). Additionally, α Syn is also

available for degradation and cleavage, which could affect both amyloid formation and vesicle binding (Figure 4-1). In this study, we have evaluated the effect of proteasomal cleavage of α Syn proteins in a system that includes synthetic liposomes. Within this *in vitro* system, we find that the reactions of α Syn degradation, self-association, and liposome binding compete with one another, but that the presence of liposomes and 20S favors the formation of the oligomeric conformation that is thought to be cytotoxic. This system therefore provides a more thorough picture of the association between α Syn familial PD point mutations and aberrant metabolism of the protein.

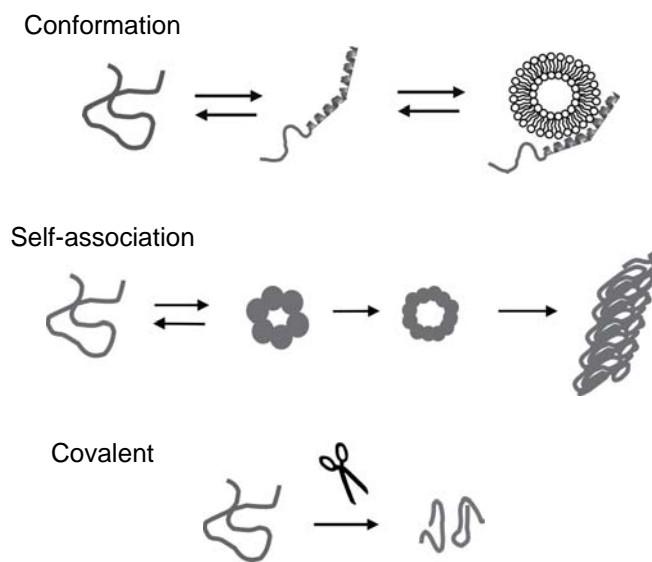


Figure 4-1. Potential reactions of α Syn. α Syn undergoes several reactions coupled to changes in its structure. (*top panel*) It forms random-coil structure in aqueous solution, but adopts α -helical structure in the presence of liposomes, lipid vesicles, or negatively-charged detergents. (*middle panel*) α Syn also self-associates to form oligomers with significant α -helical content, annular protofibrils with less α -helix and more β -strand character, and β -sheet-rich amyloid fibrils (Apetri et al., 2006). (*bottom panel*) Several covalent modifications of α Syn have also been observed, including irreversible modifications such as C-terminal truncation. Both conformational and covalent modifications affect the self-association that is associated with disease.

Results

Effects of α Syn mutations on α Syn structure

In vivo, α Syn is associated with synaptic membranes (Jensen et al., 1998; Kahle et al., 2000), and such association with lipid membranes favors a secondary structure (Bussell et al., 2005; Cole et al., 2002; Davidson et al., 1998; Eliezer et al., 2001; Jao et al., 2004) that resists degradation by the 20S proteasome *in vitro* (Bussell et al., 2005; Cole et al., 2002; Davidson et al., 1998; Eliezer et al., 2001; Jao et al., 2004; Liu et al., 2005). The three familial PD mutations have been reported to modulate the affinity of α Syn for lipid membranes. Wildtype and the mutant α Syn proteins A30P-syn, E46K-syn, and A53T-syn were recombinantly expressed in and purified from *E. coli* (Appendix A). Circular dichroism spectra were acquired on all four proteins in phosphate buffer (Appendix A), and show a random-coil structure (Figure 4-2). However, in the presence of increasing amounts of liposomes composed of a 1:1 mixture of 1-palmitoyl-2-oleoyl-*sn*-glycero-3-phosphocholine (POPC) and 1-palmitoyl-2-oleoyl-*sn*-glycero-3-phosphate (monosodium salt) (POPA) (Appendix A), all four proteins acquire α -helical structure as measured by mean residue ellipticity at 222 nm. While the helical content of all four proteins is similar at low concentrations of lipids, the helical content of A30P-syn diverges as the ratio of lipids: α Syn increases.

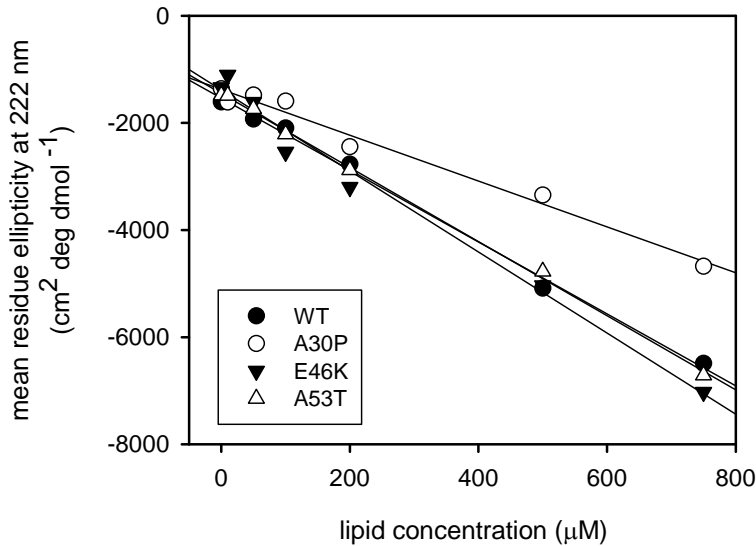


Figure 4-2. Helix formation of α Syn proteins when bound to liposomes. α Syn proteins were incubated with increasing amounts of POPA/POPC lipid vesicles prior to the acquisition of far-UV CD spectra. Shown are the averages of two independent experiments, with each sample performed in duplicate. The error bars are smaller than the size of the symbol, and indicate the standard deviation between the four experiments.

The divergence of A30P-syn helicity is not caused by a disruption of the helix by the proline mutation. 2,2,2-trifluoroethanol (TFE) was titrated into a sample of A30P-syn to induce helix formation (Appendix A). TFE produces the same amount of helix in A30P-syn as in wildtype α Syn (Figure 4-3). Therefore, the lower helical content of A30P-syn in the presence of liposomes suggests that the protein binds with lower affinity, consistent with previous studies (Choi et al., 2004; Cole et al., 2002; Nuscher et al., 2004). In contrast, in comparison to wildtype, no significant effect of A53T or E46K on liposome binding was detected by these methods (Figure 4-2).

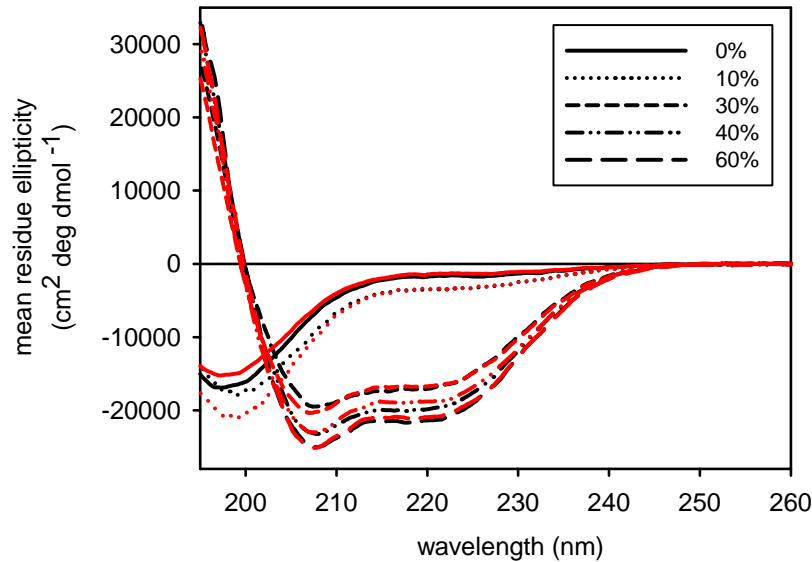


Figure 4-3. Helix formation by α Syn-A30P induced by TFE. Wildtype α Syn (black) and A30P-syn (red) were incubated with increasing amounts of 2,2,2-trifluoroethanol (TFE) prior to the acquisition of far-UV CD spectra.

Effects of the 20S proteasome on the turnover of α Syn mutants

In vitro degradation of full-length α Syn by the 20S proteasome in the absence of liposomes produces several N-terminal fragments, which previously were identified via epitope mapping and electrospray mass spectrometric analysis as polypeptides encompassing residues 1-119, 1-110, and 1-83 (Liu et al., 2005); a number of smaller fragments were also observed (data not shown). Proteasomal degradation assays were carried out on the wildtype and mutant α Syn proteins *in vitro* (Appendix A). In aqueous solution, the disease-associated mutations affect the rate of both full-length α Syn degradation and fragment production (Figure 4-4). At a ratio of 200:1 (α Syn:20S), three prominent N-terminal fragments are produced: 1-110, 1-83, and 1-73. Under these conditions, there is no measurable difference in the rate of degradation of full-length wildtype, A53T-syn, and

A30P-syn. By contrast, full-length E46K-syn is turned over more rapidly and produces a different band pattern. Wildtype α Syn primarily produces fragments consisting of residues 1-110 and 1-83 (Liu et al., 2005). A30P-syn and A53T-syn produce a fragment pattern similar to wildtype, although the A53T-syn fragments represent a smaller fraction of the total population, consistent with the slower degradation of the full-length protein. Degradation of E46K-syn readily produces a different pattern, with the 1-73 fragment appearing early in the timecourse, and all three fragments clearly observed at 10 min. Consistent with previously published work evaluating calpain-mediated degradation of α Syn (Greenbaum et al., 2005), the smallest E46K-syn fragment migrates faster on the gel than the comparable wildtype fragment. Mass spectrometric analysis showed that the two smallest fragments produced from wildtype and E46K-syn are the same fragment, 1-73 (data not shown).

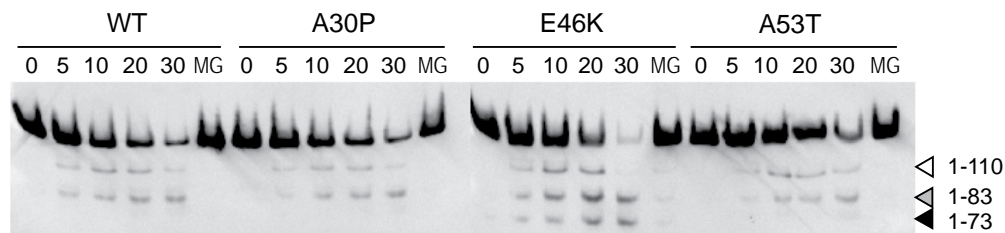


Figure 4-4. 20S proteasomal degradation of α Syn mutants associated with PD. α Syn protein (3 μ M) was incubated with purified latent 20S proteasome (15 nM) for the times (minutes) indicated. MG indicates reactions that were performed with 20S proteasome that had been preincubated with 100 μ M MG132. Specific C-terminal truncations are produced in a time-dependent manner and were identified by mass spectrometry (1-110, white triangle; 1-83, gray triangle; and 1-73, black triangle).

Since our data and those of others suggest that the mutations can alter the affinity of α Syn for vesicles and vesicle-bound α Syn is resistant to 20S degradation (Liu et al., 2005), we predicted that the mutations should also

modulate the ability of 20S to degrade each mutant protein in the presence of liposomes. Control experiments with fluorogenic peptides showed that the activity of 20S is not affected by liposomes (data not shown). At 25 and 50 μM lipids, the conformations of all four proteins are statistically indistinguishable by CD (Figure 4-2). However, at the lower concentration of lipids, all three PD-associated mutants retain the ability to produce fragments while wildtype αSyn does not (Figure 4-5). The most prominent and long-lived fragment at both lipid concentrations, regardless of mutation, is syn(1-83). At 25 μM lipids, A30P-syn, E46K-syn, and A53T-syn, but not wildtype, generate considerable amounts of this 20S-resistant truncation. The presence of 50 μM lipids reduces fragment production by A53T-syn, but the production of syn(1-83) from both A30P-syn and E46K-syn is still robust. Thus, increased amounts of the fragments, similar to those associated with the disease, are observed for all three PD-associated mutations in the presence of liposomes and the 20S proteasome.

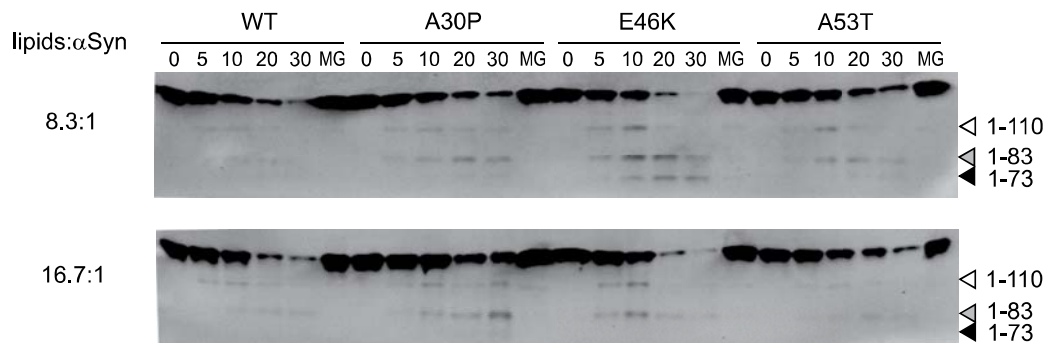


Figure 4-5. Degradation of wildtype and mutant αSyn by the 20S proteasome in the presence of liposomes. 20S-mediated degradation of αSyn proteins was carried out in the presence of either 25 μM or 50 μM liposomes. As before, “MG” samples contained proteasome that had been preincubated with 100 μM MG132, and specific C-terminal truncations are marked with triangles (1-110, white; 1-83, gray; 1-73, black).

Effect of mutations, lipid vesicles, and 20S-mediated degradation on amyloidogenesis

We have shown that the production of amyloidogenic fragments of α Syn proteins by the 20S proteasome is modulated by the presence of liposomes. To understand how those changes in fragment production affect amyloid formation, the fibrillization of α Syn into amyloid in the presence of liposomes and 20S proteasome was monitored by Thioflavin T fluorescence (Appendix A). As previously described by others, the lag time of the A30P mutant prior to nucleation is slightly longer than that of wildtype α Syn, and both E46K-syn and A53T-syn forms amyloid fibrils earlier and at a faster rate than wildtype (Figure 4-6, solid lines) (Choi et al., 2004; Conway et al., 1998; Conway et al., 2000b; Conway et al., 2000c; Greenbaum et al., 2005; Li et al., 2001; Li et al., 2002; Narhi et al., 1999). Liposomes reduce the fibrillization of E46K-syn and A53T-syn, but do not appear to affect A30P-syn at a ratio of 2.5:1 lipids: α Syn (Figure 4-7, solid lines). These results suggest that binding to liposomes can counteract the accelerating affect of the E46K and A53T mutations on amyloid formation.

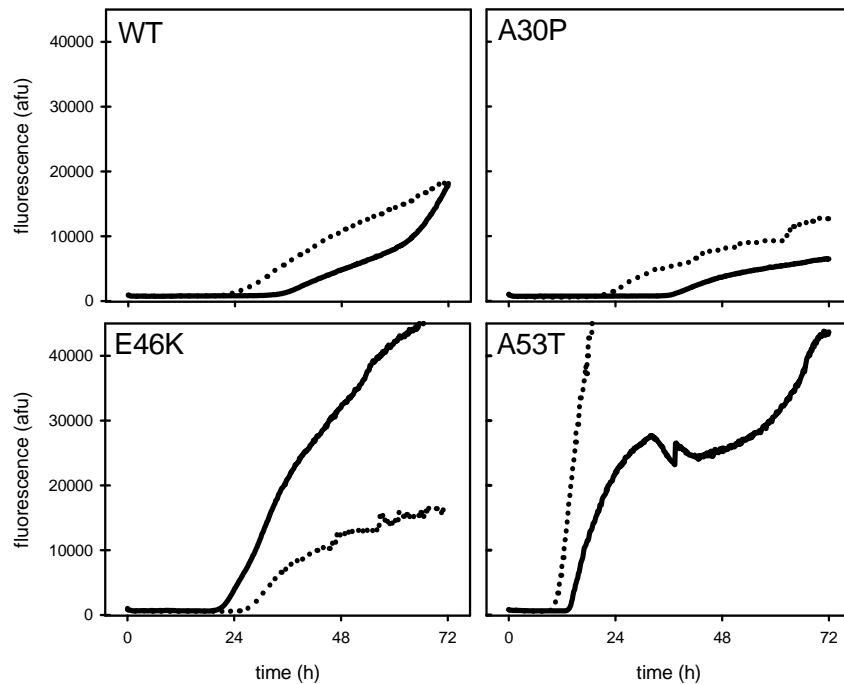


Figure 4-6. Amyloid fibril formation of α Syn proteins. Samples of wildtype and the three mutant proteins were prepared with either protein alone (solid lines) or preincubated with purified 20S proteasome for 10 min followed by the addition of 100 μ M MG132 (dotted lines). Amyloid fibril formation was then monitored by the development of fluorescence of the amyloid-binding fluorophore Thioflavin T. Shown are representative traces.

Previously, we established that the post-acidic activity of the 20S proteasome is responsible for the cleavage of wildtype α Syn into amyloidogenic fragments that accelerated amyloid formation of the full-length protein (Liu et al., 2005). In this study, 20S proteasome was added to amyloid formation reactions to create sub-stoichiometric amounts of amyloidogenic fragments. As previously observed for wildtype α Syn, the fragments were expected to accelerate amyloid formation of the full-length mutant proteins. The 20S proteasome was incubated in the reaction mixture with α Syn for ten minutes, followed by inactivation with the broad-spectrum proteasomal inhibitor MG132 to stop additional

endoproteolysis and degradation (Appendix A). The 20S proteasome created a small amount of synuclein fragments, which represented less than 1% of the total synuclein in the reaction (Figure 4-8). In all three reactions that contained mutant α Syn proteins and fragments produced by 20S, the time to nucleation was shorter than for the full-length protein alone (Figure 4-6, Figure 4-9). This confirms that the fragments observed from proteasomal cleavage of the mutant α Syn proteins are also amyloidogenic.

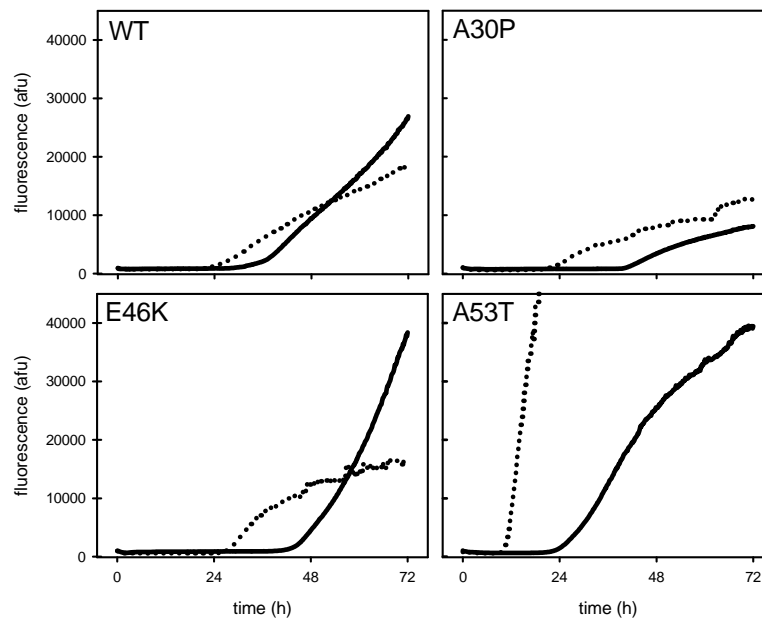


Figure 4-7. Amyloid fibril formation of α Syn proteins in the presence of liposomes. Samples of wildtype and the three mutant proteins were prepared with protein and 250 μ M liposomes (solid lines) or protein and liposomes that were preincubated with purified 20S proteasome for 10 min, followed by the addition of 100 μ M MG132 (dotted lines). Amyloid fibril formation was then monitored by the development of fluorescence of the amyloid-binding fluorophore Thioflavin T. Shown are representative traces.

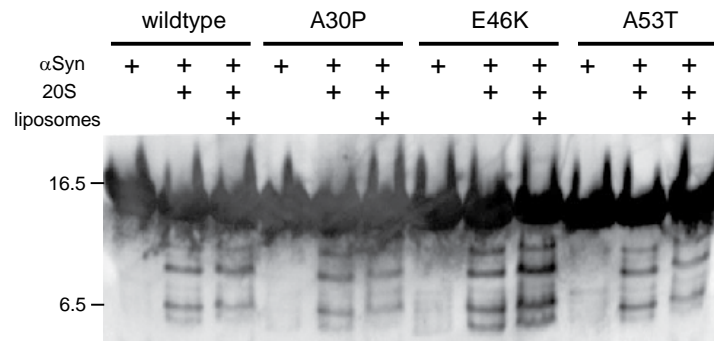


Figure 4-8. Truncations produced by the 20S proteasome under conditions of the fibrillization assay. 10 μ L of each fibrillization reaction at the beginning of the assay was immediately separated by gel electrophoresis and subjected to Western blotting with the monoclonal antibody Syn303.

The α Syn reactions of lipid-binding and proteasomal degradation are likely coupled in the cell, as binding to membranes induces structural changes in α Syn that subsequently prevent 20S degradation. Therefore, we evaluated the effects of the mutations on fibrillization under conditions where both lipid binding and 20S degradation can occur. The fibrillization of A30P-syn and E46K-syn do not differ significantly from wildtype α Syn (Figure 4-7). However, A53T-syn forms amyloid more rapidly than wildtype α Syn under these conditions. While the presence of liposomes and 20S in the *in vitro* system revealed a distinct difference between the A53T mutant and the other two PD-associated mutants, the system did not show a clear correlation between amyloid formation and PD-associated mutations under any of these experimental conditions.

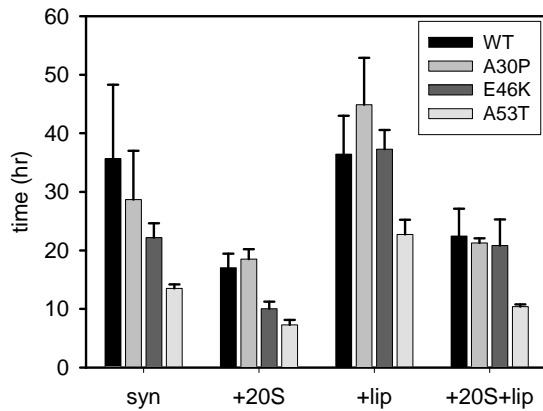


Figure 4-9. Average lag times to fibril nucleation of α Syn proteins. Error bars indicate standard error of the mean. Abscissa labels: syn, protein alone; +20S, protein and preincubation with 20S; +lip, protein and liposomes; +20S+lip, protein with both liposomes and preincubation with 20S.

Evaluation of oligomer formation in the in vitro system

In the absence of a correlation between PD-associated mutations and amyloid formation in the *in vitro* system, an analysis of pre-amyloid oligomeric species was performed (Appendix A). The “oligomer” was defined as a species that was immunoreactive with the anti-oligomer antibody I-11 (Kayed et al., 2007; Kayed et al., 2003), and is presumably closely related to the toxic species. To evaluate oligomer formation, we initiated reactions as in the fibrillization assay, but removed aliquots for a dot-blot assay using the polyclonal anti-oligomer antibody I-11 (Figure 4-10). In samples containing only α Syn, oligomers were only observed for E46K-syn and A53T-syn, and they appeared by 21 hours and 27 hours, respectively. Remarkably, in the presence of liposomes and 20S, oligomers were also seen for wildtype and A30P-syn, and the formation of oligomers in the E46K-syn and A53T-syn reactions was accelerated.

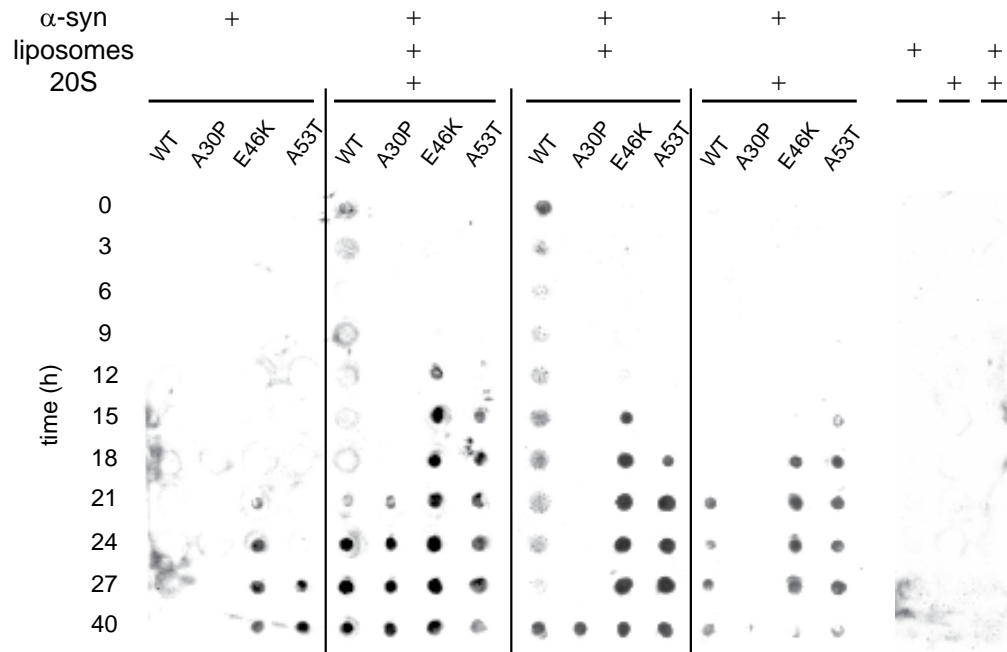


Figure 4-10. Oligomer formation of mutant α Syn proteins. α Syn proteins, 20S proteasome, and liposomes were incubated in combination as shown (*top*) and as described in Figure 5-6. Aliquots were removed at the indicated times (*left*), and subjected to dot-blotting with the I-11 anti-oligomer antibody. Shown is a representative example of three separate experiments.

(following page) **Figure 4-11. Quantitation of oligomer formation of mutant α Syn proteins.** Data from three separate and independent oligomerization assays were quantitated by densitometry. The data were normalized to the minimum and maximum signal within each experiment, and then averaged. Shown in gray bars is the mean of three replicates, and the error bars indicate the standard deviation.

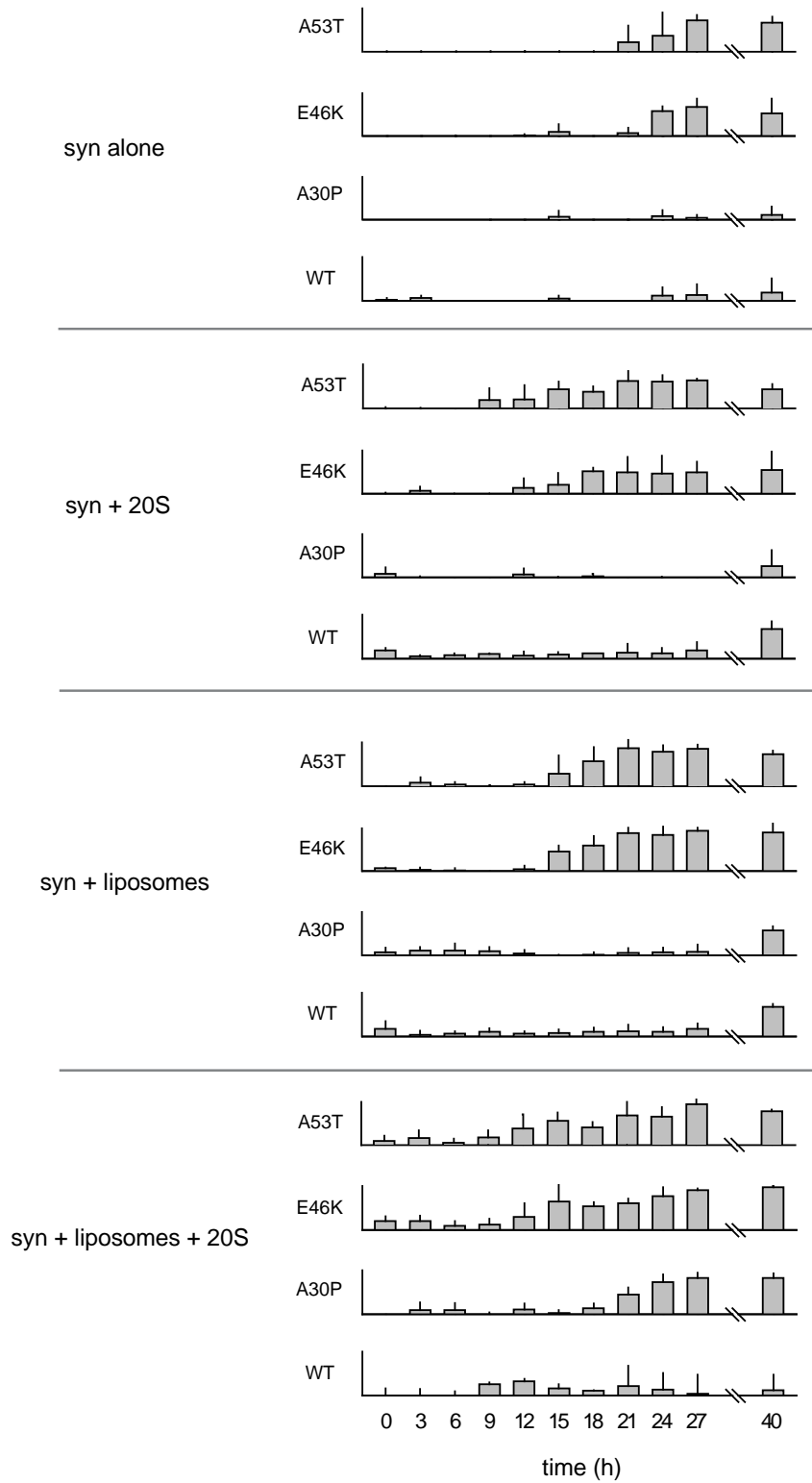


Figure 4-11. Quantitation of oligomer formation of mutant α Syn proteins.

A diffuse background signal is present at all timepoints in the samples that contain wildtype α Syn and liposomes. At later timepoints, a denser signal appears in these samples that indicated specific immunoreactivity. Interestingly, a similar diffuse background signal develops over time in all spots that contained samples with liposomes. The membrane shown in Figure 4-10 was rinsed in TBS-T and stored at 4°C. Six days later, that membrane was reprobbed with the same dilution of I-11 (Figure 4-12). In all samples that contain liposomes, a diffuse signal is detectable, and which is distinct from the darker and smaller spots contained in the non-liposome samples. The reason for this immunoreactivity is unknown, as no studies to date have shown I-11 reactivity with lipids.

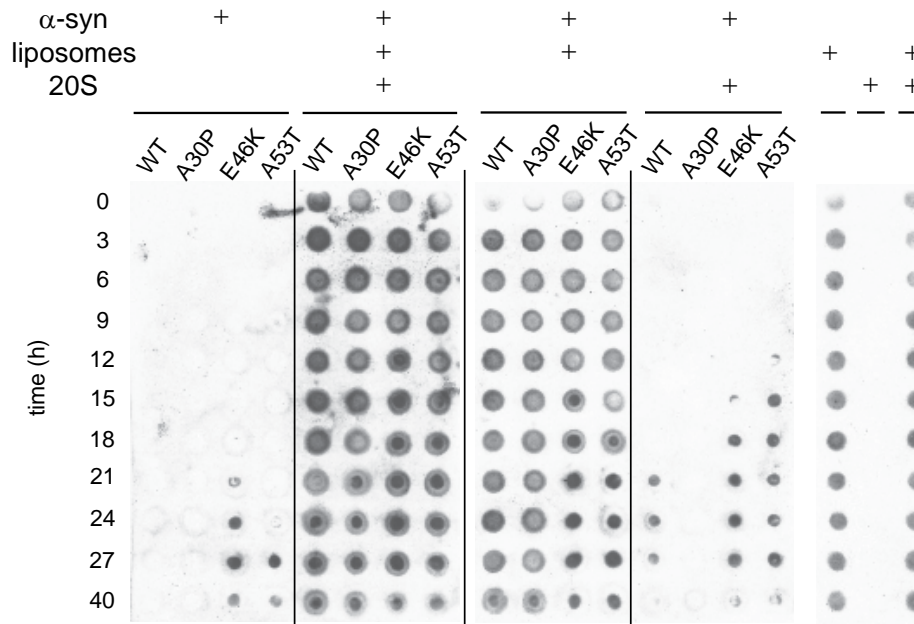


Figure 4-12. Time-dependent appearance of immunoreactive species in liposome samples. The same membranes from Figure 4-10 were stored at 4°C for six days, then reprobbed with I-11. Note the diffuse background present in all samples that contained liposomes, including the controls. The signals present in Figure 4-10 are still detectable as dense, small spots within the diffuse background spots.

To verify the oligomerization assay as a measure of a pre-amyloid conformation, the truncated α Syn proteins identified as highly amyloidogenic were analyzed by the oligomerization assay. We previously demonstrated that truncated α Syn proteins α Syn119 and α Syn110 are more amyloidogenic than wildtype. In oligomerization reactions with truncated α Syn proteins (Appendix A), we also observe a decrease in the lag time to oligomer formation (Figure 4-13). Furthermore, α Syn110 forms oligomers earlier than α Syn119, which is consistent with its increased amyloidogenicity relative to α Syn119. Wildtype α Syn did not form oligomer over the 12-hour timecourse of the experiment, which is consistent with results obtained in earlier experiments.

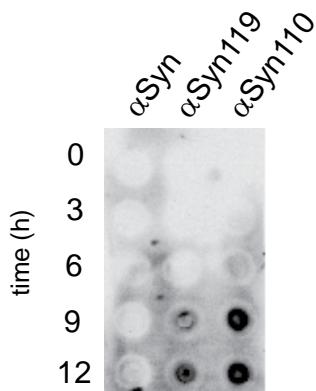


Figure 4-13. Oligomerization of truncated α Syn proteins. 100 μ M of either α Syn, α Syn119, or α Syn110 were incubated with 20 mM of ThioflavinT in 20 mM phosphate buffer with shaking at 37°C. Aliquots were removed at 0, 3, 6, 9, and 12 hours for dot blot analysis using the I-11 anti-oligomer antibody.

In additional control reactions, the A30P-syn protein never produced oligomers when incubated with 20S only, and the reaction with A30P-syn and liposomes only produced oligomers at 40 hours (Figures 4-10, 4-11). Wildtype α Syn produced small amounts of oligomers following incubation with 20S proteasome, and no oligomers were observed with liposomes alone. These results demonstrate that oligomer formation is promoted by the fragments produced by the 20S proteasome. Furthermore, the presence of both liposomes and 20S-produced fragments dramatically accelerates the formation of oligomers for all four α Syn proteins, including the wildtype.

Discussion

As observed in our previous studies, α Syn is degraded by the 20S proteasome *in vitro*, and C-terminal truncations of α Syn produced by 20S accelerate amyloid fibril formation (Liu et al., 2003; Liu et al., 2005). These observations led to a model of sporadic PD pathogenesis in which a misprocessing of α Syn by the 20S proteasome accelerates the formation of a cytotoxic conformer (Figure 4-14). In this study, the biochemical effects of the three point mutations in α Syn associated with early-onset familial PD have been evaluated in an *in vitro* system composed of α Syn, the 20S proteasome, and synthetic liposomes to mimic the lipid vesicles with which α Syn associates *in vivo*.

The individual reactions composing the *in vitro* system were first evaluated independently. The effects of the mutations on liposome binding were evaluated by CD (Figure 4-14, K_{binding}), which showed that A30P-syn has a lower affinity for liposomes than the other three α Syn proteins. This reduced K_{binding} for A30P-syn could have consequences for 20S degradation, as we have shown previously that α Syn associated with liposomes is a poor substrate for the 20S proteasome (Liu et al., 2005). Therefore, the affinity of α Syn for the lipid surface should also affect the rate of degradation; a variant that binds liposomes more tightly would have a slower rate of degradation, because fewer molecules would be unbound and therefore be a disordered substrate for the 20S. Next, the effects of the point mutations on 20S proteolysis of α Syn were assessed by an *in vitro* degradation assay (Figure 4-14, k_{endo} and k_{deg}). Liposomes were then added to the reaction to evaluate the effect of mutations when the reactions of liposome binding and 20S proteolysis are in direct competition (Figure 4-14, $K_{\text{binding}}+k_{\text{endo}},k_{\text{deg}}$).

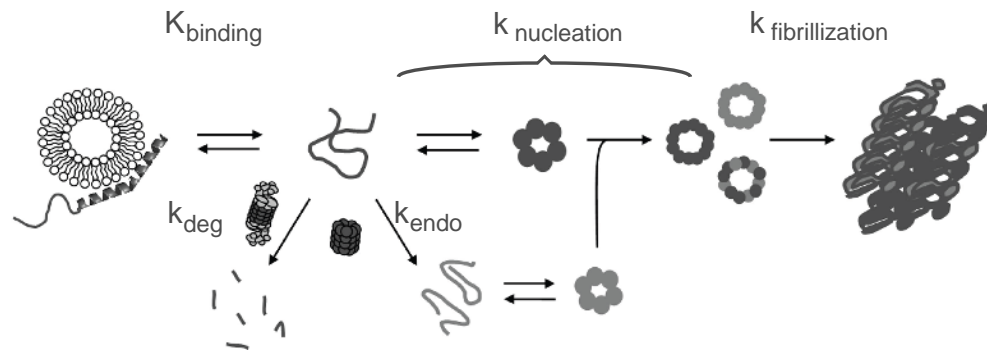


Figure 4-14. A dynamic model of Parkinson disease pathogenesis. The point mutations in α Syn that are associated with early-onset Parkinson disease have variable effects on the measurable biochemical reactions of the protein. These reactions exist within the cell as an interconnected pathway, which has been partly recreated here. In that regard, the *in vitro* system of this study evaluated the effects of the disease-associated mutations on each of these reactions independently and in combination. Correlation with the disease mutations was found in two of the reactions: 20S cleavage in the presence of liposomes (k_{endo}) and oligomer formation in the presence of liposomes and 20S ($K_{\text{binding}}+k_{\text{endo}}+k_{\text{nucleation}}$).

The α -helical content of the four proteins by CD appears to be the same at lipid:protein ratios lower than 20:1 (Figure 4-2). However, under similar conditions, the three mutant α Syn proteins behave differently when subjected to degradation by 20S proteasome (Figure 4-5). Consistent with the hypothesis that fragments produced by 20S are relevant to disease, all the three mutant α Syns produce fragments under conditions where the wildtype α Syn does not (lipid:syn ratio of 8.3:1). This distinction between the mutants and the wildtype is abolished at a slightly higher ratio of lipid:syn, 16.7:1. These data likely reflect the dynamics of the interaction, in which small amounts of unbound α Syn are available for degradation, but do not measurably influence the population measurement of structure by CD. Notably, all three mutants produce considerable amounts of N-terminal fragments in the presence of low concentrations of lipids,

whereas wildtype does not. The overall rate of endoproteolysis slows upon addition of more liposomes, although the most prominent fragments (1-110 and 1-83) continue to be observed. These data suggest that the mutants are more susceptible to proteolysis by the 20S proteasome in the presence of liposomes than the wildtype protein. Therefore, we now have a biochemical correlation of these point mutations and their association with familial early-onset disease.

The most frequently studied biochemical characteristic of α Syn is its propensity to fibrillize into amyloid in a nucleation-dependent manner (Figure 4-14, $k_{\text{nucleation}}+k_{\text{fibrillization}}$). As shown in Figure 5-6, this property is affected independently by liposomes ($K_{\text{binding}}+k_{\text{nucleation}}+k_{\text{fibrillization}}$) and by fragments produced by 20S ($K_{\text{endo}}+k_{\text{nucleation}}+k_{\text{fibrillization}}$), but neither reaction alone reveals a correlation to the presence of disease-associated mutation. Liposomes decrease the apparent $k_{\text{nucleation}}$ of fibrils of E46K- and A53T-syn, but do not affect $k_{\text{nucleation}}$ of the A30P mutant. There is a slight increase in $k_{\text{fibrillization}}$ of wildtype α Syn, which may be due to a local concentration effect on vesicle surfaces (Lee et al., 2002; Necula et al., 2003). As expected, the presence of 20S-produced fragments increases $k_{\text{nucleation}}$ and $k_{\text{fibrillization}}$ for all four proteins (Figure 4-14). This indicates that the fragments produced by the 20S proteasome from the mutant proteins are amyloidogenic, as observed for the wildtype α Syn, and that the three mutant α Syn proteins are likewise susceptible to seeding by those amyloidogenic fragments.

By measuring fibrillization in the presence of both liposomes and 20S proteasome, we evaluated the end result of multiple competing reactions: K_{binding} , k_{endo} , $k_{\text{nucleation}}$, and $k_{\text{fibrillization}}$. Each of these reactions is affected by the PD-associated mutations in different ways when evaluated independently. In the *in vitro* degradation assay with liposomes and 20S (Figure 4-5), the data demonstrate a correlation between mutation and disease in the distinct k_{endo} differences

observed between the wildtype α Syn and the mutant α Syn proteins. It can be hypothesized that this correlation would also be present in fibrillization, as the presence of amyloidogenic fragments dramatically affects $k_{\text{nucleation}}$ and $k_{\text{fibrillization}}$. However, such a correlation was not observed. A30P-syn forms amyloid at least as slowly as wildtype (Figure 4-6 and (Conway et al., 2000c)), while E46K-syn and A53T-syn are significantly more amyloidogenic than wildtype. However, in the presence of liposomes and 20S-produced fragments, only A53T-syn is highly amyloidogenic compared to wildtype protein. The A30P- and E46K-syn proteins have $k_{\text{nucleation}}$ and $k_{\text{fibrillization}}$ similar to wildtype α Syn. This suggests that the competing reactions of liposome binding, 20S endoproteolysis, and fibrillization oppose each other for the A30P and E46K point mutants.

However, all three mutations have been associated with early-onset familial disease (Kruger et al., 1998; Polymeropoulos et al., 1997; Zarranz et al., 2004). By evaluating amyloid formation, we simultaneously evaluated nucleation and amyloid fibril formation. Recent work by others has strongly implicated a pre-amyloid conformation, termed “oligomer” or “protofibril”, as being responsible for cytotoxicity. To that end, the acceleration of oligomerization, rather than amyloid formation, has been suggested as the common link between the mutants (Conway et al., 2000b; Conway et al., 2000c). If an element upstream of amyloid formation plays a role in pathogenesis, the effect of the disease-associated mutations may be absent in amyloid formation. This hypothesis was consistent with the lack of correlation between mutation and the amyloid formation data obtained from our *in vitro* system. Therefore, a direct evaluation of the oligomer species was performed. To evaluate oligomer formation in the presence of 20S-produced fragments and liposome binding, fibrillization reactions were initiated and aliquots were removed over 40 hours. The aliquots were then assayed for oligomer content in a dot-blot using the anti-

oligomer antibody I-11. When the reaction contained just α Syn protein, oligomers were observed only for E46K-syn and A53T-syn. Significantly, the addition of 20S to produce fragments promoted oligomer formation in wildtype α Syn, as well as accelerating $k_{\text{nucleation}}$ of E46K-syn and A53T-syn. When both liposomes and proteasomes were added, oligomers were present in all four protein samples. Oligomers were observed as early as 12 hours for E46K-syn and A53T-syn, with wildtype α Syn and A30P-syn producing oligomers by 21 hours. This shows that the presence of liposomes and 20S proteasome-produced fragments results in a more rapid production of the putative cytotoxic species. The increase in $k_{\text{nucleation}}$ is most notable with E46K-syn and A53T-syn. However, it is noteworthy that proteasome-produced fragments and liposomes also induce formation of oligomers in wildtype α Syn.

The *in vitro* system containing liposomes revealed multiple differences between the wildtype α Syn and the three PD-associated mutations when evaluated for C-terminal truncation by 20S proteasome and for pre-amyloid oligomer formation. These differences were not observed when the system was assessed only for amyloid formation. Interestingly, the formation of oligomers by the wildtype α Syn shows that the putative toxic species can be formed without a genetic manipulation, providing support for the hypothesis that cleavage of wildtype α Syn may have a role in the pathology of idiopathic PD, as well. By adding the 20S proteasome and liposomes to α Syn self-association reactions, it was possible to evaluate the combined effect of disease-associated mutations on the multiple reactions that are interconnected in a dynamic pathway, as well as assess the combined effect of those multiple reactions on the formation of the putative toxic species. Furthermore, the presence of 20S proteasome-produced truncations accelerates the onset of oligomers in all conditions. Pre-amyloid oligomers have been proposed to be the cytotoxic species in neurodegenerative

diseases, including Parkinson's. Therefore, these data underscore the importance of evaluating the role of α Syn and mutations associated with early-onset disease within the context of a dynamic model of α Syn metabolism (Figure 4-14), and provide support for the contribution of C-terminal cleavage of α Syn by the 20S proteasome to PD pathogenesis.

Chapter Five

Immunodetection of α -synuclein Truncations

Introduction

The deposition of aggregated α Syn is the pathologic hallmark of Lewy body diseases. A fraction of that aggregated α Syn in human brain tissue has been found to be C-terminally truncated, a modification which has been shown *in vitro* to accelerate oligomer and amyloid formation (Hoyer et al., 2004; Li et al., 2005; Liu et al., 2005). Furthermore, substoichiometric amounts of truncated forms can seed the aggregation of the full-length protein (Liu et al., 2005), which led to an attractive hypothesis that truncated α Syn contributes to early stages of pathogenesis. Consistent with that hypothesis, truncated forms of α Syn have been shown to correlate with several factors that are associated with disease. First, truncations of α Syn are present in the insoluble, fibrillar aggregates found in the brains of Parkinson disease patients, but not in aggregate fractions of control brains (Anderson et al., 2006; Liu et al., 2005). Furthermore, the presence of α Syn truncation correlates with disease progression in transgenic mouse models of PD (Li et al., 2005; Liu et al., 2005). Finally, transgenic mouse models that express C-terminally truncated forms of human α Syn develop PD-like symptoms and exhibit PD-like neuronal pathology (Tofaris et al., 2006; Wakamatsu et al., 2006). Therefore, the hypothesis is that truncated α Syn contributes to pathogenesis, but the precise role of truncated protein is also not known. Additionally, the mechanism that produces the truncated α Syn remains unidentified as well.

Multiple proteases have been suggested to metabolize α Syn, including the 20S proteasome (Bennett et al., 1999; Liu et al., 2005) calpain I (Mishizen-Eberz

et al., 2003; Mishizen-Eberz et al., 2005), and cathepsin D (Sevlever et al., 2008). Tissue fractionation and Western blotting has provided approximate molecular weights of the truncations, and subsequent epitope mapping using a panel of antibodies with varying recognition epitopes provided a general idea of the nature of the truncations (Anderson et al., 2006; Li et al., 2005; Liu et al., 2005). In an attempt to conclusively identify the cleavage sites, two groups performed mass spectrometric analysis of truncated α Syn that was purified from brain tissue. The two studies resulted in two sets of cleavage sites. The 2005 study identified two cleavage products, syn12 (12 kDa) and syn10 (10 kDa), that had cleavage sites between residues 102-109 and 118-125 (Li et al., 2005). Similar truncations were identified in the 2006 study, which named the C-terminal residues of the truncated forms as 135, 122, 119, and 115 (Anderson et al., 2006). However, neither group identified the cleavage site that produced the 10 kDa fragment, which may correspond to α Syn110 as suggested by mobility in the SDS gel and epitope mapping (Liu et al., 2005).

In addition to its central role in the Lewy body diseases, α Syn pathology also occurs in 30% of AD patients (Lewy body variant of AD, LBVAD) (Ranginwala et al., 2008). In cases with concurrent AD pathology, the α Syn pathology is generally much more severe than in cases without AD pathology (Pletnikova et al., 2005). Interactions that stimulate fibrillization have been identified *in vitro* between α Syn and the aggregated proteins A β and tau in AD plaques (Geddes, 2005; Giasson et al., 2003), while a genetic overlap was found between the genotypes of α Syn and tau pathology (Mamah et al., 2005). Both of these findings further strengthen the hypothesis that the aggregation of one promotes the aggregation of the other. However, the mechanism of this interaction is unknown. In addition to the increased full-length α Syn pathology in LBVAD, truncated forms of α Syn also appear to be more abundant in cases with

concurrent AD pathology (Pletnikova et al., 2005). Because truncations of α Syn are known to increase amyloidogenicity and there is a strong possibility for cross-seeding of AD amyloidogenic proteins, the identification of specific truncated α Syn forms may contribute to the understanding of the pathogenesis and/or the boundaries between these diseases. Ultimately, the clinical distinction between PD/PDD, DLB, and AD has direct consequences for treatment, as some medications are contra-indicated for PDD and DLB that are acceptable for use by AD patients (McKeith et al., 1992).

The current methods of identifying the presence and identity of the α Syn C-terminal truncations are labor-intensive, approximate at best, and are prohibitive for an analysis of even a moderate number of samples. Therefore, a reagent that specifically recognizes truncated forms of α Syn would be useful for higher-throughput analyses of both cultured cells and tissues.

Antibodies that incorporate the carboxylic acid group into the recognition epitope have been described (Liang et al., 1996). The use of short, synthetic peptides as antigens to produce antibodies was well-established, but often an antibody would be obtained that would react avidly against the antigen peptide but not recognize the same epitope within a protein (Liang et al., 1996). While there are several explanations, including posttranslational modification and conformational accessibility, Liang and colleagues focused on the chemical composition of the putative epitope. Using both monoclonal and polyclonal antibodies raised against peptide antigens, they showed that immunoreactivity depended on the presence of the carboxyl group as well as the amino acid sequence. Amidated, truncated, and elongated peptides were $\sim 0.1\%$ as reactive as the original peptide antigen. Therefore, one can increase the likelihood of the carboxyl group being incorporated into the recognition epitope by shortening the

peptide antigen. Supporting this finding are several studies reporting that peptide antigens shorter than 8 residues are unlikely to produce protein-reactive antibodies (*i.e.*, reactive against the full-length protein) (Dyson et al., 1988; Rothbard and Taylor, 1988; Tanaka et al., 1985). The minimum length required for immune response has been established to be between 5 and 6 residues (Edwards et al., 1995; Liang et al., 1996). Therefore, short (< 8 residues) peptides are both sufficient for eliciting a specific immune response and also increase the likelihood that the carboxyl group will be incorporated into the recognition epitope, thus preventing recognition of the full-length protein.

While the work described in this chapter was being performed, a polyclonal antibody against human α Syn119 was successfully made by ActiveSite Pharmaceuticals (Elan Pharmaceuticals) (Anderson et al., 2006). In that study, they extracted α Syn from the Lewy bodies of patients with Lewy body disease with a urea/thiourea buffer, and using their polyclonal antibody they identified α Syn119 as one of the truncated forms present in the LBs. They also found α Syn119 in the soluble extract of brain tissue from non-LBD patients. Both of these results were consistent with earlier results (Li et al., 2005; Liu et al., 2005), and proved that a polyclonal antibody selective for an extreme C-terminal epitope could be developed.

Results

Antibody production

Four peptides were identified for synthesis that corresponded to the C-terminal seven residues of four α Syn truncations: α Syn110, α Syn119, α Syn122, and α Syn123 (Table 5-1).

Table 5-1. Peptide antigens for polyclonal antibodies.

α Syn form (residues)	C-terminal sequence	Presumptive protease
α Syn110 (1-110)	EEGAPQE	20S
α Syn119 (1-119)	LEDMPVD	20S
α Syn122 (1-122)	MPVDPDN	calpain I
α Syn123 (1-123)	PVDPDNE	20S

The four antigen peptides (Table 5-1) were commercially synthesized by ProteinTech PTGLAB (Chicago, IL) with a cysteine residue on the N-terminus to enable conjugation to a carrier protein, keyhole limpet hemocyanin (Appendix A). The thiol-dependent conjugation forced the peptide to be oriented with the carboxyl terminus toward the solution, making it accessible for recognition by antibodies. Antisera were produced commercially, also by ProteinTech, and yielded pre-immune sera, two production bleeds, and one final bleed per serum (Table 5-2 and Appendix A). The pre-immune sera and the final bleed sera were aliquoted for use in experiments.

Table 5-2. Polyclonal sera raised against α Syn peptide antigens.

Truncation	α Syn110		α Syn119		α Syn122		α Syn123	
Serum ID (197x-y)	6-1	6-2	7-1	7-2	8-1	8-2	9-1	9-2

Antibody validation

The polyclonal sera were validated against the intended targets using recombinantly expressed and purified truncations of α Syn in slot blot assays (Figure 5-1) and ELISAs (Figure 5-2). Both methods showed that 7 of the 8 antibodies bind the intended target with some specificity. The slot blots showed specificity at dilutions of 1:5000 against 50 ng of antigen for all antibodies with the exception of 1976-1 (Figure 5-1).

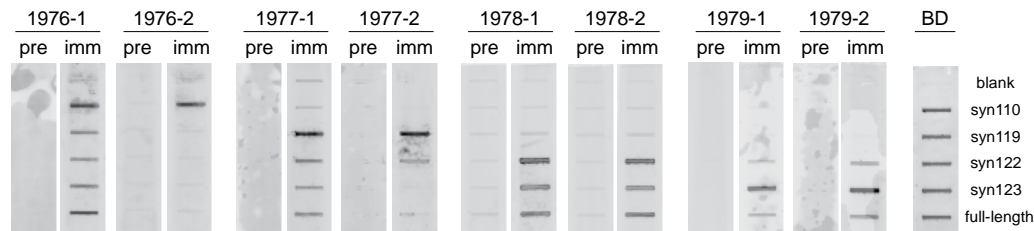


Figure 5-1. Slot blots of recombinant truncated α Syn proteins. 50 ng of recombinant protein (labeled on right) was applied to nitrocellulose membrane using a slot blot apparatus. The membranes were then blotted with 1:5000 dilutions of pre-immune or immune serum as indicated. A control blot was performed using the monoclonal anti- α Syn antibody (BD Biosciences). “Blank” indicates that no protein was applied in that slot.

ELISA data for 1976-2 and 1977-1 also demonstrated rigorous specificity for the appropriate antigens (Figure 5-2, panels A and B, respectively). At the same level of capture antigen, the antisera against syn122 and syn123 showed little specificity and considerable cross-reactivity against syn123 and syn122, respectively, as well as against full-length α Syn (Figure 5-3).

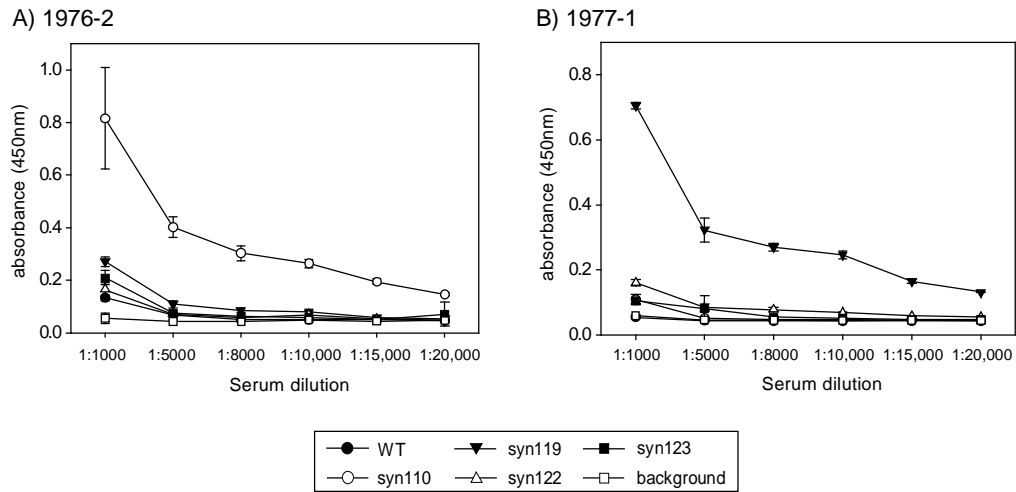


Figure 5-2. ELISAs of polyclonal antibodies against α Syn110 and α Syn119 with 2.5 μ g of capture antigen. 2.5 μ g of recombinant α Syn protein was bound to a 96-well plate. Individual wells were then incubated with the indicated dilutions of primary antibody in triplicate, followed by incubation with a 1:4000 dilution of anti-rabbit secondary antibody. Quantitation of bound antibody was performed with the chromogenic substrate OPD after 10 minutes of chromophore development. Note the different scales of the y-axis between panels A and B.

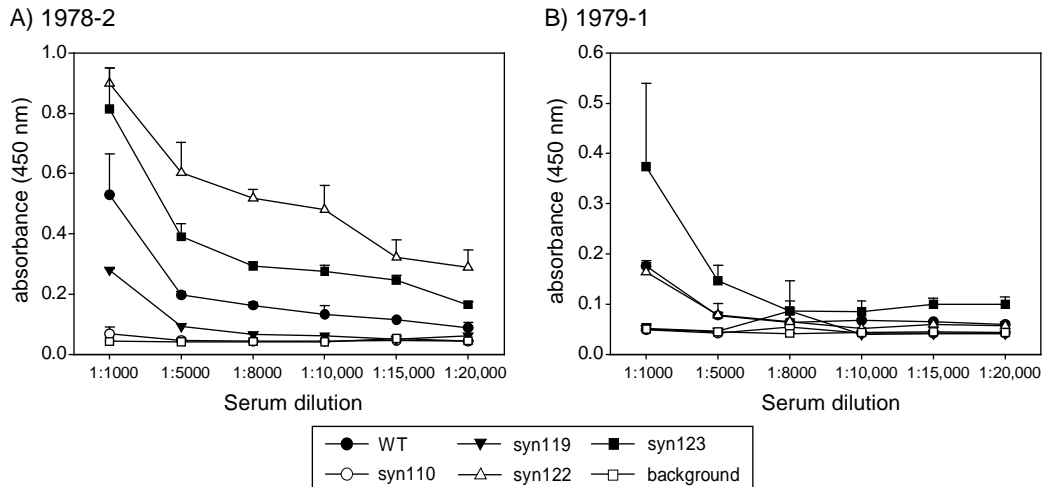


Figure 5-3. ELISAs of polyclonal antibodies against α Syn122 and α Syn123 with 2.5 μ g of capture antigen. 2.5 μ g of recombinant α Syn protein was bound to a 96-well plate. Individual wells were then incubated with the indicated dilutions of primary antibody in triplicate, followed by incubation with a 1:4000 dilution of anti-rabbit secondary antibody. Quantitation of bound antibody was performed with the chromogenic substrate OPD after 10 minutes of chromophore development. Note the different scales of the y-axis between panels A and B.

To reduce the amount of non-specific binding, additional ELISAs were performed using smaller amounts of capture antigen (Figures 5-4, 5-5). With 250 ng of capture antigen, the antibody 1978-1 displayed a measurable specificity for α Syn122, while the 1978-2 antibody showed no improvement over the data shown in Figure 5-3 (Figure 5-4, top panels). Reducing the amount of antigen to 25 ng revealed that both antisera specifically recognized syn122 at dilutions of 1:5000 and 1:10,000, although significant binding to both syn123 and full-length protein was still observed (Figure 5-4, bottom panels). For detection of α Syn122, the antiserum 1978-1 appeared to be the more specific of the two antisera.

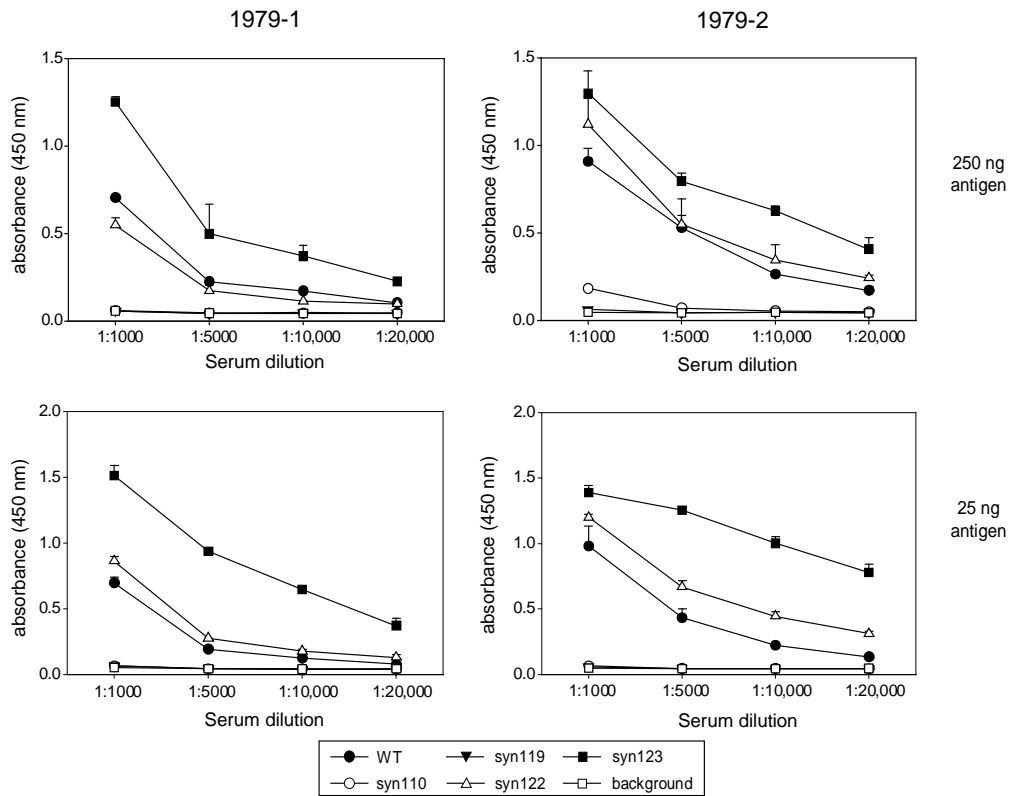


Figure 5-5. ELISAs of antibodies against α Syn123 with lower amounts of capture antigen. Recombinant α Syn protein was bound to a 96-well plate in the amounts indicated to the right. Individual wells were then incubated with the indicated dilutions of primary antibody in triplicate, followed by incubation with a 1:4000 dilution of anti-rabbit secondary antibody. Quantitation of bound antibody was performed with the chromogenic substrate OPD after 10 minutes of chromophore development (250 ng antigen) or 20 minutes (25 ng).

Western blots of in vitro degradation products of α Syn

20S proteasomal degradation assays were performed with full-length α Syn and then analyzed by Western blotting for α Syn110 or α Syn119 with the polyclonal serum 1976-2 or 1977-1, respectively (Appendix A). The 1976-2 antibody specifically recognized the α Syn110 fragment and did not react with any other α Syn species, as shown by a subsequent Western blot with a control antibody against the N-terminus of α Syn (Syn303) (Figure 5-6, panel A). The antibody 1977-1 preferentially recognized the α Syn119 product (Figure 5-6, panel B). However, 1977-1 also cross-reacted with the large amount of full-length protein in the Western blot, which is a consequence of the experimental conditions required to ensure the production and detection of α Syn119, which is highly labile to further degradation by 20S.

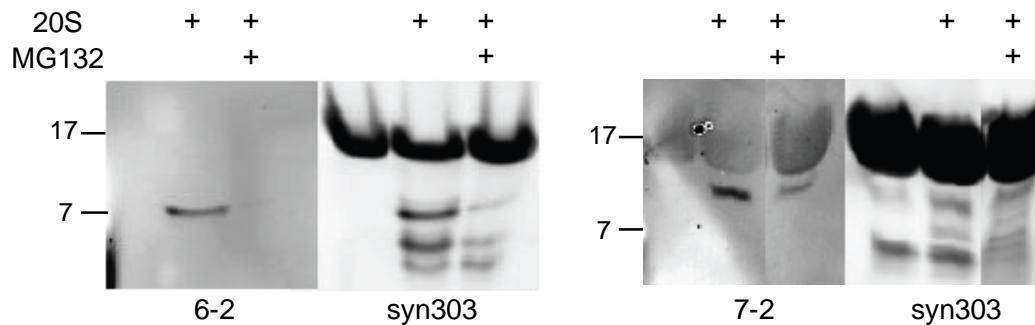


Figure 5-6. The polyclonal antibodies recognize products of proteasomal degradation of α Syn. (A) Full-length α Syn was incubated with 20S proteasome at a ratio of 500:1 α Syn:20S (Appendix A). The samples were analyzed by Western blot with either 1976-2 (anti- α Syn110) or syn303 (control), as labeled below the gels. (B) Full-length α Syn was incubated with 20S proteasome at a ratio of 5000:1 α Syn:20S to promote the formation of syn119. The samples were analyzed by Western blot with either 1977-1 (anti- α Syn119) or syn303 (control) as labeled.

Western blots of human cortical brain tissue

Sixteen samples of human cortex were obtained as described (Appendix A). The patients had been diagnosed with one of the following: Alzheimer's disease (AD), diffuse Lewy body disease (DLBD), or Lewy body variant of Alzheimer's disease (LBVAD) (Table 5-3). Samples were also obtained from postmortem tissue of non-LB age-matched patients to use as controls. The distribution of samples was as follows: six LBVAD, four DLBD, four AD, and two healthy controls. Previous fractionation of cortex and substantia nigra from PD and AD patients showed that α Syn truncations are present in the urea-soluble fraction of PD tissue, but not AD tissue (Liu et al., 2005). Immunohistochemistry analyses of DLBD and LBVAD have shown α Syn inclusions similar to those found in PD (Yokota et al., 2007), and truncated α Syn has been observed in DLBD and LBVAD samples (C. Liu, unpublished, and (Pletnikova et al., 2005)).

Table 5-3. Patient cortex samples.

Patient ID	Clinical diagnosis	Braak	CERAD	Comments
21199	LBVAD	V	C	numerous LB in cingulate
22146	CONTROL	III	0	
22180	AD	VI	C	
22365	DLBD	III	A	5 LB/100X in cingulate
22538	LBVAD	V	C	LB present in neocortex
22574	AD	V	C	
22791	CONTROL	I	0	
23647	LBVAD	IV	C	8 LB/100X in cingulate
23732	LBVAD	III	B (moderate NP)	moderate LB in neocortex
24615	AD	V	C	
24813	DLBD	II	A	40 LB/100X in cingulate; abundant LB present in frontal
25239	DLBD	II	B	moderate plaques in neocortex may be a confounding factor; 3 LB/100X field in cingulate
26198	AD	VI	C	
33605	DLBD	II	A	20 LB/100X in cingulate; LB present in frontal
34132	LBVAD	III	C (moderate plaques)	Frequent LB and LN in frontal cortex
34470	LBVAD	VI	C	5 LB/100X field and low density of LN in cingulate

Approximately half a milligram of each tissue sample was sequentially fractionated as described (Appendix A) (Liu et al., 2005). A control Western blot was performed with a monoclonal anti- α Syn antibody (BD Biosciences). While fragments were present in the soluble protein fraction (Figure 5-7, lanes marked H) of most samples, fragments were only present in the aggregated protein fractions that were soluble in either SDS or urea (Figure 5-7, lanes S and U). Furthermore, the samples that contained truncated α Syn in the aggregated fraction were exclusively from tissue with Lewy bodies (Figure 5-7, bottom panel). Truncated α Syn was not observed in the aggregated fractions of tissue without Lewy bodies (Figure 5-7, top panel). Similarly, high-molecular weight aggregates of α Syn were primarily found in the aggregated fractions of Lewy body-containing tissue, consistent with the presence of large amounts of aggregated α Syn in the Lewy bodies. These data from sixteen patient samples support earlier findings that used a much smaller data set of two patients, one AD and one PD (Liu et al., 2005).

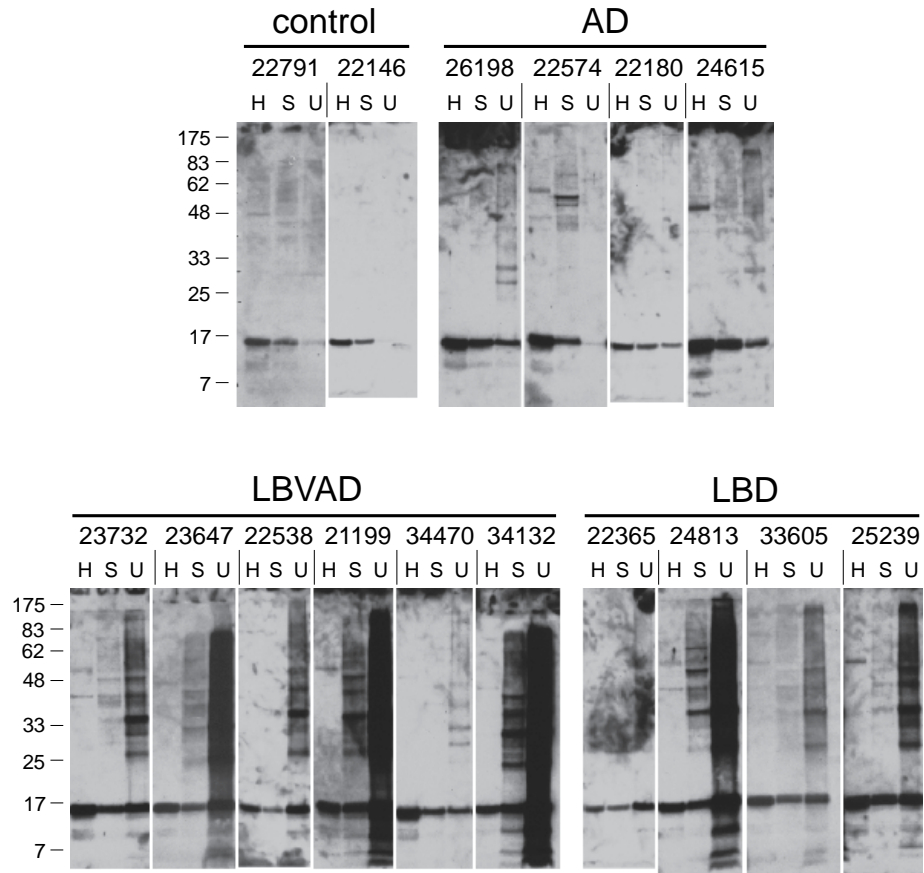


Figure 5-7. Sequential fractionation of human cortex samples. Cingulate cortex tissue was sequentially fractionated as described (Appendix A). Diagnoses and sample numbers are noted at the top of each set: AD, Alzheimer's disease; LBVAD, Lewy body variant of Alzheimer's disease; DLBD, diffuse Lewy body disease. Sequential fractionations of each sample are labeled: H, high salt soluble (750 mM NaCl); S, SDS-soluble (4% SDS); U, urea-soluble (8 M urea). Samples were probed with the monoclonal anti- α Syn antibody from BD Biosciences, which recognizes an epitope in the middle of the protein. Molecular weight markers (kDa) are identified on the right.

Western blot analyses were then performed on selected samples from this set of brain tissue. Two LBVAD samples, 21199 and 34132, and one DLBD sample, 24813, were selected for the largest amount of fragmented and aggregated α Syn. An AD sample, 24615, was selected as a non-LB control. When blotted with the polyclonal antibody directed against α Syn110 (1976-2), no reactivity was observed against any species in the 7-10 kDa range, where the recombinant α Syn110 migrates (Figure 5-8). Some very high-molecular weight bands and smears were observed above 175 kDa, which remained in the stacking gel and did not enter the separating gel.

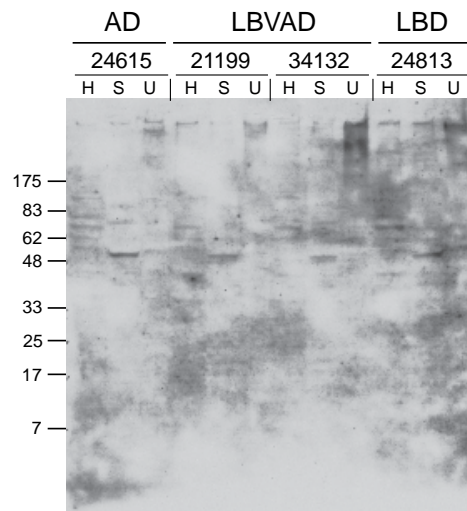


Figure 5-8. Blot for α Syn110 in cortex samples with the 1976-2 antibody. Selected samples of brain tissue were fractionated as before, then probed with the 1976-2 anti- α Syn110 antibody (1:500 dilution) and detected with ECL+ (Amersham). Molecular weight markers (kDa) are identified on the right.

Identical membranes were also probed with the two antibodies against α Syn119, 1976-1 and 1976-2 (Figure 5-9). Both antibodies revealed a band at approximately 10 kDa in the LBVAD sample 34132 (Figure 5-9, arrows). Additionally, all fractions contained a strong band of unidentified species at approximately 20 kDa. This band does not correspond to any of the bands identified with the BD anti- α Syn antibody (Figure 5-7). Furthermore, the 1977-1 antibody reproducibly reacts with high-molecular weight species in the LB-containing samples (Figure 5-9, panel A), whereas the 1977-2 antibody appears to recognize a different set of higher molecular weight species that are found in all tissue, regardless of disease pathology.

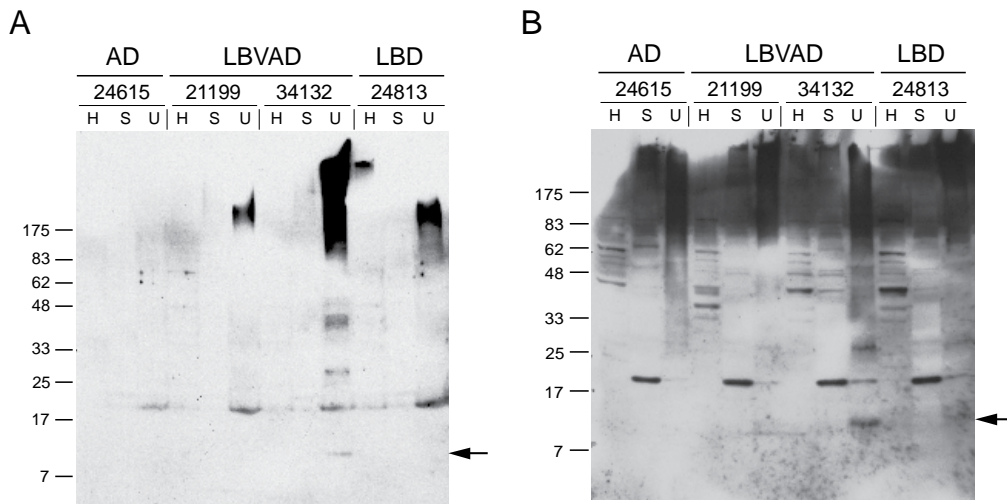


Figure 5-9. Detection of α Syn119 in cortex samples by the 1977-1 and 1977-2 antibodies. Selected samples of brain tissue were fractionated as before, then probed with either the 1977-1 (A) and 1977-2 (B) anti- α Syn119 antibody (1:1000 dilutions) and detected with ECL+ (Amersham). The arrow in each panel marks the putative α Syn119 monomer. Molecular weight markers (kDa) are identified on the right.

Immunohistochemistry of human cortical brain tissue

Immunohistochemistry analyses were performed on “tissue microarrays” composed of all sixteen samples previously analyzed by Western blot as well as additional samples. Signals were detected using the alkaline-phosphatase-based ultraView detection system (Ventana Medical Systems), which has been found to significantly increase sensitivity of brain tissue stains (Hatanpaa et al., 2008).

A commercial anti- α Syn antibody, LB509, that is used for postmortem diagnosis was used as a control (Figure 5-10, panel A). LB509 stained the tissue in an expected pattern, staining both Lewy neurites and Lewy bodies. The anti- α Syn119 antibody 1977-2 also stained Lewy neurites and Lewy bodies, although the shapes of the LNs that were recognized by 1976-2 were more dot-like than the elongated structures seen with the LB509 (Figure 5-10, panel B). Most interesting were the stains with the 1976-2 antibody against α Syn110. Unlike the previous two antibodies, 1976-2 showed a diffuse granular staining of the cytosol, while not staining any LN- or LB-like structures (Figure 5-10, panel C).

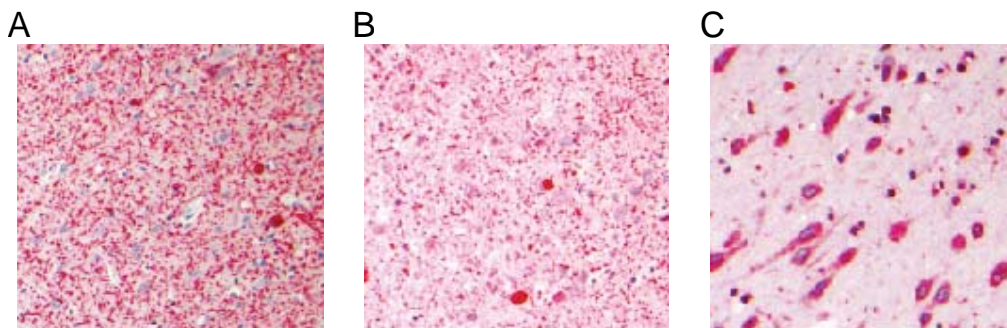


Figure 5-10. Immunohistochemical detection of α Syn in the cingulate cortex of a patient with LBVAD. Tissue sample 23647 was stained with either LB509 (A), 1977-2 (B), or 1976-2 (C). Pink indicates positive immunoreactivity, while blue is a counterstain with hematoxylin to identify the nuclei. Lewy neurites and Lewy bodies were stained with LB509 and 1977-2, while 1976-2 stains the cytosol. All images are at 200X magnification.

To determine the specificity of the 1976-2 stain, IHC was performed with the pre-immune serum (Figure 5-11, panel B). Additionally, the 1976-2 serum was pre-absorbed with 100-fold molar excess of the antigenic peptide before being used for staining (Figure 5-11, panel C). Staining was absent with the pre-immune serum and reduced by over 90% with the pre-absorbed serum, supporting the specificity of the staining observed with the 1976-2 serum.

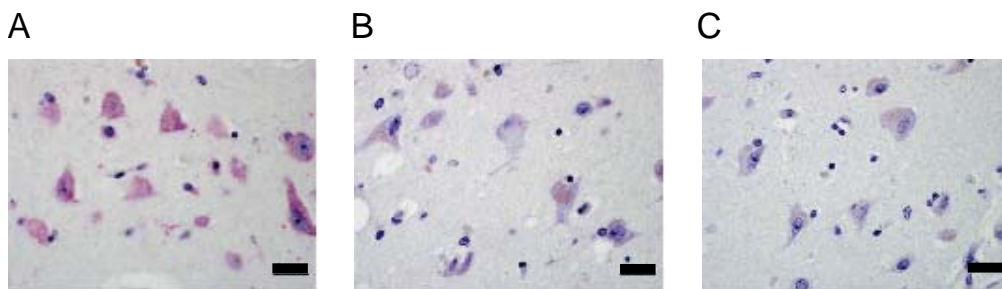


Figure 5-11. Control IHC stains for the 1976-2 serum. A tissue sample from a patient with LBVAD was stained with either 1976-2 (A), pre-immune serum (B), or 1976-2 pre-absorbed with 100-fold molar excess of the antigenic peptide (C). Pink indicates positive immunoreactivity; blue is a counterstain with hematoxylin; and the light gold pigment in some of the neurons in panels B and C is lipofuscin, a visible age-related pigment that gathers around the nucleus. All images are at 400X magnification; the scale bar represents 50 μm .

Discussion

The short peptide antigens of eight amino acid residues successfully produced antibodies that preferentially recognized the intended truncated α Syn in seven out of the eight attempts. Of those seven antisera, some showed specificity in slot blot analyses: 1976-2 against α Syn110; 1977-1 and 1977-2, against α Syn119; and 1979-1 and 1979-2, against α Syn123 (Figure 5-1). The two sera intended to recognize α Syn122, 1978-1 and 1978-2, had considerable cross-reactivity with α Syn123 and full-length protein (Figure 5-1). Quantitative analysis of antigen recognition with ELISAs was consistent with the qualitative blot analyses (Figures 5-2 through 5-5). 1976-2 and 1977-1 appeared to be the most specific sera as they differentiated the intended antigen (either α Syn110 or α Syn119, respectively) from the other forms of α Syn including the full length at relatively high antigen concentrations of 2.5 μ g (Figure 5-2). Specificity was broader for the four sera directed against α Syn122 and α Syn123, as very low amounts of antigen (25 ng) was necessary to observe selective binding to the target antigen over the other α Syn proteins (Figures 5-3, 5-4, and 5-5). The 25 ng used in the ELISAs was comparable to the 50 ng of antigen used in the slot blots. A comparison of those two data sets showed consistency in the evaluation of specificity of the four sera against α Syn122 and α Syn123.

The two most specific antibodies, 1976-2 and 1977-2, were then used for Western blots of *in vitro* 20S proteasome degradation assays of α Syn (Figure 5-6). Two experimental conditions were used to produce the desired truncations after residues 110 and 119, because α Syn119 is much more susceptible to further degradation by 20S. A larger amount of initial full-length substrate provided sufficient competition for 20S to increase the half-life of the α Syn119 endoproteolysis product. Both sera selectively recognized the intended targets,

although 1977-1 showed some cross-reactivity with the large amount of intact full-length protein that was also present in the gel (Figure 5-6, panel B). This was not unexpected, given the slot blot and ELISA analyses that showed a capability for cross-reactivity with full-length protein. Despite this cross-reactivity, the antibodies performed well in these Western blot applications.

It is well-established that truncations of α Syn are present in brain tissue of Lewy body disease patients and mouse models (Li et al., 2005; Liu et al., 2005). However, as noted above, the precise site of cleavage in the C-terminus is not known. Because most proteases cut at specific sequences, identifying the exact cleavage site would aid in the identification of specific proteases as the *in vivo* cleavage factor. Furthermore, an identified protease could also provide information on when α Syn cleavage occurs during disease progression. This would be a significant advance over the predictions and estimates of cleavage made so far. The available methodologies of epitope-mapping and mass spectrometric analyses of the fragments have suggested proteases that could be responsible, but a conclusive identification of the fragments by a truncation-specific method would provide a solid line of study to pursue regarding α Syn cleavage pathways *in vivo*.

To that end, samples of cingulate cortex brain tissue were obtained from the Alzheimer's Disease Research Center Tissue Bank at UT-Southwestern. The samples were sequentially fractionated with high salt buffer (750 mM NaCl) to remove soluble proteins and complexes, followed by 4% SDS buffer to solubilize moderately aggregated proteins, and finally by 8 M urea to solubilize highly stable protein aggregates, including amyloid fibrils. The fractions were separated by gel electrophoresis and analyzed with the monoclonal antibody against α Syn from BD Biosciences, which recognizes an epitope in the middle of the protein

and which had been previously used to identify α Syn fragments in brain tissue (Liu et al., 2005) (Figure 5-7). Consistent with those earlier results, this larger sample size showed soluble fragments of α Syn in most samples, but aggregated fragments were only found in tissue of diseased brains, along with high-molecular weight aggregates that were not disassembled by either SDS or urea (Figure 5-7, bottom panels). Based on the amount of fragments in the urea fraction detected by the BD antibody, three Lewy body disease brains were selected for further analysis with the polyclonal truncation-specific antibodies. An AD sample was also included as a non-LB control.

Consistent with the immunohistochemical studies (Figure 5-10), both the 1977-1 and 1977-2 antibodies successfully detected the presence of monomeric α Syn119 in a sample of LBVAD (Figure 5-9, arrows). Despite a significant amount of fragments in the other two LB samples by the monoclonal antibody, the polyclonal antibodies did not react with similar size fragments in those samples. Additionally, the 1976-2 antibody did not detect a monomeric form of α Syn110 in any of the Lewy body disease tissues, despite reacting positively in the immunohistochemical studies. The lack of detection by the polyclonal antibodies may be due to an insufficient amount of material in the blot to capture the antigen. This may be a consequence of the sensitivity of the polyclonal antibodies, which have been shown in control experiments with recombinant protein to be less sensitive than the commercial monoclonal antibody. The slot blots and Western blots showed that approximately 20-50 ng of protein was the limit of detection for the polyclonals (Figure 5-12), whereas the BD monoclonal antibody could detect amounts as low as 5 ng of recombinant protein (data not shown).

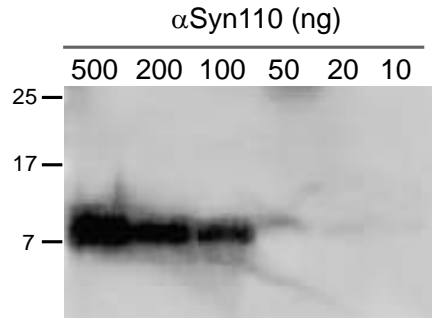


Figure 5-12. Sensitivity of 1976-2 against α Syn110 in Western blots. Recombinant α Syn110 in the amounts indicated was electrophoresed on a 12.5% SDS-polyacrylamide gel, transferred to nitrocellulose, and blotted with a 1:1000 dilution of 1976-2 into TBS-T. Following incubation with an anti-rabbit secondary, the blot was visualized with ECL+ (Amersham) on a Typhoon imager (Amersham/GE Biosciences).

Another potentially interesting result from the Western blots against α Syn119 was the presence of a ~20 kDa band in the SDS samples of all four tissues (Figure 5-9). Oddly, this band does not correspond to any of the α Syn species detected by the BD antibody, which detects the full-length protein at ~17 kDa in all samples (Figure 5-7). It is possible that the 20 kDa SDS-soluble band recognized by the 1977 set of antibodies is either an oligomer of a fragment that is clipped at both the N- and C-termini or otherwise modified. If the N-terminal cleavage is within the BD recognition epitope, it would escape detection by that antibody; as long as the C-terminal cleavage occurs immediately after residue 119, the 1977-1 and 1977-2 antibodies would recognize it. However, because the blots were performed with the crude sera without any additional affinity purification, the observed band could also be a non-specific reaction with a

protein other than α Syn. Additional experiments with a panel of antibodies against α Syn will aid in identification of this band.

Despite the limited Western blot results, the immunohistochemistry stains produced provocative patterns. The IHC method used here is an enhanced method that has been shown to be more sensitive to other amyloidogenic proteins (Hatanpaa et al., 2008), which may explain the specific immunodetection of α Syn by the 1976-2 and 1977-2 sera. The 1977-2 sera against α Syn119 show a slightly more dot-like pattern than the commercial antibody LB509 that is used for clinical diagnosis of pathology, the epitope for which is the C-terminus of α Syn (residues 122-140) (Figure 5-10, panels A and B). This may reflect a slightly different localization of α Syn119 compared to the full-length protein.

A profound difference in staining pattern was observed with the antibody against α Syn110, 1976-2. Instead of staining Lewy bodies and Lewy neurites as the other two antibodies, 1976-2 produced a diffuse granular staining that was restricted to the cytosol of the neurons (Figure 5-10, panel C). As the α Syn110 is known to be produced by the 20S proteasome *in vitro*, and the proteasome is present throughout the cytosol, it is tempting to form a hypothesis in which the α Syn110 fragments are found in the cytosol because of their recent production by the proteasome. The presence of diffuse staining of α Syn110 in the cytosol is certainly inconsistent with the fragments arising from proteolysis of the aggregates within LBs. Control stains with preimmune serum and antigen-pre-absorbed 1976-2 serum confirmed the specificity of the staining (Figure 5-11). Additional stains will also be performed, including stains for elements of the 20S proteasome that may show co-localization with the 1976-2-positive signals.

In conclusion, the production of polyclonal C-terminus specific antibodies against truncated forms of α Syn was successful, and the antibodies can be reliably used in *in vitro* applications such as ELISA and Western blots of recombinant proteins. The use of the antibodies against tissue samples produced mixed results, but the highly sensitive immunohistochemistry experiments suggest that the partitioning of α Syn fragments within neurons may hold information about the pathogenesis and perhaps even the boundaries between various diseases that contain Lewy bodies. Further experiments must be done to conclusively identify the presence of the 119 and 110 truncations in tissue, as well as their role in the development of disease. However, the preliminary results presented here suggest that both α Syn110 and α Syn 119 are present in diseased tissue but not healthy tissue. Because both of those truncations have been produced by the 20S proteasome *in vitro*, the results strongly implicate proteasomal cleavage as the truncating element *in vivo*.

Chapter Six

Degradation of disordered substrates by the 20S proteasome

Introduction

Intrinsically disordered proteins (IDPs) are now recognized as a significant fraction of all proteins in the cell, and participate in a variety of essential cell pathways (Radivojac et al., 2007; Uversky et al., 2000). The conformational flexibility of these proteins, which exist as a structural ensemble at either the secondary or tertiary structural level (Xie et al., 2007b), affords many biological advantages. With regard to protein-protein interactions, the sampling of a wide variety of conformations by IDPs enables a diversity for binding to other proteins that is unmatched by the “lock-and-key” mechanism (Radivojac et al., 2007). While an acquisition of ordered structure upon binding its partner has an entropic cost, the ability of the disordered protein to form a large interaction surface can provide highly favorable enthalpies to the overall binding reaction, such as in the formation of the coiled-coil structure of the SNARE complex (Ernst and Brunger, 2003). As intrinsic disorder is an essential biological feature of many proteins, there must be mechanisms for the expression, folding, and turnover of these proteins in the cell that ensure the proper function of these highly dynamic structures. Notably, the regions of disorder must be overlooked by the protein quality control machinery during synthesis, but some pathway must also exist for these proteins to later be recognized for routine protein turnover or for regulation.

Despite the essential function of IDPs, many have been implicated in neurodegenerative diseases that involve the aggregation of proteins. Aggregation is primarily a gain-of-toxic function, and the proteins that form toxic

conformations all contain some element of intrinsically disorder (*e.g.*, α Syn in Lewy body diseases, A β and tau in Alzheimer's disease, and the prion protein in spongiform encephalopathies such as Creutzfeldt-Jakob). The conformational states of these proteins that are partially unfolded (*i.e.*, "pre-molten globule") have been implicated as the species that precipitate the nucleation of toxic aggregates (Uversky and Fink, 2004). Regardless of starting structure, the formation of amyloid from monomeric proteins requires a significant structural rearrangement of the monomer into the cross-beta sheet structure of the amyloid fibril (Fink, 1998). Such rearrangements can be induced in highly stable proteins such as lysozyme and BSA through ultrasonication (Stathopoulos et al., 2004), perhaps by exposing highly amyloidogenic sequences within the protein that are normally protected (Tartaglia et al., 2008). Therefore, it is reasonable to expect that the intrinsic conformational flexibility of the monomer contributes to the propensity of a protein to aggregate. Supporting this hypothesis was a study in which a sequence that is conserved between three amyloidogenic proteins (α Syn, A β , and prion) was engineered into non-amyloidogenic proteins. When the sequence was inserted into IDPs, the resulting chimeras formed aggregates. Insertion of the same sequence into the well-folded proteins thioredoxin and protein G did not promote aggregation (Ji et al., 2005).

Some IDPs are degraded by the 20S proteasome *in vitro*. These proteins include the proteins p21^{CIP} and α Syn, which are entirely random coil in solution (Liu et al., 2003; Tofaris et al., 2001). *In vivo*, the turnover of p21 is an essential regulatory step in the cell growth pathway (Schafer, 1998). Furthermore, the proteins DHFR, ferritin, and lysozyme are substrates for 20S degradation when they have been thermodynamically destabilized by oxidation (Amici et al., 2004; Shringarpure et al., 2001). Structural destabilization by the removal of metal ion cofactors can also increase the susceptibility of a protein to 20S-mediated

degradation, as exemplified by the apo form of SOD1 (Di Noto et al., 2005). These data indicate that the 20S proteasome may function as a sensor of thermodynamic instability. To that end, an operational definition of IDPs was proposed that identifies an IDP as a protein that is susceptible to degradation by the 20S proteasome (Tsvetkov et al., 2008). However, such a definition is difficult to reconcile with the observation that IDPs do not appear to be more susceptible to proteasomal turnover *in vivo*, where there is no significant difference between the halflives of IDPs and well-ordered proteins (Tompa et al., 2008). Additionally, artificially disordered proteins, such as carboxymethylated casein, are not always equal substitutes for naturally occurring IDPs, such as α Syn and p21^{CIP}, as substrates for the 20S proteasome (Liu et al., 2003; McGuire et al., 1989). Therefore, elements of a potential substrate must participate in its recognition as a substrate by the 20S proteasome.

The entry of a targeted substrate, such as a polyubiquitinated protein, into the lumen of the 20S is well-known to be regulated by the binding of one or two multisubunit regulatory complexes. In all proteasomes, polypeptides enter and exit the lumen through annuli controlled by the α rings on either end of the proteasome. Access to the lumen is restricted by the N-termini of the alpha subunits, which overlay one another to form a “gate”. The alpha subunit ring binds to the activator complexes PA700 and PA28 (Gray et al., 1994; Peters et al., 1993; Yoshimura et al., 1993), which reorder the gate to allow access to the catalytic lumen (Whitby et al., 2000). Low concentrations of SDS have also been shown to increase 20S peptidase activity against fluorogenic peptides, presumably by also changing the conformation of the gate (Tanaka et al., 1988). The regulatory function of the gate was conclusively shown using mutants of the yeast 20S, in which deletions of the α 3 and α 7 subunit N-termini significantly altered

proteasomal activity. The single mutant $\alpha 3\Delta N$ stimulated the rate of peptide hydrolysis over 10-fold compared to the wildtype 20S, while the double mutant $\alpha 3\alpha 7\Delta N$ hydrolyzed carboxymethylated casein at a rate tenfold greater than the wildtype (Bajorek et al., 2003; Groll et al., 2000). The *in vitro* degradation experiments described above were performed with purified 20S proteasome without ATP, ruling out the participation of the PA700 activator complex. Because the gate is usually closed, a substrate that enables its own entry into the proteasome must enable a conformational rearrangement of the gate.

These studies demonstrated that the 20S proteasome is capable of protein degradation independently of activator complexes. Because the 20S is known to be present in the cell apart from any activator complex (Brooks et al., 2000; Peters et al., 1994), this evidence suggested a physiological role for 20S in the turnover of a subset of proteins. For such a role, the 20S must first recognize some element of the potential substrate. There is significant evidence that structural disorder is that element, from complete random coil to local structural destabilization. After the recognition of the substrate, the substrate must be allowed access to the catalytic sites in the lumen. The role of the gate formed by the 20S alpha subunits is unknown, although some conformational rearrangement must take place to allow polypeptide entry.

This study set out to characterize the interaction between the 20S proteasome and IDP substrates. To understand the elements of a protein that make it a substrate for 20S degradation, mutant forms of RNase Sa and α Syn were used as models. The function of 20S as a stability sensor was confirmed by the increasing susceptibility of destabilized RNase Sa mutants to degradation. However, truncated forms of α Syn were found to have different rates of degradation, despite containing equal amounts of disorder. Therefore, the

presence of disorder may be necessary but is not sufficient for 20S degradation. To more fully understand the mechanism of substrate recognition and degradation by the 20S, we evaluated the composition of the 20S proteasome from multiple independent purifications. Two-dimensional gel analyses enabled the correlation of a modification of the $\alpha 6(\alpha 1)$ subunit with the enzymatic activity against IDPs, which has not been previously identified as a regulatory element for proteasomal activity. Finally, additional substrates for the modified form of 20S were identified in mouse liver extracts.

Results

20S-mediated degradation of RNase Sa destabilized mutants – Several mutants of RNase Sa were identified by the Pace research group (Texas A&M University) as thermodynamically destabilized: $\Delta 2-6$, R68Y, Y51F, Y80F, and Y30F (Pace et al., 2001). Additionally, the point mutant D79Y was more stable than the wildtype RNase Sa. As a measure of the stability of each protein, the midpoint of the melting curve (T_m) of each mutant was determined by monitoring the CD signal over a thermal melting curve (Figure 6-1). The same proteins were subjected to degradation by the 20S proteasome (M39 preparation, C. Liu, unpublished) (Figure 6-1). The rate of degradation by 20S correlated with the thermodynamic stability of the proteins, as the mutants with a lower T_m were more rapidly degraded.

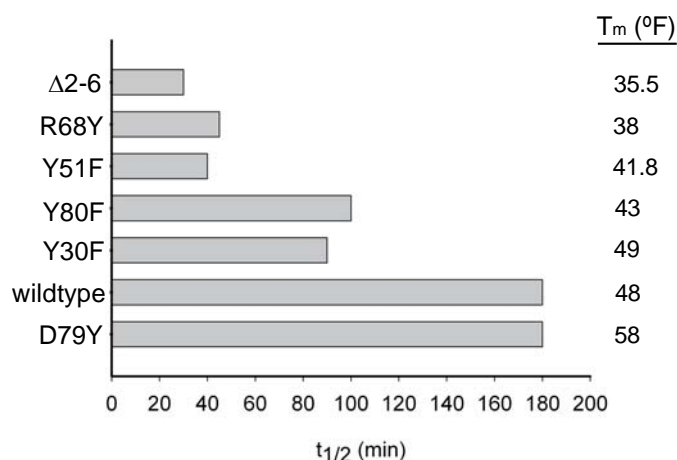


Figure 6-1. Rate of RNase Sa degradation by 20S is correlated with thermodynamic stability. *Left panel*, quantitation of the half-life of RNase proteins when incubated with the 20S proteasome. *Right panel*, the T_m of each protein as determined by thermal denaturation. (Data acquired by C. Liu and N. Pace, unpublished.)

20S-mediated degradation of truncated α Syn – α Syn terminal truncations were recombinantly expressed in and purified from *E. coli*, then subjected to degradation by the 20S proteasome (M57 preparation). Despite the approximately equal amount of random coil structure formed by each truncation (Figures 6-2 and 6-3, panels A), the proteasome exhibited different rates of degradation of each substrate (Figures 6-2 and 6-3, panels B). The C-terminal truncation α Syn119 was rapidly cleaved into a product that migrated comparably to α Syn110 (Figure 6-2, panel B). The rate of cleavage and turnover of full-length α Syn was slower than α Syn119, but faster than α Syn110 as measured by the appearance of truncated products (Figure 6-2, panel B). The susceptibility of the C-terminal truncations to degradation, from most to least, is α Syn119 > α Syn > α Syn110.

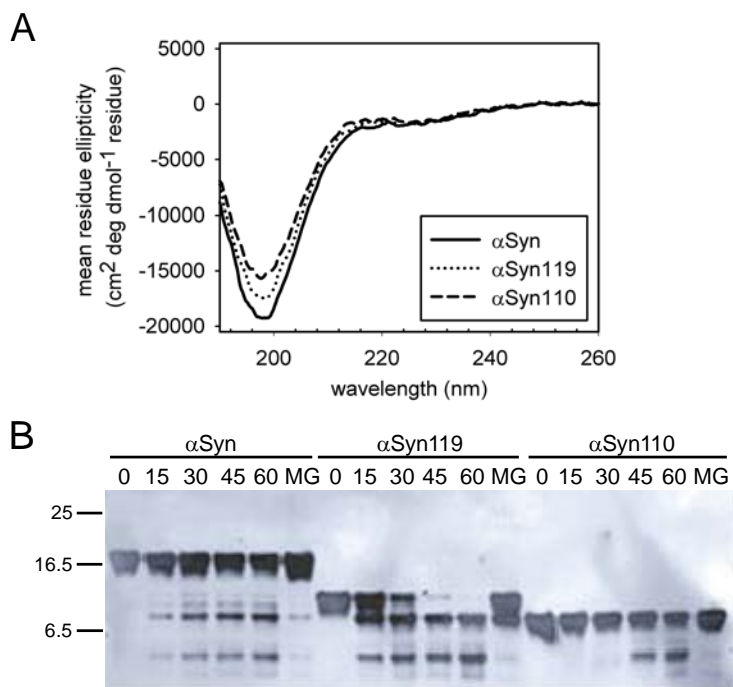


Figure 6-2. C-terminal truncations of αSyn are selectively degraded by 20S. (A) Mean residue ellipticity of αSyn C-terminal truncations. (B) 20S degradation of αSyn proteins (1000:1 αSyn :20S). The last lane of each set was a reaction performed with 20S that had been pre-incubated with the inhibitor MG132.

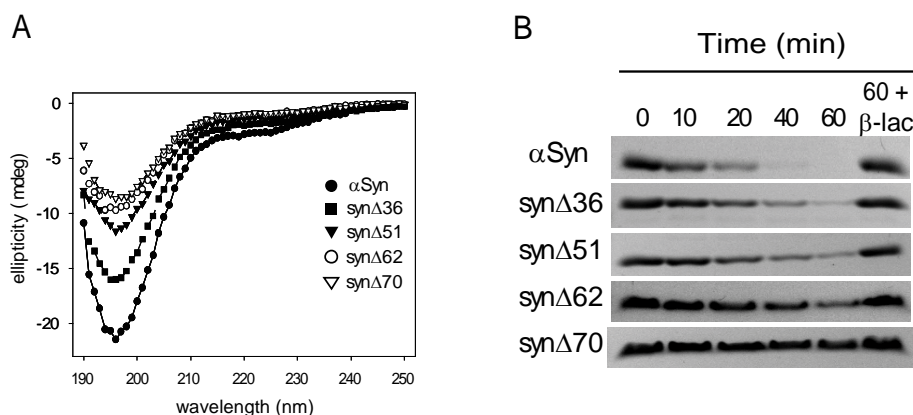


Figure 6-3. N-terminal truncations of α Syn are also selectively degraded by 20S. (A) Ellipticity of α Syn truncations (units in millidegrees). (B) 20S degradation of N-terminally truncated α Syn proteins (200:1 α Syn:20S). The last lane was a reaction performed with 20S that had been pre-incubated with the inhibitor β -lactacystin.

When full-length α Syn turnover was compared to the degradation of N-terminal deletions, all the deletion mutants were slower than full-length (Figure 6-3, panel B). The rate of degradation was inversely correlated with the size of the deletion from the N-terminus; the order of susceptibility to degradation (from most to least): α Syn > α Syn Δ 36 > α Syn Δ 51 > α Syn Δ 62 > α Syn Δ 70. Therefore, while 20S is capable of degrading intrinsically disordered proteins, it does not degrade all IDPs at the same rate, and some IDPs (such as α Syn Δ 70 and α Syn110) appear to be resistant to 20S degradation.

Degradation of α Syn by different 20S preparations – There are multiple protocols for the purification of 20S proteasome from bovine erythrocytes. Two preparations from different protocols were evaluated for degradation of the IDP model substrate α Syn: M57 (Appendix A, “endoproteolytic” protocol) and M58 (Appendix A, “latent” protocol). M57 was purified via a protocol that incorporates an ammonium sulfate cut to separate the 20S from PA700, while the M58 protocol omitted that step. When incubated with the fluorogenic tetrapeptide substrate Suc-LLVY-AMC, the baseline peptidase activity of M57 is higher than that of M58 (data not shown). Because M58 has such low intrinsic peptidase activity, it has been used exclusively for studies that stimulate activity by peptides that mimic the C-terminal tails of several PA700 subunits (Gillette et al., 2008). When the M58 proteasome was incubated with α Syn, no degradation or endoproteolytic cleavage was observed (Figure 6-4). Therefore, the two purification protocols yield 20S proteasomes with different peptidase and protease activities.

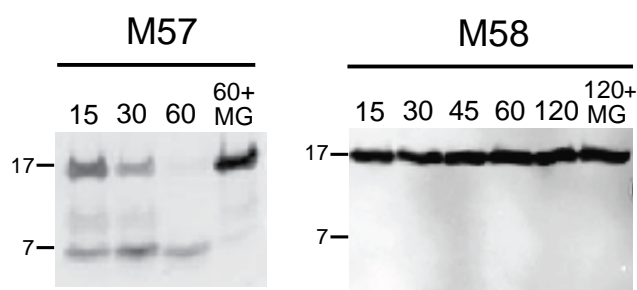


Figure 6-4. α Syn is not degraded by all 20S proteasome preparations. α Syn was incubated with the indicated 20S proteasome at a ratio of 250:1 α Syn:20S at 37°C. Aliquots were removed at the times indicated (in minutes). Control reactions were performed with 20S that had been pre-incubated with the inhibitor MG132. α Syn was detected by Western blotting with the syn303 monoclonal antibody.

Multiple preparations of 20S proteasome followed the same protocol as that used for M57: M39, M49, and M51. When incubated with α Syn, these preparations also degraded full-length α Syn, while also producing C-terminal truncations as seen in degradation assays performed with M57 (Figure 6-5). This established that the enhanced protease activity of the M57-style preparation is reproducible, and not simply an artifact of a single preparation.

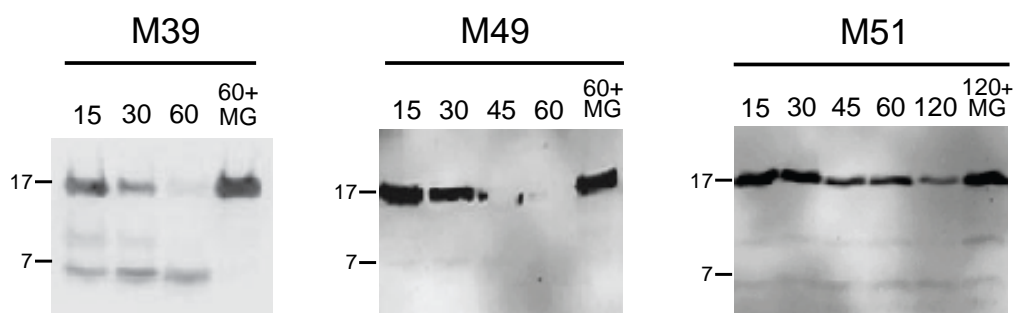


Figure 6-5. The endoproteolytic activity of 20S is reproducible. α Syn was incubated with the indicated 20S proteasome at a ratio of 250:1 α Syn:20S at 37°C. Aliquots were removed at the times indicated (in minutes). As before, control reactions were performed with 20S that had been pre-incubated with the inhibitor MG132. α Syn was detected by Western blotting with the syn303 monoclonal antibody.

Activation of 20S peptidase activity with PA28 – Latent and active forms of purified 20S proteasome have been described in the literature, with the difference in activity ascribed to a change in the conformation of the gate (Tanaka et al., 1989). To test if the endoproteolytic activity of M57 against α Syn was dependent on the existence of an intact, closed gate, an activation assay with the ATP-independent activator complex PA28 was performed. The PA28 complex binds

to the alpha ring of the 20S proteasome and reorders the gate, enabling the diffusion of small peptide substrates into the lumen for ATP-independent proteolysis. Recombinant PA28 α was incubated with 20S proteasome at a molar ratio of 100:1 PA28 α :20S and evaluated for both hydrolysis of the fluorogenic tetrapeptide substrate Suc-LLVY-AMC (Figure 6-6, panel A) and degradation of α Syn (Figure 6-6, panel B). As expected, the PA28 α stimulated proteasomal cleavage of the fluorogenic peptide. By contrast, the open gate did not stimulate α Syn degradation; the 20S proteasome complexed with PA28 degraded α Syn more slowly than 20S alone.

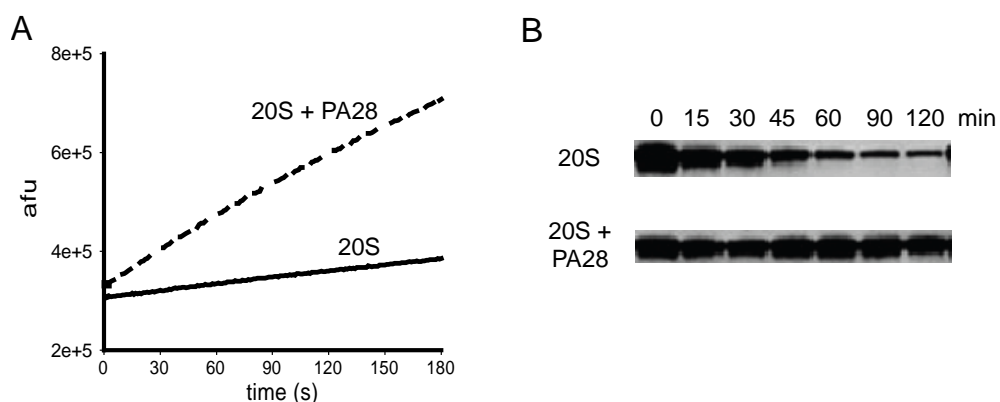


Figure 6-6. PA28 activation inhibits the 20S proteasome against α Syn. (A) Peptide hydrolysis of Suc-LLVY-AMC (50 μ M) by M57 20S (2 nM) in the absence and presence of 20 nM recombinant PA28 α . (B) Degradation of 5 μ M α Syn by 20 nM M57 20S (250:1 α Syn:20S) in the absence and presence of 200 nM PA28 α . Aliquots were removed at the times indicated and α Syn was detected by Western blotting with svn303.

Native gel electrophoresis of 20S proteasomes – As described above, there are two different protocols for the preparation of 20S proteasome from bovine erythrocytes, and the preps differ in activity against the α Syn substrate (Figure 6-4). The preparations look similar by one-dimensional SDS-PAGE, but migrated differently by native gel electrophoresis (Figure 6-7). The difference in migration suggested that there was a compositional difference between the two preparations, which could be the source of the observed difference in activity.

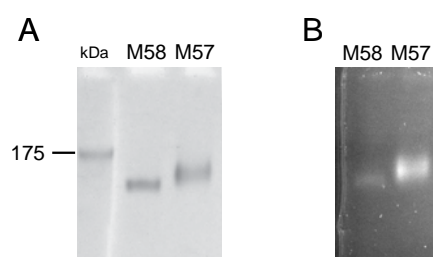


Figure 6-7. Native gel electrophoresis of M57 and M58 proteasomes. (A) Coomassie-stained native gel electrophoresis of 5 μ g each M58 and M57 proteasomes. Also shown is a molecular weight marker in the “kDa” lane (New England Biolabs, prestained premixed markers, #P7708S), which was used for internal reference only and does not correspond to the actual molecular weight of the native complexes. (B) Prior to staining, a peptidase overlay assay was performed to assess activity. The gel was incubated in 50 μ M of Suc-LLVY-AMC fluorogenic peptide substrate for 20 minutes at 37°C prior to image acquisition at ex360/em465 nm.

Two-dimensional gel analysis of 20S proteasomes – Two-dimensional gel analysis was performed on the M57 and M58 proteasomes, using isoelectric focusing in the first dimension and SDS-PAGE in the second. An overlay of the 2D gel of each prep revealed that nearly all the proteasomal subunits were identical between the two proteasome preps with the notable exception of two areas (Figure 6-8). The M58 proteasome contained three spots with a neutral pI and a molecular weight just above 33 kDa that were not present in the M57 prep (Figure 6-8, pink spots marked with arrows). The M57 proteasome had three spots with a more acidic pI and a molecular weight less than 33 kDa that were not present in the M58 prep (Figure 6-8, cyan spots marked with arrowheads).



Figure 6-8. Overlay of M57 and M58 proteasomes. Coomassie blue-stained 2D gels of the proteasome preps M58 (pink) is overlaid on the similarly stained 2D gel of M57 (cyan). Arrows denote spots specific to the latent M58 preparation, while arrowheads mark spots unique to the endoproteolytic M57 proteasome.

The most acidic spot unique to M57 was excised and submitted for identification by mass spectrometry (Figure 6-9). The peptides generated by tryptic digest covered 38% of the protein sequence and were matched portions of the PSMA1 gene product, which has been variously identified as $\alpha 6$ (Baumeister/Coux nomenclature), $\alpha 1$ (GenBank/SwissProt nomenclature) and C2 (an historical and obsolete nomenclature). Henceforth, this subunit will be referred to as $\alpha 6(\alpha 1)$, which emphasizes the commonly used name of $\alpha 6$ while parenthetically acknowledging the GenBank/SwissProt nomenclature ($\alpha 1$) that is used for all database searches. This identification was confirmed by Western blotting with the monoclonal antibody MCP106 specific for $\alpha 6(\alpha 1)$ (BioMol International) (Figure 6-10).

```

1  MFRNQYDNDV TVWSPQGRIH QIEYAMEAVK QGSATVGLKS KTHAVLVALK
51  RAQSELAAHQ KKILHVDNHI GISIAGLTAD ARLLCNFMRQ ECLDSRFVFD
101 RPLPVSRLVS LIGSKTQIPT QRYGRRPYGV GLLIAGYDDM GPHIFQTCPS
151 ANYFDCRAMS IGARSQSART YLERHMSEFM ECNLNELVKH GLRALRETLP
201 AEQDLTTKNV SIGIVGKDLE FTIYDDDDVS PFLEGLEERP QRKAQPTQPA
251 DEPAEKADEP MEH

```

Figure 6-9. Mass spectrometric identification of $\alpha 6(\alpha 1)$. The sequence of $\alpha 6(\alpha 1)$ is shown in black, with sequence numbering on the right. In bold red are the peptides that were identified by mass spectrometry from the tryptic digest of the most acidic M57-specific spot.



Figure 6-10. Confirmation of the M57-unique spots as $\alpha6(\alpha1)$. M57 proteasome was subjected to 2D electrophoresis, then analyzed for total proteasome by Coomassie stain and $\alpha6(\alpha1)$ by Western blotting. Shown here is the overlay of the Western blot, which used a 1:1000 dilution of the MCP106 monoclonal antibody (green, 5 μg total protein), on a Coomassie stained gel (pink, 15 μg total protein).

A blot of the 2D separation of M58 proteasome showed that the M58-unique spots (Figure 6-11, pink spots) were also $\alpha 6(\alpha 1)$. Therefore, a change in both the pI and the molecular weight of $\alpha 6(\alpha 1)$ is associated with the endoproteolytic activity of the 20S proteasome.



Figure 6-11. Confirmation of the M58-unique spots as $\alpha 6(\alpha 1)$. M58 proteasome was subjected to 2D electrophoresis then analyzed for total proteasome by Coomassie stain and $\alpha 6(\alpha 1)$ by Western blotting. Shown here is the overlay of the Western blot, which used a 1:1000 dilution of the MCP106 monoclonal antibody (green, 5 μg total protein), on a Coomassie stained gel (pink, 15 μg total protein).

The other three proteasome preparations that exert endoproteolytic activity, M39, M40, and M51, also contained the three $\alpha 6(\alpha 1)$ spots that were unique to as shown by overlays of Coomassie-blue-stained 2D separations of these preparations (Figure 6-12). The modification of $\alpha 6(\alpha 1)$ is reproducibly associated with the endoproteolytic activity of the 20S proteasome.

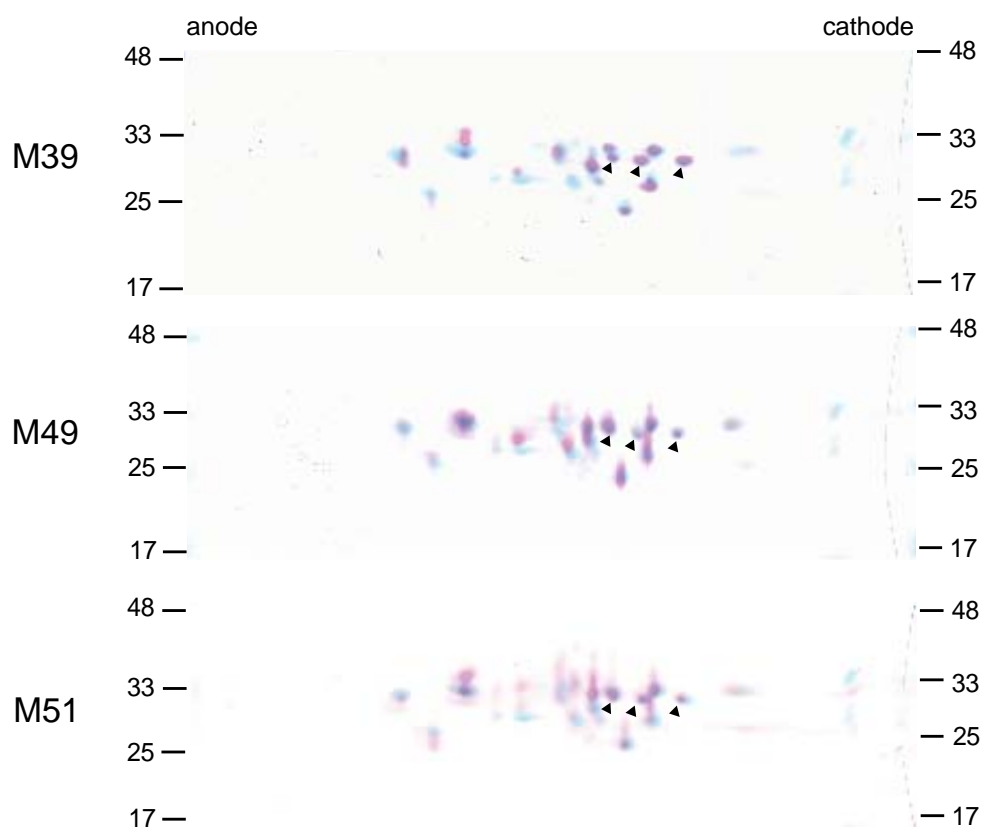


Figure 6-12. All four endoproteolytic 20S proteasomes contain the same $\alpha 6(\alpha 1)$ modified subunits. Coomassie blue-stained 2D gels of the proteasome preps M39, M49, and M51 (pink) are overlaid on the similarly stained 2D gel of M57 (cyan). Arrowheads note the spots unique to the endoproteolytic proteasome preparations.

Treatment of 20S proteasome with λ phosphatase – The difference in molecular weight and pI of the $\alpha 6(\alpha 1)$ subunit between the M57 and M58 proteasomes suggested that a post-translational modification may account for the biochemical changes. Both M57 and M58 proteasomes were incubated for 1 hour with recombinant λ phosphatase in reaction buffer (New England Biolabs), then separated by 2D gel electrophoresis and blotted for $\alpha 6(\alpha 1)$. The pattern of $\alpha 6(\alpha 1)$ spots in M57 did not change significantly. However, a new set of spots appears in M58 that are more basic than the $\alpha 6(\alpha 1)$ spots of untreated M58, which indicated that $\alpha 6(\alpha 1)$ in the M58 proteasome is at least partially phosphorylated. Therefore, there is an additional modification that distinguishes M57 $\alpha 6(\alpha 1)$ from M58 $\alpha 6(\alpha 1)$.

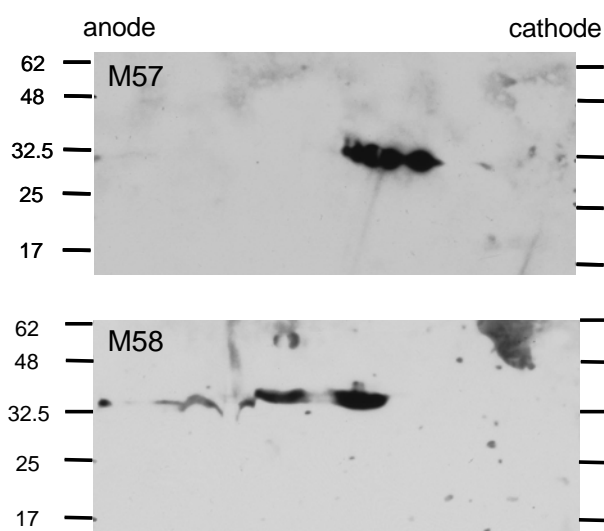


Figure 6-13. λ phosphatase treatment of M57 and M58 proteasomes. 2.5 μg of either M57 or M58 was incubated with 100 units of λ phosphatase (New England Biolabs) for 1 hour at 30°C. The samples were then subjected to 2D electrophoresis as described and blotted with for $\alpha 6(\alpha 1)$.

Fractionation of mouse livers and treatment with 20S proteasome – A variety of IDP substrates have been used for evaluating the activity of 20S *in vitro*, including α Syn, p21^{CIP}, and RNase Sa. In an effort to identify additional substrates for 20S degradation, which may provide insight into the physiological role of the endoproteolytic form of 20S *in vivo*, protein extracts from mouse livers were subjected to 20S degradation *in vitro*. Mouse liver tissue was lysed by homogenization and the resulting soluble fraction brought to 1 M ammonium sulfate. The unbound fraction of the ammonium sulfate supernatants was then subjected to degradation by the M57 20S proteasome. Following SDS-PAGE and Coomassie-blue staining, two bands were identified as undergoing apparent degradation during the 20S incubation, at 55 kDa and 35 kDa (Figure 6-14). The bands were not affected by incubation with 20S that had been pre-inhibited with the inhibitor MG132, which indicated that the proteins in those bands had been specifically degraded over time in a proteasome-dependent manner. A sample of the untreated tissue fraction was electrophoresed along with the degradation assay samples, and these two bands were cut from the untreated lane and submitted for protein identification by tryptic digest and mass spectrometry. The 55 kDa band was identified as protein disulfide isomerase, and the peptides from the 35 kDa band were matched to glyceraldehyde-3-phosphate dehydrogenase.

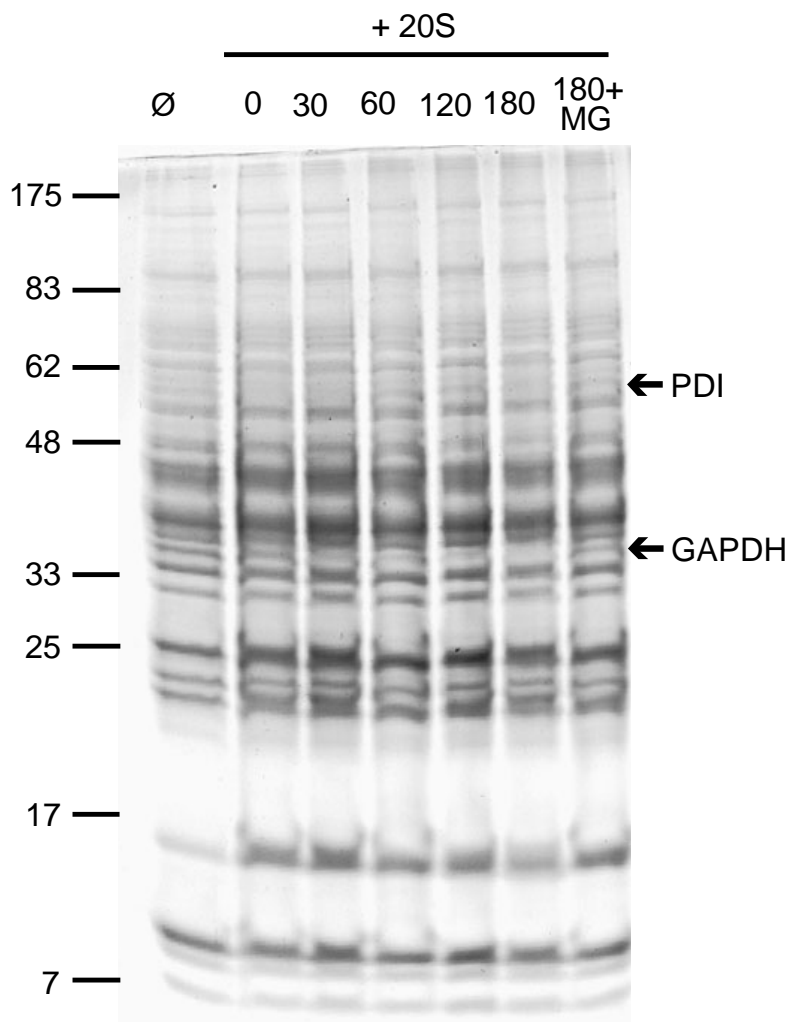


Figure 6-14. Substrates of the 20S proteasome in a fraction from mouse liver. The soluble fraction of mouse liver tissue was treated with 1 M $(\text{NH}_4)_2\text{SO}_4$ and incubated with phenyl sepharose. The flowthrough was recovered (lane \emptyset). A portion of the flowthrough was diluted to 1 mg/mL with 70 μM αSyn and incubated with 200 nM M57 20S 37°C. Aliquots were removed at the times indicated. A control reaction was performed with 20S that had been pre-incubated with MG132. The gel was stained with Coomassie blue. The bands marked with arrows were excised from the flowthrough lane and submitted for protein identification by mass spectrometry, which produced the identifications labeled on the right: protein disulfide isomerase (PDI) and glyceraldehyde-3-phosphate dehydrogenase (GAPDH).

Discussion

Degradation of proteins by the 20S proteasome has been described by several groups using proteasomes from a variety of sources (Table 3-1). All of these proteins contain some disorder, due to destabilization by oxidation (Shringarpure et al., 2003), the removal of metal ion cofactors (Di Noto et al., 2005), or point mutations (Amici et al., 2004). The presence of disorder has been established as sufficient for degradation by the 20S proteasome (Liu et al., 2003). Interestingly, the extent of structural destabilization of a protein can be detected by the 20S, as evidenced by the variable susceptibility of a panel of RNase Sa point mutants to 20S degradation (Figure 6-1). An inverse correlation was found between the structural stability of the proteins, as measured by the melting point (T_m), and the rate of degradation by 20S. This data suggested that the 20S proteasome acts as a sensor for thermodynamic stability and/or intrinsic disorder.

In that regard, Tsvetkov and colleagues defined an IDP as a protein that is susceptible to 20S-mediated degradation (Tsvetkov et al., 2008). However, while many IDPs are substrates for the 20S proteasome, including p21^{CIP} and α Syn (Liu et al., 2003), not all disordered proteins are equally good substrates (Figures 6-2 and 6-3). C-terminal and N-terminal truncations of α Syn have approximately equal amounts of random coil structure, and yet the 20S proteasome degrades these truncations at different rates (Figures 6-2 and 6-3). Notably, the N-terminal truncation α Syn Δ 70 does not appear to be degraded at all, and only a small amount of α Syn110 is cleaved after 45 minutes, when most of the other proteins have been noticeably degraded. Therefore, the presence of disorder in a protein is not sufficient for that protein to be a substrate of the 20S proteasome.

An additional level of complexity in the mechanism of 20S-substrate recognition was that different purification protocols yield proteasomes that have different activities against IDP substrates. Proteasomes purified by a protocol that is identified here as the “endoproteolytic” protocol are able to degrade the model IDP substrate full-length α Syn (preparation numbers M39, M49, M51, and M57) (Figures 6-4 and 6-5). Proteasome that was purified by a different protocol, the “latent” protocol, does not degrade α Syn (preparation M58) (Figure 6-4). Therefore, there must exist an element (or elements) of the 20S proteasome that enable degradation of IDPs, in addition to the as-yet identified characteristics of the IDP that enables degradation by 20S.

All proteasomal substrates must enter the catalytic lumen through the gate formed by the N-terminal tails of the alpha subunits. To identify whether the gate played a role in the ability of α Syn to be recognized and degraded by the M57 20S, the proteasome was activated by pre-incubation with a recombinant PA28 α activator complex (Figure 6-6). The addition of PA28 α increased the rate of peptidase activity, indicating an opening of the gate. By contrast, the rate of degradation of α Syn was decreased, which showed that simply opening the gate was not only insufficient to enable α Syn degradation but may have also inhibited substrate recognition. Since the PA28 α oligomer binds to the alpha ring, it is possible that the binding site(s) for α Syn on the proteasome may be sterically occluded by the activator complex.

To further elucidate the interaction between the substrate and 20S, attention was directed toward the difference in activity between the two 20S preps. In addition to the difference in protease and peptidase activities, the two proteasomes migrate differently in a native gel (Figure 6-7), which suggested that there was a compositional difference between the two enzymes. Analysis of the

two preparations by two-dimensional electrophoresis identified two areas of difference, where one preparation had spots and the other did not (Figure 6-8). Subsequent mass spectrometry identified the spots unique to M57 as the $\alpha 6(\alpha 1)$ subunit (Figure 6-9), which was confirmed by Western blotting (Figure 6-10). The M58-unique spots were also identified as $\alpha 6(\alpha 1)$ by Western blotting (Figure 6-11). These data conclusively identified the difference between the M57 and M58 proteasomes, as well as the accompanying difference activity profiles, to an as-yet unidentified modification of the $\alpha 6(\alpha 1)$ subunit.

Previously published reports have identified several post-translational modifications of the $\alpha 6(\alpha 1)$ subunit (Table 6-1). These modifications include N-terminal acetylation (Claverol et al., 2002; Tokunaga et al., 1990; Uttenweiler-Joseph et al., 2008), oxidation (Zong et al., 2008), C-terminal truncation (Arizti et al., 1993; Arribas et al., 1994), and phosphorylation (Fernandez Murray et al., 2000). The existence of functionally relevant *in vivo* modifications remains an open question. For example, a subsequent mass spectrometric study was not able to replicate the N-terminal acetylation data (Claverol et al., 2002).

Table 6-1. Identified post-translational modifications of $\alpha 6(\alpha 1)$.

source organism	PTM	Reference
Yeast	Phosphorylation	Claverol et al., 2002
Rat	C-terminal truncation N-terminal acetylation	Arizti et al., 1993 Tokunaga et al., 1990
Mouse	Oxidation	Zong et al., 2008
Human	N-terminal acetylation	Uttenweiler-Joseph et al., 2008

Given that $\alpha 6(\alpha 1)$ was previously found to be phosphorylated, M57 and M58 were treated with λ phosphatase in an effort to identify that modification (Figure 6-11). M58 appeared to be partially phosphorylated, as a new set of spots appeared following incubation with the phosphatase. The M57 pattern was only slightly changed, indicating little if any phosphorylation.

Additionally, two isoforms of the human and rat $\alpha 6(\alpha 1)$ subunit have been identified, termed “long” and “short”, that differ by five amino acids at the N terminus (Coux et al., 1994; Silva Pereira et al., 1992). The short isoform is translated from a shortened mRNA message that lacks the first fifteen nucleotides of exon 2, which encode residues 2-6. Similarly, long and short forms of $\alpha 6(\alpha 1)$ have been observed in fruit flies (Covi et al., 1999), although these were not experimentally confirmed as splice variants. The loss of residues 2-6 has been predicted to change the pI by approximately half a pH unit, from 7.28 for the long isoform to 6.90 for the short isoform, as calculated by MWCALC algorithm (Claverol et al., 2002). By contrast, using the pI/MW algorithm available on the ExPASy server (Gasteiger et al., 2005), the long isoform was predicted to have a pI of 6.51 and a molecular weight of 30.2 kDa, while the short isoform was predicted to have a pI of 6.15 and a molecular weight of 29.6 kDa. Neither the change in pI and the change in molecular weight is consistent with the observed difference in the $\alpha 6(\alpha 1)$ between the M58 and M57 preps. The observed molecular weight shift is too large to be caused by the loss of just five amino acids. The smaller molecular weight M57 $\alpha 6$ spots are more basic than the larger $\alpha 6$ spots of M58, which is inconsistent with the prediction of the short splicing isoform being more acidic. Therefore, the splice variants identified in human tissue cannot account for the novel M57 $\alpha 6$ forms. Additionally, there is only one isoform of the $\alpha 6(\alpha 1)$ subunit reported for the bovine sequence. Assays do not

appear to have been performed on the bovine DNA to identify alternative start sites or alternative splice sites.

The tryptic peptides of the M57 $\alpha 6(\alpha 1)$ spot did not cover the N- or C-termini, which have been separately documented to be changes in sequence by splicing (Ni et al., 1995; Silva Pereira et al., 1992) and cleavage (Arizti et al., 1993), respectively. Experiments are currently underway to identify the N-terminal sequence of the preparation-specific spots, which tests the hypothesis that the change in pI and mobility is due to a splice variant. Isolation of the full-length subunit from the complex has proven to be experimentally difficult, as attempts at purifying $\alpha 6(\alpha 1)$ via reversed-phase HPLC separation did not yield a sufficient amount for whole-mass analysis by mass spectrometry.

Previous work identified the alpha subunits $\alpha 3$ and $\alpha 7$ as capable of regulating proteasomal activity (Bajorek et al., 2003; Groll et al., 2000). Deletion of the N-terminus of $\alpha 3$ increased the basal peptidase activity of 20S (Groll et al., 2000), while a double deletion of the N-termini of both $\alpha 3$ and $\alpha 7$ increased protease activity against carboxymethylated casein (Bajorek et al., 2003). The modification of $\alpha 6(\alpha 1)$ that correlates with the endoproteolytic activity of natural IDPs is the first identification of $\alpha 6(\alpha 1)$ as a participant in the regulation of 20S proteasomal activity, and the first modification not produced by experimental design. The modification of $\alpha 6(\alpha 1)$ may contribute to a conformational change in the gate that creates an intermediate state, between latent and active, that allows luminal entry of peptide substrates but retains a regulatory capability that is selective for certain protein substrates.

The physiological relevance of the modification is underscored by the identification of multiple substrates for the 20S proteasome in tissue extracts. Protein extracts of rodent livers that have been enriched for proteins that do not bind a hydrophobic interaction column contain multiple species that appear to be degraded by the 20S proteasome *in vitro* (Figure 6-14). One of the identified substrates was glyceraldehyde-3-phosphate dehydrogenase (GAPDH), which has been implicated in neurodegenerative disease and therefore makes the metabolism of GAPDH an area of interest (Mazzola and Sirover, 2002). A second substrate was identified as protein disulfide isomerase, which is important for proper protein folding in the endoplasmic reticulum, including the loading of antigenic peptides onto MHC class I molecules and reducing disulfides in preparation for ER-assisted degradation (ERAD) (Appenzeller-Herzog and Ellgaard, 2008). PDI has also been implicated in neurodegeneration; it was found to be upregulated in cell culture models of PD, as well as present in LBs of human PD patients (Conn et al., 2004). The protein sequences of GAPDH and PDI were analyzed using the disorder prediction algorithm DisEMBL (Linding et al., 2003). The algorithm predicted some regions of moderate disorder by two of the three definitions of disorder, but no region in either protein was predicted to be disordered by all three definitions (data not shown). A more detailed analysis of these sequences is necessary to identify potential regions that might be recognized by 20S, and *in vitro* degradation assays with purified proteins should be performed to empirically determine their susceptibility to degradation.

In addition to GAPDH and PDI, several proteins in cell extracts were found to be degraded by 20S (Tsvetkov et al., 2008). A functional role for the 20S proteasome *in vivo* is likely given the prevalence of 20S particles in the cell (Brooks et al., 2000; Peters et al., 1994). One role for 20S has been proposed to be the turnover of nascent polypeptide chains that resulted from aborted ribosomal translation (Qian et al., 2006). However, the data presented here suggest that the *in vivo* function for 20S is potentially more substantial, and that the turnover of IDPs may be partially mediated by the 20S proteasome in a highly regulated manner.

Chapter Seven

Prospectus for Future Work

The work described in this dissertation may be continued through two lines of research. The first focuses on the relationship between the truncated α Syn proteins and Lewy body diseases, and the second is to further study and elucidate the mechanism by which the 20S proteasome recognizes and degrades intrinsically disordered proteins.

Regarding the polyclonal antibodies that are specific for the C-termini of truncated forms of α Syn, the next effort should be to increase the affinity of the antibodies for the target proteins in tissue to enable their conclusive identification. Signal strength proved to be the limiting factor for detecting α Syn110 and α Syn119 in the Western blots of tissue extracts, with only α Syn119 being faintly detected. The published report from Elan Pharmaceuticals demonstrated that a high-affinity, specific polyclonal antibody for α Syn119 is possible (Anderson et al., 2006). Perhaps the Western blot conditions tested so far have not exhausted the possibilities to enhance the interaction between the polyclonal antibodies and the antigens, such that low nanogram to pictogram quantities can be detected by Western blot. Most of the experiments, including the *in vitro* Western blots and ELISAs and the immunohistochemistry of the brain tissue, were performed with crude sera. Purification of the IgG from the sera from three of the antibodies, 1976-2, 1977-1, and 1977-2, removed significant amounts of serum proteins (data not shown), and thus may enhance the signals obtained from Western blots with the variation of just a few more parameters. A conclusive identification of the truncated species of α Syn in brain tissue will provide valuable information to the identity of the protease(s) responsible for producing these highly amyloidogenic forms of α Syn.

Furthermore, the polyclonal antibodies were able to distinguish truncations from other forms of α Syn as shown by slot blot analysis (Figure 5-1). While some antibodies were more specific than others, this is sufficient data to warrant the development of monoclonal antibodies against α Syn truncations. Monoclonal antibodies have several advantages over polyclonals. These advantages include the potential for greater specificity due to the selection of a single recognition epitope, and the ability to produce unlimited amounts of the antibody from hybridomas in cell culture.

Ideally, the use of antibodies against truncated α Syn would find a wider use in the search for understanding and identifying pathogenesis. Because C-terminally truncated α Syn appears to participate in pathogenesis, as evidenced by multiple mouse models, the development of cell culture assays that monitor the production of α Syn truncations could make use of the terminus-specific antibodies through ELISAs, which would enable high-throughput screening of gene products and small molecules for the inhibition of α Syn truncation. An even more impressive and ambitious goal may be to use terminus-specific antibodies for clinical diagnosis of LBDs. Many groups are searching for markers of Parkinson's disease and other Lewy body diseases that can be easily screened in patients, such as proteins that circulate in the blood or cerebrospinal fluid. Should a truncated form of α Syn prove to be a marker for early stages of LBD, an antibody specific for that form could be useful for both research and diagnostic purposes.

A more near-term application of antibodies against truncated α Syn would be to analyze the brain tissue of mouse models of PD for the presence of truncated α Syn. These reagents could directly test the hypothesis that C-terminal truncated α Syn is formed by a disruption of the ubiquitin-proteasome system. For example,

the truncation-specific antibodies could be used to evaluate the brain tissue from the PA700-knockdown mouse model of neurodegeneration, in which the 26S proteasome is compromised but the 20S proteasome remains functional (Bedford et al., 2008). If an increase in the production of truncated α Syn was observed, it would provide strong support for our model of pathogenesis in which a dysfunctional UPS enhances the role of the 20S proteasome in protein turnover, increasing the chance that cytotoxic fragments will be produced.

Regardless of the identity of the protease that is responsible for α Syn truncation *in vivo*, the phenomenon of intrinsically disordered protein degradation by the 20S proteasome is both interesting, from a macromolecular machine perspective, and potentially revolutionary to cell biology, given the prevalence of IDPs in the cell. The first priority for this project is to precisely identify the modification of the $\alpha 6(\alpha 1)$ subunit that correlates with the endoproteolytic activity. Currently, the subunit from both endoproteolytic and latent preps is being analyzed by N-terminal sequencing. Because the mammalian $\alpha 6(\alpha 1)$ subunit is known to exist in two splicing isoforms that differ in five amino acids at the N-terminus, five cycles of the Edman degradation reaction will show what isoform(s) are in the proteasome preparations.

If the Edman degradation does not reveal a difference between the N-termini of the $\alpha 6(\alpha 1)$ subunits from the M57 and M58 proteasome preparations, then other methods will be necessary to identify the nature of the modification. As noted above, the isolation of $\alpha 6(\alpha 1)$ subunit by reversed-phase HPLC may work, although additional conditions would need to be screened to disassociate the 20S complex while still allowing the individual subunits to be sufficiently soluble in the mobile phase for elution from the column. Other methods for

isolating the $\alpha 6(\alpha 1)$ subunit should also be investigated, including electroelution and passive elution from the 2D gel. However, the conditions required for whole-mass analysis by mass spectrometry exclude the use of any detergents, which rules out any method of separation that involves SDS electrophoresis. A solution-based separation of subunits based on pI may also be useful, although the amount of proteasome required for even the smallest-scale analysis will be considerable (in the high microgram to low milligram quantities), given the unavoidable dilution of the applied sample into the final collected fractions.

Once the modification is identified, additional work must be done to understand the mechanism by which the modification functions. *In vitro* manipulation should be performed to convert one form of the proteasome into the other, as measured by both structural analysis (2D electrophoresis) and activity assays. Another primary goal should be to identify the same modified form of the proteasome *in vivo*. Western blots for $\alpha 6(\alpha 1)$ subunit are currently being performed on 2D gels of mammalian cell culture lysates. Similar analysis should also be done for reserved samples of the early steps of 20S purification for two purposes: first, to evaluate if the modified form of the $\alpha 6(\alpha 1)$ subunit is present in the starting material, and second, to identify the step that distinguishes the modified form from the unmodified form. Depending on the nature of the modification, if it is present *in vivo* then there are a variety of assays that could be performed in cell culture to manipulate the modification through cell signaling pathways.

Much work remains to be done to understand the precise elements of intrinsically disordered denatured proteins that make them susceptible to 20S. α Syn is an acceptable and well-characterized model substrate, but as we and

others have demonstrated, there is a variety of proteins that are diverse in structure and conformational flexibility that are also substrates for the 20S proteasome. Manipulations of sequence, structure, and stability could be performed on substrates other than α Syn and assayed for susceptibility to 20S degradation. A particularly promising place to start is with the two potential substrates for 20S that were identified in mouse liver tissue, GAPDH and PDI, should be recombinantly expressed and purified for *in vitro* confirmation of their ability to be degraded by 20S. If they are confirmed as substrates, then the structure and sequence of these proteins should be analyzed for regions of intrinsic disorder, as well as for sequence motifs that may serve as novel “degrons” for 20S-mediated proteolysis.

Appendix A

Materials and Methods

General materials and experimental methods that were used throughout this work are described here. Within each of the chapters, specific experimental conditions are detailed as necessary.

Recombinant expression and purification of α -synuclein

α Syn was expressed and purified as described (Liu et al., 2005). Briefly, α Syn was recombinantly expressed in BL21(DE3) *Escherichia coli* (see Table A-1 for expression vectors). Following inoculation from an overnight culture, the cultures were allowed to grow to an OD of 0.6 before induction with 1 mM IPTG per 1 L of culture. After 4 hours of induction, the cells were pelleted at 5000 \times g. The pelleted cells were resuspended in lysis buffer (20 mM Tris, pH 7.6 at 4°C, 20 mM NaCl, and Complete protease inhibitor (Roche)). Lysis was executed by 2 min of sonication in an ice water bath, at power output 5 and 50% duty cycle. The lysed cell suspension was centrifuged at 40,000 \times g for 20 min at 4°C, and the supernatant was removed to a fresh tube and heated to 90°C for 10 min. Aggregated material was again removed by centrifugation at 40,000 \times g for 20 min at 4°C. The resulting supernatant was brought to 1M (NH₄)₂SO₄ and incubated for 45 min at 4°C with 8 mL of a 50% slurry of equilibrated phenyl-sepharose beads per 30 mL of cleared lysate. The unbound fraction was separated from the beads by filtration through a BioRad glass column, and then brought to 3M (NH₄)₂SO₄ and incubated for 2 hr at 4°C. Following centrifugation at 40,000 \times g for 20 min at 4°C, the supernatant was discarded and the pellet resuspended in 5-10 mL of 20 mM Tris (pH 7.6 at 4°C), 20 mM NaCl. The resuspension was transferred to 3500 MWCO dialysis tubing. The solution was then dialyzed a minimum of 3 times against 100 volumes of 20 mM Tris (pH 7.6 at 4°C), 20 mM

NaCl, 1 mM EDTA at 4°C over 36 hours. The eluate was then subjected to chromatography over a DEAE anion exchange column. The protein was bound in 20 mM Tris (pH 7.6 at 4°C) and 20 mM NaCl and eluted over an 8-25% gradient of 20 mM Tris (pH 7.6 at 4°C) and 1 M NaCl. Fractions were analyzed for purity and concentration by SDS-PAGE and Coomassie blue staining. The fractions with pure protein were pooled, and the solution was transferred to 3500 MWCO dialysis tubing for dialysis into 120 volumes of 20 mM sodium phosphate, pH 7.6 in three equal exchanges. The protein was then concentrated to >250 μM in Amicon centrifugal concentrators with a MWCO of 3000-5000. Aliquots were snap-frozen in liquid N₂ before being stored at -80°C.

Table A-1. Bacterial expression constructs for αSyn proteins.

Protein product	Expression vector
αSyn	pRK172
αSyn	pET28a
His ₆ - αSyn	pET28a
A30P-αSyn	pRK172
E46K-αSyn	pRK172
His ₆ -E46K-αSyn	pET28a
A53T-αSyn	pRK172
αSyn110	pET28a
αSyn119	pET28a
αSyn120	pET28a
αSyn122	pET28a
αSyn123	pET28a
E46K-αSyn119	pET28a
A53T-αSyn110	pET28a
A53T-αSyn120	pET28a

Circular dichroism measurement of α -synuclein

10 μ M α Syn in 350 μ L of 20 mM phosphate buffer (pH 7.2) was incubated for 5 min at room temperature. When indicated, liposomes or liposome buffer were also added. Wavelength scan measurements were taken in duplicate on a JASCO J-810 spectrophotometer in increments of 0.1 nm, with 3 repetitions per sample and an averaging time of 1 sec. For each sample, corresponding background spectra were automatically subtracted using the background correction algorithm of the JASCO Spectra Analysis program.

Bovine proteasome purification: endoproteolytic 20S

20S proteasome was purified from bovine red blood cells essentially as described (McGuire and DeMartino, 1986). Bovine erythrocytes were washed in PBS (137 mM NaCl, 2.7 mM KCl, 8.1 mM Na₂HPO₄, 14.7 mM KH₂PO₄, pH 7.4) and frozen at -80°C. Following thawing at 4°C, cells were lysed in Buffer “50+5” (50 mM Tris (pH 7.6 at 4°C), 5 mM β -mercaptoethanol (β -ME), 20% glycerol). Following centrifugation (11,500 \times g, 1 hr, 4°C), the supernatant incubated batchwise with DE52 anion exchange resin and eluted with Buffer 50+5. The eluate was brought to 40% ammonium sulfate, and the supernatant was separated from precipitate by centrifugation. The supernatant was extensively dialyzed against Buffer 50+5 and purified over a DEAE Fractogel anion exchange column. The elution peak was determined based on both peptidase activity for chymotrypsin-like activity and protease activity against ¹⁴C-casein. The pooled fractions were concentrated on an XM-300 filter (BioRad) and separated on a Sephacryl S300 size exclusion column. The elution peak was again determined by peptidase and protease activities and by gel electrophoresis. The pooled fractions were dialyzed against 20 mM potassium phosphate buffer (5 mM KH₂PO₄/K₂HPO₄, pH 7.6 with HCl, 5 mM β -ME, 20% glycerol). Following separation over hydroxyapatite resin, the peak fraction was again determined by

peptidase and protease activities and by gel electrophoresis. The pooled fractions were dialyzed overnight against Buffer X (20 mM Tris (pH 7.6 at 5°C), 20 mM NaCl, 100 μ M MgCl₂, 100 μ M EDTA, 450 μ M DTT, 20% glycerol), concentrated on an XM-300 filter, and snap-frozen in liquid nitrogen prior to storage at -80°C.

Bovine proteasome purification: latent 20S

20S proteasome was purified from bovine red blood cells as follows. All steps were performed at 4°C. Bovine erythrocytes were washed in PBS (137 mM NaCl, 2.7 mM KCl, 8.1 mM Na₂HPO₄, 14.7 mM KH₂PO₄, pH 7.4) and lysed in 5.5 volumes of Buffer H without glycerol (20 mM Tris-HCl, pH 7.6 at 4°C, 20 mM NaCl, 1 mM EDTA, 5 mM β -ME). The lysate was centrifuged (11,500 \times g, 1 hr, 4°C) to pellet the insoluble material and the resulting supernatant was incubated batchwise with DE52 anion exchange resin in Buffer X (20 mM Tris (pH 7.6 at 5°C), 20 mM NaCl, 100 μ M MgCl₂, 100 μ M EDTA, 450 μ M DTT) and eluted with Buffer X + 400 mM NaCl. The eluate was dialyzed against Buffer X, then separated over a DEAE-Fractogel anion exchange column using a 1400 mL gradient of Buffer X + 50 mM NaCl and Buffer X + 450 mM NaCl. The 20S peak was collected and concentrated on an XM-300 filter (BioRad) before size exclusion chromatography over a Sephacryl S300 column in Buffer X + 120 mM NaCl. The elution peak was again collected and then dialyzed against Buffer K (20 mM KH₂PO₄/K₂HPO₄, pH 7.6 with HCl, 0.1 mM EDTA, pH 7.6, 1 mM MgCl₂, 5 mM β ME, 20% glycerol). The dialysate was bound to a HAP column (2.5cm \times 9cm; 10 g total resin) in Buffer K and eluted over a 500 mL gradient of Buffer K from 20 mM KH₂PO₄/K₂HPO₄ to 250 mM KH₂PO₄/K₂HPO₄. The 20S peak was collected and dialyzed against Buffer X with 120 mM NaCl, then concentrated on a PM-10 filter. The concentrated protein was then again subjected to size exclusion chromatography over the S300 column in Buffer X + 120 mM NaCl, and the eluted 20S was dialyzed against Buffer H + 20% glycerol.

The protein was then concentrated to 2.2 mg/mL, aliquoted, and snap-frozen in liquid N₂ prior to storage at -80°C.

Proteasome peptidase activity assay

Indicated amounts of proteasome and activating complex, when used, were dispensed into the well of a black, clear-bottom 96-well Corning Costar assay plate (#3631). When indicated, the plate was preincubated at the described temperature. The fluorogenic peptide substrate was diluted to a working stock of 50 μM in 50 mM Tris-HCl (pH 8.0 at 37°C) with 5 mM β-ME and preheated to 37°C. 250 μL of the working stock was dispensed into each well of the assay plate and immediately placed into a fluorescence plate reader preheated to 37°C. Samples were read over 20 minutes at appropriate excitation/emission wavelengths (Table A-2) on one of two plate readers: either a Bio-Tek FL600 Microplate Fluorescence Reader or a Molecular Devices SpectraMax5.

Table A-2. Fluorogenic peptide substrates.

Target activity	Peptide-fluorophore	Excitation λ (nm)	Emission λ (nm)
Chymotrypsin	Suc-LLVY-AMC	360	465
Trypsin	Suc-VVR-AMC	360	465
PGPH	Suc-LLE-βNA	340	405

Native gel electrophoresis of proteasome

Proteasomes were diluted into 4X non-denaturing sample buffer (10 mM Tris-HCl, pH 6.8 at 4°C, 15% glycerol, trace bromophenol blue) prior to loading onto a 4% non-denaturing polyacrylamide gel (45 mM Tris, 40 mM boric acid, 0.05 mM EDTA, 1 mM β -ME) and electrophoresed in native gel running buffer (45 mM Tris, 40 mM borate, 0.05 mM EDTA) for 4 hr at 70 V at 4°C. After electrophoresis, the gel was incubated in 50 μ M Suc-LLVY-AMC (diluted from DMSO stock into 50 mM Tris-HCl, pH 8.0 at 37°C, 5 mM β -ME) for 20 minutes at 37°C. The gel was then imaged on an Alpha Innotech fluorescence imager with appropriate filters set for the excitation and emission wavelengths of AMC.

Two-dimensional gel electrophoresis of proteasome

20S proteasome (5 μ g – 20 μ g, in less than 15 μ L) was diluted into a final volume of 125 μ L of rehydration buffer (7 M urea, 2 M thiourea, 4% CHAPS, 65 mM DTT, 0.02% Pharmolytes (pH 3-10), trace amount of bromophenol blue) and incubated at room temperature for 2 hours with occasional mixing. The isoelectric focusing gel strip (ReadyStrip IPG Strip, 7 cm, linear gradient, pH 3-10 BioRad #163-2000) as passively rehydrated with the sample overnight at room temperature. The next day, the strip was subjected to isoelectric focusing in BioRad Protean IEF Cell using a six-step program at 20°C: 50V, 10hr; 500V, 250 Vhr; 1000V, 500Vhr; 5000V, 7500 Vhr; 50V, 12 hr; 50 V, 24 hr (the last steps are holding steps and were occasionally omitted as time permitted). The strip was then incubated in 5 mL equilibration buffer (50 mM Tris-HCl, pH 8.8, 6M urea, 30% glycerol, 2% SDS, 65 mM DTT, trace amount bromophenol blue) in a 15-mL conical tube for 15 min at room temperature with shaking. The strip was then loaded onto the top of a 1.5 mm 12.5% polyacrylamide gel (no stacking gel), flanked by two 5-mm wide strips of filter paper that had been spotted with ~10 μ L

of molecular weight marker (New England Biolabs, #P7708S). The IEF strip was overlaid with sealing solution (0.5% agarose in cathode buffer), then electrophoresed at 30V for 20 minutes until the sample entered the separating gel, when the voltage was increased to 90V for approximately 5 hours. The gel was then either transferred to a membrane for blotting or stained with Coomassie blue.

In vitro RNase Sa degradation assay

3 μ g of RNase Sa was incubated with 200 nM M39 20S proteasome in reaction buffer (20 mM Tris-HCl, 20 mM NaCl, 1 mM EDTA, 10% glycerol) at 27 °C. Aliquots were removed at the indicated timepoints and mixed with SDS sample buffer that did not contain β -ME. Control reactions were performed with 20S proteasome that had been inhibited by β -lactocystin. Samples were loaded onto SDS polyacrylamide gels without preheating, and the gels stained with Coomassie blue.

In vitro α Syn degradation assay

20S proteasomal degradation of α Syn was carried out as previously described (Liu et al., 2005). Briefly, α Syn was incubated with 20S proteasome at indicated concentrations at 37°C in Buffer A (20 mM Tris-HCl, 20 mM NaCl, 1 mM EDTA, pH 7.1 at 37°C). When appropriate, control buffers or additional reagents were included in the reaction mixture. Aliquots were removed at indicated timepoints and the degradation reaction stopped by the addition of 5X SDS sample buffer and the samples held on ice prior to boiling at 100°C. Samples were separated on a 12.5% Tricine SDS polyacrylamide gel and transferred to 0.45 μ m nitrocellulose. The membrane was then subjected to Western blotting with a 1:1000 dilution in TBS-T with 3% BSA and 0.02% NaN_3 of the monoclonal antibody Syn303, which recognizes amino acids 2-4.

Liposome preparation

Liposomes were prepared essentially as described (Eliezer et al., 2001). 1-palmitoyl-2-oleoyl-*sn*-glycero-3-phosphocholine (POPC) and 1-palmitoyl-2-oleoyl-*sn*-glycero-3-phosphate (monosodium salt) (POPA) were obtained from Avanti Polar Lipids, Inc. Equimolar amounts of the lipids were combined, and the chloroform evaporated under nitrogen followed by lyophilization for a minimum of 3 hr. Following resuspension to a final concentration of 2.5 mM in lipid buffer (100 mM NaCl, 10 mM Na₂HPO₄, pH 7.4), the solution was sonicated for 4 cycles of 2 min each (power 3, 40% duty cycle), at which point the optical density approached that of buffer.

α -synuclein fibrillization assay

500 μ L reactions of 100 μ M α Syn were prepared as previously described, with some modification (Liu et al., 2005). Samples also either contained lipid buffer or 250 μ M lipids in the form of vesicles. Where present, 20S proteasome, was added at a final concentration of 20 nM. Samples were incubated at 37°C for 10 min followed by the addition of the proteasomal inhibitor MG132 at a final concentration of 100 μ M. After mixing, the sample was centrifuged at 16,000 \times *g* for 30 sec at room temperature prior to initiating the Thioflavin T assay. The aggregation reaction was performed in triplicate in microtiter plates with a Teflon bead, essentially as described (Liu et al., 2005). The plates were sealed with an ABI-PRISM optical adhesive cover (Applied Biosystems), and shaken continuously for 8 min 20 sec of every 10 min at 37°C. Thioflavin T fluorescence was monitored at 450 nm excitation/482 nm emission on a Molecular Devices fluorescence plate reader. An aliquot of the reaction mix was reserved for analysis of fragment production by SDS-PAGE and western blotting.

α -synuclein oligomerization assay

650 μ L reactions containing 100 μ M α Syn were prepared as for the fibrillization reactions described above. The reaction was then performed in quadruplicate, with 150 μ L aliquoted into four separate wells of a 96-well plate. At appointed times, a 10 μ L aliquot was removed from one of the quadruplicates and spotted 2 μ L at a time onto a 0.45 μ m nitrocellulose membrane. After all the timepoints had been acquired, the membrane was blocked in TBS with 0.05% Tween-20 (TBS-LowTween) with 10% milk. The membrane was then blotted with a 1:8000 dilution of I-11 anti-oligomer antibody (generous gift of R. Kaye, UTMB) in TBS-LowTween with 5% milk, followed by a 1:10,000 dilution of anti-rabbit secondary (Jackson Immuno-Research, #111-035-144; resuspended in water and stored in aliquots at -20°C) in TBS-LowTween with 5% milk. Detection was performed with SuperSignal West Dura Extended Duration Substrate (Pierce, #34075).

Polyclonal antibody development

Rabbit polyclonal antibodies were produced by Proteintech Group, Inc. The antigens used for immunization were synthetic peptide heptamers, synthesized by Proteintech Group, Inc., conjugated to the carrier protein keyhole limpet hemocyanin. The peptides are identical to the last seven amino acids of each of four truncations of α Syn: α Syn110, α Syn119, α Syn122, and α Syn123. For each antigen, two rabbits were immunized. Preimmune sera were also collected from each animal. The crude serum from the final bleed of each rabbit was diluted 1:5000 in TBS-T (Tris-buffered saline with 0.05% Tween-20) and used in a slot-blot against a panel of recombinant α Syn proteins: full-length α Syn, α Syn110, α Syn119, α Syn122, and α Syn123 (50 ng each). Additionally, 5 μ M purified recombinant α Syn was incubated with 10 nM 20S proteasome (500:1

α Syn:20S) or 75 μ M α Syn with 15 nM 20S (5000:1 α Syn:20S) in reaction buffer (20 mM Tris, 20 mM NaCl, 1mM EDTA, pH 7.2 at 37°C) for 15 minutes at 37°C. Aliquots were removed and subjected to Western blotting using a 1:5000 dilution of each polyclonal terminus-specific serum in TBS-T. In both assays, all C-terminally truncated fragments of α Syn were identified in control blots using either the monoclonal anti- α Syn antibody (BD Biosciences) or the N-terminal specific α Syn antibody Syn303 (recognition epitope: residues 2-4).

Enzyme-linked immunosorbent assay (ELISA)

This assay was adapted from a previously published protocol (Harlow and Lane, 1988). Recombinant α Syn proteins (full-length, α Syn110, α Syn119, α Syn122, and α Syn123) were diluted in 20 mM phosphate buffer (pH 7.2) to working stocks of 5-20 μ g/mL as needed to attain the desired amount of final protein (μ g) in 50 μ L. The protein solutions were then applied to the wells of a 96-well Corning Costar EIA/RIA clear polystyrene plate that was high-binding certified (#9018), 50 μ L of the working stock per well. A plastic lid was placed on the plate to prevent evaporation, and the plate was incubated 6-8 hours at room temperature on a plate rocker. The plate was then washed twice with 300 μ L/well phosphate buffered saline (PBS: 137 mM NaCl, 2.7 mM KCl, 10 mM Na₂HPO₄, 1.76 mM KH₂PO₄, pH 7.2)). 300 μ L of blocking solution (3% bovine serum albumin, 0.02% sodium azide in PBS) was then applied to each well and the plate again incubated for 5-8 hours at room temperature on the rocker. The plate was again washed twice as before. Dilutions of primary polyclonal antibodies were prepared in blocking solution, added to the wells at 50 μ L/well, and incubated for 2 hours at room temperature on the plate rocker. Following 4 washes with PBS, the secondary antibody (anti-rabbit, Jackson ImmunoResearch #111-035-005) was diluted into PBS + 3% BSA, dispensed onto the plate at 100 μ L/well, and

incubated at room temperature for 2 hours on the plate rocker. The plate was then washed 4 times with PBS. 100 μ L/well of OPD substrate (Pierce; 10X OPD buffer #34062, OPD #34005) was applied to the plate and then allowed to develop for 10-20 minutes at room temperature. During this time, absorbance was read at regular intervals on a Molecular Devices SpectraMax absorbance plate reader at 450 nm. The assay was stopped by the addition of 50 μ L/well of 2.5 M sulfuric acid, at which time the absorbance was read for a final time at a wavelength of 490 nm.

Dissection and storage of human brain tissue

Samples of human brain tissue were obtained from the Alzheimer's Disease Center at UT-Southwestern, for which the samples had been obtained and stored as follows. At autopsy, one of the cerebral hemispheres was sectioned coronally at 1-cm intervals. The slabs were placed in plastic bags and then stored at -80°C . Approximately 0.5 grams of frozen cortical tissue was dissected from the anterior cingulate gyrus and used for biochemical studies. A signed consent for brain autopsy had been obtained from the next of kin or legal representative in each case.

Sequential fractionation of human brain tissue

Samples of cingulate cortex from human patients were sequentially fractionated as described (Liu et al., 2005). All centrifugations were performed at $100,000\times g$. The tissue was homogenized in liquid N_2 with a ceramic mortar and pestle and transferred to a preweighed 1.5 mL microcentrifuge tube. After weighing the recovered tissue, the sample was resuspended in Buffer A (20 mM Tris-HCl, pH 7.6 at 4°C , 750 mM NaCl, 5 mM EDTA with Complete Protease Inhibitor (Roche)) at a concentration of 6 mL per gram of tissue. The suspension was centrifuged at 4°C , and the supernatant was saved as the high-salt soluble

fraction. The pellets were washed twice with the same volume of Buffer A. The pellets were then resuspended in 3 mL/g in Buffer B (20 mM Tris-HCl, pH 7.6 at 25°C, 4% SDS with Complete Protease Inhibitor (Roche)). Following centrifugation at 25°C, the supernatant was saved as the SDS-soluble fraction, and the pellets washed twice with the same volume of Buffer B. The pellets were then resuspended in Buffer C (20 mM Tris-HCl, pH 7.6 at 25°C, 8 M urea) and sonicated for 15 seconds at 50% duty cycle, power output 2. The suspension was centrifuged at 25°C, and the supernatant was saved as the urea-soluble fraction. The fractions were diluted into 1X SDS sample buffer, separated by gel electrophoresis in a 12.5% Tricine polyacrylamide gel, and transferred to nitrocellulose. Western blots were performed using each of the terminus-specific antibodies as the primary antibody at the indicated dilutions. To verify the fractionation, control Western blots were performed using a monoclonal anti- α Syn antibody (BD Biosciences) at a 1:5000 dilution in TBS-T with 3% BSA and 0.02% NaN₃.

Immunohistochemistry of patient brain samples

Tissue microarrays (TMAs) had been prepared for a previous study and were available as resource in the beginning of this study. Each punch of tissue was 1.5 mm in diameter. The TMAs were prepared using a tissue microarrayer (Beecher Instruments, Sun Prairie, WI). The tissue sections were pretreated with proteinase K (#53020; Dako, Carpinteria, CA) for 15 min before incubation in a 1:500 dilution of the primary antisera. The slides were detected using the alkaline-phosphatase based ultraView Red detection system (Ventana Medical Systems, Tucson, AZ) with the chromogen Fast Red/Naphthol. The entire immunotaining procedure was performed using the Benchmark XT automated stainer (Ventana).

Fractionation of mouse liver tissue

Eleven perfused mouse livers were harvested at the time of animal sacrifice and immediately placed in a beaker containing cold homogenizing medium (HM, 0.25 M sucrose, 1 mM DTT in PBS (137 mM NaCl, 2.7 mM KCl, 10 mM Na₂HPO₄, 1.76 mM KH₂PO₄, pH 7.2)). The samples were washed in HM, the wet weight of the livers measured, and then flash-frozen in liquid N₂ prior to storage at -80°C. Six weeks later, the livers were thawed on ice, minced to a paste-like consistency, and then rinsed with 5 volumes of HM. The tissue was then subjected to 8 passes in a Dounce homogenizer in 2 volumes of HM plus Complete Protease Inhibitor (Roche). The resulting homogenate was passed through four layers of cheesecloth that had been pre-moistened with HM. The volume of the homogenate was then brought to twice the liver weight (final w/v = 50%) and the solution centrifuged at 150,000×g for 30 min at 4°C. The resulting supernatant was flash-frozen in liquid N₂ for overnight storage at -80°C. The following morning, the solution was re-centrifuged at 125,000×g for 30 min at 4°C. The pellet was reserved and resuspended in HM+protease inhibitor for later analysis. The supernatant was divided into four equal fractions and brought to either 0.5 M, 1.0 M, 1.5 M, or 2.0 M (NH₄)₂SO₄. These fractions were then centrifuged in a benchtop centrifuge at 16,000×g for 10 min at 4°C to pellet precipitated proteins, and then the resulting supernatant incubated with charged phenyl sepharose beads (Amersham) for 30 min at 4°C. The unbound fraction was collected, and the beads washed with 1 mL of the appropriate concentration of (NH₄)₂SO₄. The wash flowthrough was reserved for later analysis. All samples were desalted by overnight dialysis against PBS with 10 mM EDTA and 1 mM phenylmethylsulfonylfluoride at 4°C. The total protein concentration of each sample was determined by the Bradford assay, a CD spectrum of each was taken, and aliquots of the samples were electrophoresed on an SDS

polyacrylamide gel for Coomassie blue staining. Samples were divided into 6×200 μ L aliquots and flash-frozen in liquid N₂.

20S degradation assay with mouse liver fractions

An aliquot of the 1.0 M (NH₄)₂SO₄ fraction was thawed on ice and the total protein concentration determined by the Bradford assay. The fraction was brought to 1.0 mg/mL in Buffer A (20 mM Tris-HCl, 20 mM NaCl, 1 mM EDTA, pH 7.1 at 37°C) with 0.1 mg/mL α Syn protein added (as a marker for functional 20S degradation) and 100 nM M57 20S. The reaction was incubated at 37°C, with timepoints taken as indicated. A simultaneous reaction was performed with 20S that had been pre-inhibited with 0.1 mM MG132. The samples were electrophoresed on a large 12.5% SDS polyacrylamide gel, then stained with Coomassie blue.

Appendix B

Chapter Collaborations

Chapter Three

Collaborators for the work described in Chapter Three are as follows: David Thompson and George DeMartino, Ph.D. (UT-Southwestern, Department of Physiology), for essential and extensive assistance in purifying the M57 20S from bovine erythrocytes; Rakez Kayed, Ph.D. (University of Texas Medical Branch at Galveston, Texas), for the kind gift of the anti-oligomer antibody and for providing training assistance in its use; Yan Li in the UTSW Protein Chemistry Technology Core for whole-mass spectrometric identification of the synE46K(1-73) fragment; Arynn Yaeger (UT-Southwestern, Department of Physiology) for assistance in expression and purification of the α Syn proteins; and Virginia M.-Y. Lee, Ph.D. (University of Pennsylvania School of Medicine), for the kind gift of the antibody Syn303.

Chapter Four

Collaborators for the work described in Chapter Four are as follows: Kimmo Hatanpaa, M.D., Ph.D. (UT-Southwestern Department of Neuropathology), for providing brain tissue samples, executing the immunohistochemistry experiments, and experimental design and discussion; Chan Foong, M.S. (UT-Southwestern Department of Neuropathology), for dissection and recovery of the brain tissue samples; Arynn Yaeger (UT-Southwestern, Department of Physiology) for assistance with the development of ELISAs; and Virginia M.-Y. Lee, Ph.D. (University of Pennsylvania School of Medicine), for the kind gift of the antibody Syn303.

Chapter Five

Collaborators for the work described in Chapter Five are as follows: Nick Pace, Ph.D. (Texas A&M University), for the gift of the RNase Sa mutant proteins and determination of the T_m values; Chang-wei Liu, Ph.D. (currently of University of Colorado Health Sciences Center at Denver), for the degradation assays of the RNase Sa mutant proteins and of the α Syn N-terminal truncations and for the CD analysis of the α Syn N-terminal truncations; David Thompson and George DeMartino, Ph.D. (UT-Southwestern, Department of Physiology) for proteasome preparations; Thomas Gillette (UT-Southwestern, Department of Physiology) for the kind sharing of the monoclonal anti- $\alpha 6(\alpha 1)$ antibody; Junmei Zhang and Yan Li (UT-Southwestern Protein Chemistry Technology Center) for mass spectrometry identification and analysis of the $\alpha 6(\alpha 1)$ subunit; Aryn Yaeger (UT-Southwestern, Department of Physiology) for the development and execution of the liver fractionation assays; and Virginia M.-Y. Lee, Ph.D. (University of Pennsylvania School of Medicine), for the kind gift of the antibody Syn303.

References

- Aarsland, D., Ballard, C., Larsen, J. P., and McKeith, I. (2001). A comparative study of psychiatric symptoms in dementia with Lewy bodies and Parkinson's disease with and without dementia. *Int J Geriatr Psychiatry* 16, 528-536.
- Aarsland, D., Perry, R., Brown, A., Larsen, J. P., and Ballard, C. (2005a). Neuropathology of dementia in Parkinson's disease: a prospective, community-based study. *Ann Neurol* 58, 773-776.
- Aarsland, D., Perry, R., Larsen, J. P., McKeith, I. G., O'Brien, J. T., Perry, E. K., Burn, D., and Ballard, C. G. (2005b). Neuroleptic sensitivity in Parkinson's disease and parkinsonian dementias. *J Clin Psychiatry* 66, 633-637.
- Ahn, M., Kim, S., Kang, M., Ryu, Y., and Kim, T. D. (2006). Chaperone-like activities of alpha-synuclein: alpha-synuclein assists enzyme activities of esterases. *Biochem Biophys Res Commun* 346, 1142-1149.
- Alim, M. A., Ma, Q. L., Takeda, K., Aizawa, T., Matsubara, M., Nakamura, M., Asada, A., Saito, T., Kaji, H., Yoshii, M., *et al.* (2004). Demonstration of a role for alpha-synuclein as a functional microtubule-associated protein. *J Alzheimers Dis* 6, 435-442; discussion 443-439.
- Alvarez-Castelao, B., and Castano, J. G. (2005). Mechanism of direct degradation of IkkappaBalpha by 20S proteasome. *FEBS Lett* 579, 4797-4802.
- Alvarez-Garcia, O., Vega-Naredo, I., Sierra, V., Caballero, B., Tomas-Zapico, C., Camins, A., Garcia, J. J., Pallas, M., and Coto-Montes, A. (2006). Elevated oxidative stress in the brain of senescence-accelerated mice at 5 months of age. *Biogerontology* 7, 43-52.
- Amici, M., Sagratini, D., Pettinari, A., Pucciarelli, S., Angeletti, M., and Eleuteri, A. M. (2004). 20S proteasome mediated degradation of DHFR: implications in neurodegenerative disorders. *Arch Biochem Biophys* 422, 168-174.
- Ancolio, K., Alves da Costa, C., Ueda, K., and Checler, F. (2000). Alpha-synuclein and the Parkinson's disease-related mutant Ala53Thr-alpha-synuclein do not undergo proteasomal degradation in HEK293 and neuronal cells. *Neurosci Lett* 285, 79-82.
- Anderson, J. P., Walker, D. E., Goldstein, J. M., de Laat, R., Banducci, K., Caccavello, R. J., Barbour, R., Huang, J., Kling, K., Lee, M., *et al.* (2006). Phosphorylation of Ser-129 is the dominant pathological modification of alpha-synuclein in familial and sporadic Lewy body disease. *J Biol Chem* 281, 29739-29752.
- Apetri, M. M., Maiti, N. C., Zagorski, M. G., Carey, P. R., and Anderson, V. E. (2006). Secondary structure of alpha-synuclein oligomers: characterization by raman and atomic force microscopy. *J Mol Biol* 355, 63-71.
- Appenzeller-Herzog, C., and Ellgaard, L. (2008). The human PDI family: versatility packed into a single fold. *Biochim Biophys Acta* 1783, 535-548.

- Arizti, P., Arribas, J., and Castano, J. G. (1993). Modulation of the multicatalytic proteinase complex by lipids, interconversion and proteolytic processing. *Enzyme Protein* 47, 285-295.
- Arribas, J., Arizti, P., and Castano, J. G. (1994). Antibodies against the C2 COOH-terminal region discriminate the active and latent forms of the multicatalytic proteinase complex. *J Biol Chem* 269, 12858-12864.
- Bajorek, M., Finley, D., and Glickman, M. H. (2003). Proteasome disassembly and downregulation is correlated with viability during stationary phase. *Curr Biol* 13, 1140-1144.
- Baker, J. M., Hudson, R. P., Kanelis, V., Choy, W. Y., Thibodeau, P. H., Thomas, P. J., and Forman-Kay, J. D. (2007). CFTR regulatory region interacts with NBD1 predominantly via multiple transient helices. *Nat Struct Mol Biol* 14, 738-745.
- Baumeister, W., Walz, J., Zuhl, F., and Seemuller, E. (1998). The proteasome: paradigm of a self-compartmentalizing protease. *Cell* 92, 367-380.
- Bedford, L., Hay, D., Devoy, A., Paine, S., Powe, D. G., Seth, R., Gray, T., Topham, I., Fone, K., Rezvani, N., *et al.* (2008). Depletion of 26S proteasomes in mouse brain neurons causes neurodegeneration and Lewy-like inclusions resembling human pale bodies. *J Neurosci* 28, 8189-8198.
- Bennett, M. C., Bishop, J. F., Leng, Y., Chock, P. B., Chase, T. N., and Mouradian, M. M. (1999). Degradation of alpha-synuclein by proteasome. *J Biol Chem* 274, 33855-33858.
- Berlett, B. S., and Stadtman, E. R. (1997). Protein oxidation in aging, disease, and oxidative stress. *J Biol Chem* 272, 20313-20316.
- Bernado, P., Bertocini, C. W., Griesinger, C., Zweckstetter, M., and Blackledge, M. (2005). Defining long-range order and local disorder in native alpha-synuclein using residual dipolar couplings. *J Am Chem Soc* 127, 17968-17969.
- Bertocini, C. W., Jung, Y. S., Fernandez, C. O., Hoyer, W., Griesinger, C., Jovin, T. M., and Zweckstetter, M. (2005). Release of long-range tertiary interactions potentiates aggregation of natively unstructured alpha-synuclein. *Proc Natl Acad Sci U S A* 102, 1430-1435.
- Beyer, K. (2006). Alpha-synuclein structure, posttranslational modification and alternative splicing as aggregation enhancers. *Acta Neuropathol* 112, 237-251.
- Bisaglia, M., Schievano, E., Caporale, A., Peggion, E., and Mammi, S. (2006). The 11-mer repeats of human alpha-synuclein in vesicle interactions and lipid composition discrimination: a cooperative role. *Biopolymers* 84, 310-316.
- Bisaglia, M., Tessari, I., Pinato, L., Bellanda, M., Giraud, S., Fasano, M., Bergantino, E., Bubacco, L., and Mammi, S. (2005). A topological model of the interaction between alpha-synuclein and sodium dodecyl sulfate micelles. *Biochemistry* 44, 329-339.

- Bove, J., Zhou, C., Jackson-Lewis, V., Taylor, J., Chu, Y., Rideout, H. J., Wu, D. C., Kordower, J. H., Petrucelli, L., and Przedborski, S. (2006). Proteasome inhibition and Parkinson's disease modeling. *Ann Neurol* 60, 260-264.
- Bracken, C., Iakoucheva, L. M., Romero, P. R., and Dunker, A. K. (2004). Combining prediction, computation and experiment for the characterization of protein disorder. *Curr Opin Struct Biol* 14, 570-576.
- Brannigan, J. A., Dodson, G., Duggleby, H. J., Moody, P. C., Smith, J. L., Tomchick, D. R., and Murzin, A. G. (1995). A protein catalytic framework with an N-terminal nucleophile is capable of self-activation. *Nature* 378, 416-419.
- Brooks, P., Fuertes, G., Murray, R. Z., Bose, S., Knecht, E., Rechsteiner, M. C., Hendil, K. B., Tanaka, K., Dyson, J., and Rivett, J. (2000). Subcellular localization of proteasomes and their regulatory complexes in mammalian cells. *Biochem J* 346 Pt 1, 155-161.
- Bussell, R., Jr., and Eliezer, D. (2003). A structural and functional role for 11-mer repeats in alpha-synuclein and other exchangeable lipid binding proteins. *J Mol Biol* 329, 763-778.
- Bussell, R., Jr., and Eliezer, D. (2004). Effects of Parkinson's disease-linked mutations on the structure of lipid-associated alpha-synuclein. *Biochemistry* 43, 4810-4818.
- Bussell, R., Jr., Ramlall, T. F., and Eliezer, D. (2005). Helix periodicity, topology, and dynamics of membrane-associated alpha-synuclein. *Protein Sci* 14, 862-872.
- Carrard, G., Bulteau, A. L., Petropoulos, I., and Friguet, B. (2002). Impairment of proteasome structure and function in aging. *Int J Biochem Cell Biol* 34, 1461-1474.
- Chandra, S., Chen, X., Rizo, J., Jahn, R., and Sudhof, T. C. (2003). A broken alpha-helix in folded alpha-synuclein. *J Biol Chem* 278, 15313-15318.
- Chandra, S., Gallardo, G., Fernandez-Chacon, R., Schluter, O. M., and Sudhof, T. C. (2005). Alpha-synuclein cooperates with CSPalpha in preventing neurodegeneration. *Cell* 123, 383-396.
- Chartier-Harlin, M. C., Kachergus, J., Roumier, C., Mouroux, V., Douay, X., Lincoln, S., Levecque, C., Larvor, L., Andrieux, J., Hulihan, M., *et al.* (2004). Alpha-synuclein locus duplication as a cause of familial Parkinson's disease. *Lancet* 364, 1167-1169.
- Chen, Q., Thorpe, J., and Keller, J. N. (2005). Alpha-synuclein alters proteasome function, protein synthesis, and stationary phase viability. *J Biol Chem* 280, 30009-30017.
- Choi, W., Zibae, S., Jakes, R., Serpell, L. C., Davletov, B., Crowther, R. A., and Goedert, M. (2004). Mutation E46K increases phospholipid binding and assembly into filaments of human alpha-synuclein. *FEBS Lett* 576, 363-368.
- Chu, C. T., Caruso, J. L., Cummings, T. J., Ervin, J., Rosenberg, C., and Hulette, C. M. (2000). Ubiquitin immunohistochemistry as a diagnostic aid for community pathologists evaluating patients who have dementia. *Mod Pathol* 13, 420-426.

- Claverol, S., Burlet-Schiltz, O., Girbal-Neuhauser, E., Gairin, J. E., and Monsarrat, B. (2002). Mapping and structural dissection of human 20 S proteasome using proteomic approaches. *Mol Cell Proteomics* 1, 567-578.
- Cole, N. B., Murphy, D. D., Grider, T., Rueter, S., Brasaemle, D., and Nussbaum, R. L. (2002). Lipid droplet binding and oligomerization properties of the Parkinson's disease protein alpha-synuclein. *J Biol Chem* 277, 6344-6352.
- Conn, K. J., Gao, W., McKee, A., Lan, M. S., Ullman, M. D., Eisenhauer, P. B., Fine, R. E., and Wells, J. M. (2004). Identification of the protein disulfide isomerase family member PD1p in experimental Parkinson's disease and Lewy body pathology. *Brain Res* 1022, 164-172.
- Conway, K. A., Harper, J. D., and Lansbury, P. T. (1998). Accelerated in vitro fibril formation by a mutant alpha-synuclein linked to early-onset Parkinson disease. *Nat Med* 4, 1318-1320.
- Conway, K. A., Harper, J. D., and Lansbury, P. T., Jr. (2000a). Fibrils formed in vitro from alpha-synuclein and two mutant forms linked to Parkinson's disease are typical amyloid. *Biochemistry* 39, 2552-2563.
- Conway, K. A., Lee, S. J., Rochet, J. C., Ding, T. T., Harper, J. D., Williamson, R. E., and Lansbury, P. T., Jr. (2000b). Accelerated oligomerization by Parkinson's disease linked alpha-synuclein mutants. *Ann N Y Acad Sci* 920, 42-45.
- Conway, K. A., Lee, S. J., Rochet, J. C., Ding, T. T., Williamson, R. E., and Lansbury, P. T., Jr. (2000c). Acceleration of oligomerization, not fibrillization, is a shared property of both alpha-synuclein mutations linked to early-onset Parkinson's disease: implications for pathogenesis and therapy. *Proc Natl Acad Sci U S A* 97, 571-576.
- Cooper, A. A., Gitler, A. D., Cashikar, A., Haynes, C. M., Hill, K. J., Bhullar, B., Liu, K., Xu, K., Strathearn, K. E., Liu, F., *et al.* (2006). Alpha-synuclein blocks ER-Golgi traffic and Rab1 rescues neuron loss in Parkinson's models. *Science* 313, 324-328.
- Coux, O., Nothwang, H. G., Silva Pereira, I., Recillas Targa, F., Bey, F., and Scherrer, K. (1994). Phylogenetic relationships of the amino acid sequences of prosome (proteasome, MCP) subunits. *Mol Gen Genet* 245, 769-780.
- Covi, J. A., Belote, J. M., and Mykles, D. L. (1999). Subunit compositions and catalytic properties of proteasomes from developmental temperature-sensitive mutants of *Drosophila melanogaster*. *Arch Biochem Biophys* 368, 85-97.
- Croke, R. L., Sallum, C. O., Watson, E., Watt, E. D., and Alexandrescu, A. T. (2008). Hydrogen exchange of monomeric alpha-synuclein shows unfolded structure persists at physiological temperature and is independent of molecular crowding in *Escherichia coli*. *Protein Sci* 17, 1434-1445.
- Cuervo, A. M., Stefanis, L., Fredenburg, R., Lansbury, P. T., and Sulzer, D. (2004). Impaired degradation of mutant alpha-synuclein by chaperone-mediated autophagy. *Science* 305, 1292-1295.

- David, D. C., Layfield, R., Serpell, L., Narain, Y., Goedert, M., and Spillantini, M. G. (2002). Proteasomal degradation of tau protein. *J Neurochem* *83*, 176-185.
- Davidson, W. S., Jonas, A., Clayton, D. F., and George, J. M. (1998). Stabilization of alpha-synuclein secondary structure upon binding to synthetic membranes. *J Biol Chem* *273*, 9443-9449.
- Davies, K. J., and Shringarpure, R. (2006). Preferential degradation of oxidized proteins by the 20S proteasome may be inhibited in aging and in inflammatory neuromuscular diseases. *Neurology* *66*, S93-96.
- de Laureto, P. P., Tosatto, L., Frare, E., Marin, O., Uversky, V. N., and Fontana, A. (2006). Conformational properties of the SDS-bound state of alpha-synuclein probed by limited proteolysis: unexpected rigidity of the acidic C-terminal tail. *Biochemistry* *45*, 11523-11531.
- Dedmon, M. M., Lindorff-Larsen, K., Christodoulou, J., Vendruscolo, M., and Dobson, C. M. (2005). Mapping long-range interactions in alpha-synuclein using spin-label NMR and ensemble molecular dynamics simulations. *J Am Chem Soc* *127*, 476-477.
- Denny, J. B. (2004). Growth-associated protein of 43 kDa (GAP-43) is cleaved nonprocessively by the 20S proteasome. *Eur J Biochem* *271*, 2480-2493.
- Di Noto, L., Whitson, L. J., Cao, X., Hart, P. J., and Levine, R. L. (2005). Proteasomal degradation of mutant superoxide dismutases linked to amyotrophic lateral sclerosis. *J Biol Chem* *280*, 39907-39913.
- Drescher, M., Godschalk, F., Veldhuis, G., van Rooijen, B. D., Subramaniam, V., and Huber, M. (2008a). Spin-label EPR on alpha-synuclein reveals differences in the membrane binding affinity of the two antiparallel helices. *ChemBiochem* *9*, 2411-2416.
- Drescher, M., Veldhuis, G., van Rooijen, B. D., Milikisyants, S., Subramaniam, V., and Huber, M. (2008b). Antiparallel arrangement of the helices of vesicle-bound alpha-synuclein. *J Am Chem Soc* *130*, 7796-7797.
- Dunker, A. K., Brown, C. J., Lawson, J. D., Iakoucheva, L. M., and Obradovic, Z. (2002). Intrinsic disorder and protein function. *Biochemistry* *41*, 6573-6582.
- Dunker, A. K., Lawson, J. D., Brown, C. J., Williams, R. M., Romero, P., Oh, J. S., Oldfield, C. J., Campen, A. M., Ratliff, C. M., Hipps, K. W., *et al.* (2001). Intrinsically disordered protein. *J Mol Graph Model* *19*, 26-59.
- Dunker, A. K., and Obradovic, Z. (2001). The protein trinity--linking function and disorder. *Nat Biotechnol* *19*, 805-806.
- Dunker, A. K., Obradovic, Z., Romero, P., Garner, E. C., and Brown, C. J. (2000). Intrinsic protein disorder in complete genomes. *Genome Inform Ser Workshop Genome Inform* *11*, 161-171.
- Dyson, H. J., Lerner, R. A., and Wright, P. E. (1988). The physical basis for induction of protein-reactive antipeptide antibodies. *Annu Rev Biophys Chem* *17*, 305-324.

- Edwards, R. J., Singleton, A. M., Murray, B. P., Davies, D. S., and Boobis, A. R. (1995). Short synthetic peptides exploited for reliable and specific targeting of antibodies to the C-termini of cytochrome P450 enzymes. *Biochem Pharmacol* *49*, 39-47.
- El-Agnaf, O. M., Jakes, R., Curran, M. D., Middleton, D., Ingenito, R., Bianchi, E., Pessi, A., Neill, D., and Wallace, A. (1998a). Aggregates from mutant and wild-type alpha-synuclein proteins and NAC peptide induce apoptotic cell death in human neuroblastoma cells by formation of beta-sheet and amyloid-like filaments. *FEBS Lett* *440*, 71-75.
- El-Agnaf, O. M., Jakes, R., Curran, M. D., and Wallace, A. (1998b). Effects of the mutations Ala30 to Pro and Ala53 to Thr on the physical and morphological properties of alpha-synuclein protein implicated in Parkinson's disease. *FEBS Lett* *440*, 67-70.
- Eliezer, D., Kutluay, E., Bussell, R., Jr., and Browne, G. (2001). Conformational properties of alpha-synuclein in its free and lipid-associated states. *J Mol Biol* *307*, 1061-1073.
- Ernst, J. A., and Brunger, A. T. (2003). High resolution structure, stability, and synaptotagmin binding of a truncated neuronal SNARE complex. *J Biol Chem* *278*, 8630-8636.
- Fenteany, G., Standaert, R. F., Lane, W. S., Choi, S., Corey, E. J., and Schreiber, S. L. (1995). Inhibition of proteasome activities and subunit-specific amino-terminal threonine modification by lactacystin. *Science* *268*, 726-731.
- Ferdous, A., Kodadek, T., and Johnston, S. A. (2002). A nonproteolytic function of the 19S regulatory subunit of the 26S proteasome is required for efficient activated transcription by human RNA polymerase II. *Biochemistry* *41*, 12798-12805.
- Fernandez-Chacon, R., Wolfel, M., Nishimune, H., Tabares, L., Schmitz, F., Castellano-Munoz, M., Rosenmund, C., Montesinos, M. L., Sanes, J. R., Schneggenburger, R., and Sudhof, T. C. (2004). The synaptic vesicle protein CSP alpha prevents presynaptic degeneration. *Neuron* *42*, 237-251.
- Fernandez Murray, P., Biscoglio, M. J., and Passeron, S. (2000). Purification and characterization of *Candida albicans* 20S proteasome: identification of four proteasomal subunits. *Arch Biochem Biophys* *375*, 211-219.
- Fink, A. L. (1998). Protein aggregation: folding aggregates, inclusion bodies and amyloid. *Fold Des* *3*, R9-23.
- Fitzgerald, P., Mandel, A., Bolton, A. E., Sullivan, A. M., and Nolan, Y. (2008). Treatment with phosphatidylglycerol-based nanoparticles prevents motor deficits induced by proteasome inhibition: implications for Parkinson's disease. *Behav Brain Res* *195*, 271-274.
- Forster, A., Masters, E. I., Whitby, F. G., Robinson, H., and Hill, C. P. (2005). The 1.9 Å structure of a proteasome-11S activator complex and implications for proteasome-PAN/PA700 interactions. *Mol Cell* *18*, 589-599.
- Forster, A., Whitby, F. G., and Hill, C. P. (2003). The pore of activated 20S proteasomes has an ordered 7-fold symmetric conformation. *Embo J* *22*, 4356-4364.

- Fredenburg, R. A., Rospigliosi, C., Meray, R. K., Kessler, J. C., Lashuel, H. A., Eliezer, D., and Lansbury, P. T., Jr. (2007). The impact of the E46K mutation on the properties of alpha-synuclein in its monomeric and oligomeric states. *Biochemistry* 46, 7107-7118.
- Gasteiger, E., Hoogland, C., Gattiker, A., Duvaud, S., Wilkins, M. R., Appel, R. D., and Bairoch, A. (2005). Protein Identification and Analysis Tools on the ExPASy Server, In *The Proteomics Protocols Handbook*, J. M. Walker, ed. (Totowa, New Jersey: Humana Press), pp. 571-608.
- Geddes, J. W. (2005). alpha-Synuclein: a potent inducer of tau pathology. *Exp Neurol* 192, 244-250.
- Giasson, B. I., Forman, M. S., Higuchi, M., Golbe, L. I., Graves, C. L., Kotzbauer, P. T., Trojanowski, J. Q., and Lee, V. M. (2003). Initiation and synergistic fibrillization of tau and alpha-synuclein. *Science* 300, 636-640.
- Gillette, T. G., Kumar, B., Thompson, D., Slaughter, C. A., and DeMartino, G. N. (2008). Differential roles of the COOH termini of AAA subunits of PA700 (19 S regulator) in asymmetric assembly and activation of the 26 S proteasome. *J Biol Chem* 283, 31813-31822.
- Gitler, A. D., Bevis, B. J., Shorter, J., Strathearn, K. E., Hamamichi, S., Su, L. J., Caldwell, K. A., Caldwell, G. A., Rochet, J. C., McCaffery, J. M., *et al.* (2008). The Parkinson's disease protein alpha-synuclein disrupts cellular Rab homeostasis. *Proc Natl Acad Sci U S A* 105, 145-150.
- Gray, C. W., Slaughter, C. A., and DeMartino, G. N. (1994). PA28 activator protein forms regulatory caps on proteasome stacked rings. *J Mol Biol* 236, 7-15.
- Greenbaum, E. A., Graves, C. L., Mishizen-Eberz, A. J., Lupoli, M. A., Lynch, D. R., Englander, S. W., Axelsen, P. H., and Giasson, B. I. (2005). The E46K mutation in alpha-synuclein increases amyloid fibril formation. *J Biol Chem* 280, 7800-7807.
- Gregersen, N. (2006). Protein misfolding disorders: pathogenesis and intervention. *J Inherit Metab Dis* 29, 456-470.
- Groettrup, M., Soza, A., Eggers, M., Kuehn, L., Dick, T. P., Schild, H., Rammensee, H. G., Koszinowski, U. H., and Kloetzel, P. M. (1996). A role for the proteasome regulator PA28alpha in antigen presentation. *Nature* 381, 166-168.
- Groll, M., Bajorek, M., Kohler, A., Moroder, L., Rubin, D. M., Huber, R., Glickman, M. H., and Finley, D. (2000). A gated channel into the proteasome core particle. *Nat Struct Biol* 7, 1062-1067.
- Groll, M., Ditzel, L., Lowe, J., Stock, D., Bochtler, M., Bartunik, H. D., and Huber, R. (1997). Structure of 20S proteasome from yeast at 2.4 Å resolution. *Nature* 386, 463-471.
- Halle, B. (2002). Flexibility and packing in proteins. *Proc Natl Acad Sci U S A* 99, 1274-1279.
- Han, H., Weinreb, P. H., and Lansbury, P. T., Jr. (1995). The core Alzheimer's peptide NAC forms amyloid fibrils which seed and are seeded by beta-amyloid: is NAC a common trigger or target in neurodegenerative disease? *Chem Biol* 2, 163-169.

Harlow, E., and Lane, D., eds. (1988). *Antibodies: A Laboratory Manual* (Cold Spring Harbor, New York: Cold Spring Harbor Laboratory).

Hatanpaa, K. J., Bigio, E. H., Cairns, N. J., Womack, K. B., Weintraub, S., Morris, J. C., Foong, C., Xiao, G., Hladik, C., Mantanona, T. Y., and White, C. L., 3rd (2008). TAR DNA-binding protein 43 immunohistochemistry reveals extensive neuritic pathology in FTLD-U: a midwest-southwest consortium for FTLD study. *J Neuropathol Exp Neurol* 67, 271-279.

Hishikawa, N., Hashizume, Y., Yoshida, M., and Sobue, G. (2001). Widespread occurrence of argyrophilic glial inclusions in Parkinson's disease. *Neuropathol Appl Neurobiol* 27, 362-372.

Hoyer, W., Cherny, D., Subramaniam, V., and Jovin, T. M. (2004). Impact of the acidic C-terminal region comprising amino acids 109-140 on alpha-synuclein aggregation in vitro. *Biochemistry* 43, 16233-16242.

Hurtig, H. I., Trojanowski, J. Q., Galvin, J., Ewbank, D., Schmidt, M. L., Lee, V. M., Clark, C. M., Glosser, G., Stern, M. B., Gollomp, S. M., and Arnold, S. E. (2000). Alpha-synuclein cortical Lewy bodies correlate with dementia in Parkinson's disease. *Neurology* 54, 1916-1921.

Ibanez, P., Bonnet, A. M., DeBarges, B., Lohmann, E., Tison, F., Pollak, P., Agid, Y., Durr, A., and Brice, A. (2004). Causal relation between alpha-synuclein gene duplication and familial Parkinson's disease. *Lancet* 364, 1169-1171.

Ikeuchi, T., Kakita, A., Shiga, A., Kasuga, K., Kaneko, H., Tan, C. F., Idezuka, J., Wakabayashi, K., Onodera, O., Iwatsubo, T., *et al.* (2008). Patients homozygous and heterozygous for SNCA duplication in a family with parkinsonism and dementia. *Arch Neurol* 65, 514-519.

Inden, M., Kondo, J., Kitamura, Y., Takata, K., Nishimura, K., Taniguchi, T., Sawada, H., and Shimohama, S. (2005). Proteasome inhibitors protect against degeneration of nigral dopaminergic neurons in hemiparkinsonian rats. *J Pharmacol Sci* 97, 203-211.

Iseki, E., Togo, T., Suzuki, K., Katsuse, O., Marui, W., de Silva, R., Lees, A., Yamamoto, T., and Kosaka, K. (2003). Dementia with Lewy bodies from the perspective of tauopathy. *Acta Neuropathol* 105, 265-270.

Iwata, A., Maruyama, M., Akagi, T., Hashikawa, T., Kanazawa, I., Tsuji, S., and Nukina, N. (2003). Alpha-synuclein degradation by serine protease neurosin: implication for pathogenesis of synucleinopathies. *Hum Mol Genet* 12, 2625-2635.

Jao, C. C., Der-Sarkissian, A., Chen, J., and Langen, R. (2004). Structure of membrane-bound alpha-synuclein studied by site-directed spin labeling. *Proc Natl Acad Sci U S A* 101, 8331-8336.

Jellinger, K. A. (2007). Morphological substrates of parkinsonism with and without dementia: a retrospective clinico-pathological study. *J Neural Transm Suppl*, 91-104.

Jellinger, K. A. (2008). A critical evaluation of current staging of alpha-synuclein pathology in Lewy body disorders. *Biochim Biophys Acta*.

- Jensen, P. H., Nielsen, M. S., Jakes, R., Dotti, C. G., and Goedert, M. (1998). Binding of alpha-synuclein to brain vesicles is abolished by familial Parkinson's disease mutation. *J Biol Chem* 273, 26292-26294.
- Ji, L. N., Du, H. N., Zhang, F., Li, H. T., Luo, X. Y., Hu, J., and Hu, H. Y. (2005). An unstructured region is required by GAV homologue for the fibrillization of host proteins. *Protein J* 24, 209-218.
- Jo, E., Darabie, A. A., Han, K., Tandon, A., Fraser, P. E., and McLaurin, J. (2004). alpha-Synuclein-synaptosomal membrane interactions: implications for fibrillogenesis. *Eur J Biochem* 271, 3180-3189.
- Jo, E., Fuller, N., Rand, R. P., St George-Hyslop, P., and Fraser, P. E. (2002). Defective membrane interactions of familial Parkinson's disease mutant A30P alpha-synuclein. *J Mol Biol* 315, 799-807.
- Jo, E., McLaurin, J., Yip, C. M., St George-Hyslop, P., and Fraser, P. E. (2000). alpha-Synuclein membrane interactions and lipid specificity. *J Biol Chem* 275, 34328-34334.
- Kahle, P. J., Neumann, M., Ozmen, L., Muller, V., Jacobsen, H., Schindzielorz, A., Okochi, M., Leimer, U., van Der Putten, H., Probst, A., *et al.* (2000). Subcellular localization of wild-type and Parkinson's disease-associated mutant alpha -synuclein in human and transgenic mouse brain. *J Neurosci* 20, 6365-6373.
- Kayed, R., Head, E., Sarsoza, F., Saing, T., Cotman, C. W., Neucula, M., Margol, L., Wu, J., Breydo, L., Thompson, J. L., *et al.* (2007). Fibril specific, conformation dependent antibodies recognize a generic epitope common to amyloid fibrils and fibrillar oligomers that is absent in prefibrillar oligomers. *Mol Neurodegener* 2, 18.
- Kayed, R., Head, E., Thompson, J. L., McIntire, T. M., Milton, S. C., Cotman, C. W., and Glabe, C. G. (2003). Common structure of soluble amyloid oligomers implies common mechanism of pathogenesis. *Science* 300, 486-489.
- Kim, H. Y., Heise, H., Fernandez, C. O., Baldus, M., and Zweckstetter, M. (2007). Correlation of amyloid fibril beta-structure with the unfolded state of alpha-synuclein. *Chembiochem* 8, 1671-1674.
- Kim, S., Jeon, B. S., Heo, C., Im, P. S., Ahn, T. B., Seo, J. H., Kim, H. S., Park, C. H., Choi, S. H., Cho, S. H., *et al.* (2004). Alpha-synuclein induces apoptosis by altered expression in human peripheral lymphocyte in Parkinson's disease. *Faseb J* 18, 1615-1617.
- Kim, S. J., Sung, J. Y., Um, J. W., Hattori, N., Mizuno, Y., Tanaka, K., Paik, S. R., Kim, J., and Chung, K. C. (2003). Parkin cleaves intracellular alpha-synuclein inclusions via the activation of calpain. *J Biol Chem* 278, 41890-41899.
- Kim, Y. S., Laurine, E., Woods, W., and Lee, S. J. (2006). A novel mechanism of interaction between alpha-synuclein and biological membranes. *J Mol Biol* 360, 386-397.

Kitada, T., Asakawa, S., Hattori, N., Matsumine, H., Yamamura, Y., Minoshima, S., Yokochi, M., Mizuno, Y., and Shimizu, N. (1998). Mutations in the parkin gene cause autosomal recessive juvenile parkinsonism. *Nature* *392*, 605-608.

Klucken, J., Ingelsson, M., Shin, Y., Irizarry, M. C., Hedley-Whyte, E. T., Frosch, M. P., Growdon, J. H., McLean, P. J., and Hyman, B. T. (2006). Clinical and biochemical correlates of insoluble alpha-synuclein in dementia with Lewy bodies. *Acta Neuropathol (Berl)* *111*, 101-108.

Kohler, A., Cascio, P., Leggett, D. S., Woo, K. M., Goldberg, A. L., and Finley, D. (2001). The axial channel of the proteasome core particle is gated by the Rpt2 ATPase and controls both substrate entry and product release. *Mol Cell* *7*, 1143-1152.

Kordower, J. H., Kanaan, N. M., Chu, Y., Suresh Babu, R., Stansell, J., 3rd, Terpstra, B. T., Sortwell, C. E., Steece-Collier, K., and Collier, T. J. (2006). Failure of proteasome inhibitor administration to provide a model of Parkinson's disease in rats and monkeys. *Ann Neurol* *60*, 264-268.

Kruger, R., Kuhn, W., Muller, T., Woitalla, D., Graeber, M., Kosel, S., Przuntek, H., Epplen, J. T., Schols, L., and Riess, O. (1998). Ala30Pro mutation in the gene encoding alpha-synuclein in Parkinson's disease. *Nat Genet* *18*, 106-108.

LeBlanc, R., Catley, L. P., Hideshima, T., Lentzsch, S., Mitsiades, C. S., Mitsiades, N., Neubergh, D., Goloubeva, O., Pien, C. S., Adams, J., *et al.* (2002). Proteasome inhibitor PS-341 inhibits human myeloma cell growth in vivo and prolongs survival in a murine model. *Cancer Res* *62*, 4996-5000.

Lee, D. H., and Goldberg, A. L. (1998). Proteasome inhibitors: valuable new tools for cell biologists. *Trends Cell Biol* *8*, 397-403.

Lee, H. J., Choi, C., and Lee, S. J. (2002). Membrane-bound alpha-synuclein has a high aggregation propensity and the ability to seed the aggregation of the cytosolic form. *J Biol Chem* *277*, 671-678.

Lee, J. C., Gray, H. B., and Winkler, J. R. (2005). Tertiary contact formation in alpha-synuclein probed by electron transfer. *J Am Chem Soc* *127*, 16388-16389.

Lee, J. C., Lai, B. T., Kozak, J. J., Gray, H. B., and Winkler, J. R. (2007). Alpha-synuclein tertiary contact dynamics. *J Phys Chem B* *111*, 2107-2112.

Li, J., Uversky, V. N., and Fink, A. L. (2001). Effect of familial Parkinson's disease point mutations A30P and A53T on the structural properties, aggregation, and fibrillation of human alpha-synuclein. *Biochemistry* *40*, 11604-11613.

Li, J., Uversky, V. N., and Fink, A. L. (2002). Conformational behavior of human alpha-synuclein is modulated by familial Parkinson's disease point mutations A30P and A53T. *Neurotoxicology* *23*, 553-567.

- Li, W., Lesuisse, C., Xu, Y., Troncoso, J. C., Price, D. L., and Lee, M. K. (2004). Stabilization of alpha-synuclein protein with aging and familial parkinson's disease-linked A53T mutation. *J Neurosci* *24*, 7400-7409.
- Li, W., West, N., Colla, E., Pletnikova, O., Troncoso, J. C., Marsh, L., Dawson, T. M., Jakala, P., Hartmann, T., Price, D. L., and Lee, M. K. (2005). Aggregation promoting C-terminal truncation of alpha-synuclein is a normal cellular process and is enhanced by the familial Parkinson's disease-linked mutations. *Proc Natl Acad Sci U S A* *102*, 2162-2167.
- Liang, T. C., Luo, W., Hsieh, J. T., and Lin, S. H. (1996). Antibody binding to a peptide but not the whole protein by recognition of the C-terminal carboxy group. *Arch Biochem Biophys* *329*, 208-214.
- Lindersson, E., Beedholm, R., Hojrup, P., Moos, T., Gai, W., Hendil, K. B., and Jensen, P. H. (2004). Proteasomal inhibition by alpha-synuclein filaments and oligomers. *J Biol Chem* *279*, 12924-12934.
- Linding, R., Jensen, L. J., Diella, F., Bork, P., Gibson, T. J., and Russell, R. B. (2003). Protein disorder prediction: implications for structural proteomics. *Structure* *11*, 1453-1459.
- Lippa, C. F., Duda, J. E., Grossman, M., Hurtig, H. I., Aarsland, D., Boeve, B. F., Brooks, D. J., Dickson, D. W., Dubois, B., Emre, M., *et al.* (2007). DLB and PDD boundary issues: diagnosis, treatment, molecular pathology, and biomarkers. *Neurology* *68*, 812-819.
- Liu, C. W., Corboy, M. J., DeMartino, G. N., and Thomas, P. J. (2003). Endoproteolytic activity of the proteasome. *Science* *299*, 408-411.
- Liu, C. W., Giasson, B. I., Lewis, K. A., Lee, V. M., Demartino, G. N., and Thomas, P. J. (2005). A precipitating role for truncated alpha-synuclein and the proteasome in alpha-synuclein aggregation: implications for pathogenesis of Parkinson disease. *J Biol Chem* *280*, 22670-22678.
- Liu, C. W., Li, X., Thompson, D., Wooding, K., Chang, T. L., Tang, Z., Yu, H., Thomas, P. J., and DeMartino, G. N. (2006). ATP binding and ATP hydrolysis play distinct roles in the function of 26S proteasome. *Mol Cell* *24*, 39-50.
- Liu, C. W., Millen, L., Roman, T. B., Xiong, H., Gilbert, H. F., Noiva, R., DeMartino, G. N., and Thomas, P. J. (2002a). Conformational remodeling of proteasomal substrates by PA700, the 19 S regulatory complex of the 26 S proteasome. *J Biol Chem* *277*, 26815-26820.
- Liu, Y., Fallon, L., Lashuel, H. A., Liu, Z., and Lansbury, P. T., Jr. (2002b). The UCH-L1 gene encodes two opposing enzymatic activities that affect alpha-synuclein degradation and Parkinson's disease susceptibility. *Cell* *111*, 209-218.
- Lowe, J., Stock, D., Jap, B., Zwickl, P., Baumeister, W., and Huber, R. (1995). Crystal structure of the 20S proteasome from the archaeon *T. acidophilum* at 3.4 Å resolution. *Science* *268*, 533-539.
- Luheshi, L. M., Crowther, D. C., and Dobson, C. M. (2008). Protein misfolding and disease: from the test tube to the organism. *Curr Opin Chem Biol* *12*, 25-31.

- Ma, C. P., Slaughter, C. A., and DeMartino, G. N. (1992). Identification, purification, and characterization of a protein activator (PA28) of the 20 S proteasome (macropain). *J Biol Chem* *267*, 10515-10523.
- Ma, C. P., Willy, P. J., Slaughter, C. A., and DeMartino, G. N. (1993). PA28, an activator of the 20 S proteasome, is inactivated by proteolytic modification at its carboxyl terminus. *J Biol Chem* *268*, 22514-22519.
- Madine, J., Doig, A. J., and Middleton, D. A. (2006). A study of the regional effects of alpha-synuclein on the organization and stability of phospholipid bilayers. *Biochemistry* *45*, 5783-5792.
- Maiti, N. C., Apetri, M. M., Zagorski, M. G., Carey, P. R., and Anderson, V. E. (2004). Raman spectroscopic characterization of secondary structure in natively unfolded proteins: alpha-synuclein. *J Am Chem Soc* *126*, 2399-2408.
- Mamah, C. E., Lesnick, T. G., Lincoln, S. J., Strain, K. J., de Andrade, M., Bower, J. H., Ahlskog, J. E., Rocca, W. A., Farrer, M. J., and Maraganore, D. M. (2005). Interaction of alpha-synuclein and tau genotypes in Parkinson's disease. *Ann Neurol* *57*, 439-443.
- Manning-Bog, A. B., McCormack, A. L., Li, J., Uversky, V. N., Fink, A. L., and Di Monte, D. A. (2002). The herbicide paraquat causes up-regulation and aggregation of alpha-synuclein in mice: paraquat and alpha-synuclein. *J Biol Chem* *277*, 1641-1644.
- Marsh, J. A., Singh, V. K., Jia, Z., and Forman-Kay, J. D. (2006). Sensitivity of secondary structure propensities to sequence differences between alpha- and gamma-synuclein: implications for fibrillation. *Protein Sci* *15*, 2795-2804.
- Marui, W., Iseki, E., Nakai, T., Miura, S., Kato, M., Ueda, K., and Kosaka, K. (2002). Progression and staging of Lewy pathology in brains from patients with dementia with Lewy bodies. *J Neurol Sci* *195*, 153-159.
- Mazzola, J. L., and Sirover, M. A. (2002). Alteration of intracellular structure and function of glyceraldehyde-3-phosphate dehydrogenase: a common phenotype of neurodegenerative disorders? *Neurotoxicology* *23*, 603-609.
- McFarlane, D., Dybdal, N., Donaldson, M. T., Miller, L., and Cribb, A. E. (2005). Nitration and increased alpha-synuclein expression associated with dopaminergic neurodegeneration in equine pituitary pars intermedia dysfunction. *J Neuroendocrinol* *17*, 73-80.
- McGuire, M. J., and DeMartino, G. N. (1986). Purification and characterization of a high molecular weight proteinase (macropain) from human erythrocytes. *Biochim Biophys Acta* *873*, 279-289.
- McGuire, M. J., McCullough, M. L., Croall, D. E., and DeMartino, G. N. (1989). The high molecular weight multicatalytic proteinase, macropain, exists in a latent form in human erythrocytes. *Biochim Biophys Acta* *995*, 181-186.
- McKeith, I., Fairbairn, A., Perry, R., Thompson, P., and Perry, E. (1992). Neuroleptic sensitivity in patients with senile dementia of Lewy body type. *Bmj* *305*, 673-678.

- McKeith, I. G., Galasko, D., Kosaka, K., Perry, E. K., Dickson, D. W., Hansen, L. A., Salmon, D. P., Lowe, J., Mirra, S. S., Byrne, E. J., *et al.* (1996). Consensus guidelines for the clinical and pathologic diagnosis of dementia with Lewy bodies (DLB): report of the consortium on DLB international workshop. *Neurology* *47*, 1113-1124.
- McNaught, K. S., Belizaire, R., Jenner, P., Olanow, C. W., and Isacson, O. (2002a). Selective loss of 20S proteasome alpha-subunits in the substantia nigra pars compacta in Parkinson's disease. *Neurosci Lett* *326*, 155-158.
- McNaught, K. S., Bjorklund, L. M., Belizaire, R., Isacson, O., Jenner, P., and Olanow, C. W. (2002b). Proteasome inhibition causes nigral degeneration with inclusion bodies in rats. *Neuroreport* *13*, 1437-1441.
- McNaught, K. S., Perl, D. P., Brownell, A. L., and Olanow, C. W. (2004). Systemic exposure to proteasome inhibitors causes a progressive model of Parkinson's disease. *Ann Neurol* *56*, 149-162.
- Mishizen-Eberz, A. J., Guttman, R. P., Giasson, B. I., Day, G. A., 3rd, Hodara, R., Ischiropoulos, H., Lee, V. M., Trojanowski, J. Q., and Lynch, D. R. (2003). Distinct cleavage patterns of normal and pathologic forms of alpha-synuclein by calpain I in vitro. *J Neurochem* *86*, 836-847.
- Mishizen-Eberz, A. J., Norris, E. H., Giasson, B. I., Hodara, R., Ischiropoulos, H., Lee, V. M., Trojanowski, J. Q., and Lynch, D. R. (2005). Cleavage of alpha-synuclein by calpain: potential role in degradation of fibrillized and nitrated species of alpha-synuclein. *Biochemistry* *44*, 7818-7829.
- Mitchell, T. W., Ekroos, K., Blanksby, S. J., Hulbert, A. J., and Else, P. L. (2007). Differences in membrane acyl phospholipid composition between an endothermic mammal and an ectothermic reptile are not limited to any phospholipid class. *J Exp Biol* *210*, 3440-3450.
- Mittag, T., and Forman-Kay, J. D. (2007). Atomic-level characterization of disordered protein ensembles. *Curr Opin Struct Biol* *17*, 3-14.
- Monaco, J. J., and Nandi, D. (1995). The genetics of proteasomes and antigen processing. *Annu Rev Genet* *29*, 729-754.
- Mott, J. D., Pramanik, B. C., Moomaw, C. R., Afendis, S. J., DeMartino, G. N., and Slaughter, C. A. (1994). PA28, an activator of the 20 S proteasome, is composed of two nonidentical but homologous subunits. *J Biol Chem* *269*, 31466-31471.
- Munishkina, L. A., Phelan, C., Uversky, V. N., and Fink, A. L. (2003). Conformational behavior and aggregation of alpha-synuclein in organic solvents: modeling the effects of membranes. *Biochemistry* *42*, 2720-2730.
- Murphy, D. D., Rueter, S. M., Trojanowski, J. Q., and Lee, V. M. (2000). Synucleins are developmentally expressed, and alpha-synuclein regulates the size of the presynaptic vesicular pool in primary hippocampal neurons. *J Neurosci* *20*, 3214-3220.

- Murray, I. V., Giasson, B. I., Quinn, S. M., Koppaka, V., Axelsen, P. H., Ischiropoulos, H., Trojanowski, J. Q., and Lee, V. M. (2003). Role of alpha-synuclein carboxy-terminus on fibril formation in vitro. *Biochemistry* 42, 8530-8540.
- Mykles, D. L. (1996). Differential effects of bovine PA28 on six peptidase activities of the lobster muscle proteasome (multicatalytic proteinase). *Arch Biochem Biophys* 325, 77-81.
- Myung, J., Kim, K. B., and Crews, C. M. (2001). The ubiquitin-proteasome pathway and proteasome inhibitors. *Med Res Rev* 21, 245-273.
- Narhi, L., Wood, S. J., Steavenson, S., Jiang, Y., Wu, G. M., Anafi, D., Kaufman, S. A., Martin, F., Sitney, K., Denis, P., *et al.* (1999). Both familial Parkinson's disease mutations accelerate alpha-synuclein aggregation. *J Biol Chem* 274, 9843-9846.
- Necula, M., Chirita, C. N., and Kuret, J. (2003). Rapid anionic micelle-mediated alpha-synuclein fibrillization in vitro. *J Biol Chem* 278, 46674-46680.
- Ni, R., Tomita, Y., Tokunaga, F., Liang, T. J., Noda, C., Ichihara, A., and Tanaka, K. (1995). Molecular cloning of two types of cDNA encoding subunit RC6-I of rat proteasomes. *Biochim Biophys Acta* 1264, 45-52.
- Nuscher, B., Kamp, F., Mehnert, T., Odoy, S., Haass, C., Kahle, P. J., and Beyer, K. (2004). Alpha-synuclein has a high affinity for packing defects in a bilayer membrane: a thermodynamics study. *J Biol Chem* 279, 21966-21975.
- Ortega, J., Heymann, J. B., Kajava, A. V., Ustrell, V., Rechsteiner, M., and Steven, A. C. (2005). The axial channel of the 20S proteasome opens upon binding of the PA200 activator. *J Mol Biol* 346, 1221-1227.
- Outeiro, T. F., Kontopoulos, E., Altmann, S. M., Kufareva, I., Strathearn, K. E., Amore, A. M., Volk, C. B., Maxwell, M. M., Rochet, J. C., McLean, P. J., *et al.* (2007). Sirtuin 2 inhibitors rescue alpha-synuclein-mediated toxicity in models of Parkinson's disease. *Science* 317, 516-519.
- Pace, C. N., Horn, G., Hebert, E. J., Bechert, J., Shaw, K., Urbanikova, L., Scholtz, J. M., and Sevcik, J. (2001). Tyrosine hydrogen bonds make a large contribution to protein stability. *J Mol Biol* 312, 393-404.
- Pandey, N., Schmidt, R. E., and Galvin, J. E. (2006). The alpha-synuclein mutation E46K promotes aggregation in cultured cells. *Exp Neurol* 197, 515-520.
- Peng, K., Vucetic, S., Radivojac, P., Brown, C. J., Dunker, A. K., and Obradovic, Z. (2005). Optimizing long intrinsic disorder predictors with protein evolutionary information. *J Bioinform Comput Biol* 3, 35-60.
- Peters, J. M., Cejka, Z., Harris, J. R., Kleinschmidt, J. A., and Baumeister, W. (1993). Structural features of the 26 S proteasome complex. *J Mol Biol* 234, 932-937.

- Peters, J. M., Franke, W. W., and Kleinschmidt, J. A. (1994). Distinct 19 S and 20 S subcomplexes of the 26 S proteasome and their distribution in the nucleus and the cytoplasm. *J Biol Chem* 269, 7709-7718.
- Pickart, C. M., and Cohen, R. E. (2004). Proteasomes and their kin: proteases in the machine age. *Nat Rev Mol Cell Biol* 5, 177-187.
- Pletnikova, O., West, N., Lee, M. K., Rudow, G. L., Skolasky, R. L., Dawson, T. M., Marsh, L., and Troncoso, J. C. (2005). Abeta deposition is associated with enhanced cortical alpha-synuclein lesions in Lewy body diseases. *Neurobiol Aging* 26, 1183-1192.
- Polymeropoulos, M. H., Lavedan, C., Leroy, E., Ide, S. E., Dehejia, A., Dutra, A., Pike, B., Root, H., Rubenstein, J., Boyer, R., *et al.* (1997). Mutation in the alpha-synuclein gene identified in families with Parkinson's disease. *Science* 276, 2045-2047.
- Qian, S. B., Princiotta, M. F., Bennink, J. R., and Yewdell, J. W. (2006). Characterization of rapidly degraded polypeptides in mammalian cells reveals a novel layer of nascent protein quality control. *J Biol Chem* 281, 392-400.
- Radivojac, P., Iakoucheva, L. M., Oldfield, C. J., Obradovic, Z., Uversky, V. N., and Dunker, A. K. (2007). Intrinsic disorder and functional proteomics. *Biophys J* 92, 1439-1456.
- Ramakrishnan, M., Jensen, P. H., and Marsh, D. (2003). Alpha-synuclein association with phosphatidylglycerol probed by lipid spin labels. *Biochemistry* 42, 12919-12926.
- Ranginwala, N. A., Hynan, L. S., Weiner, M. F., and White, C. L., 3rd (2008). Clinical criteria for the diagnosis of Alzheimer disease: still good after all these years. *Am J Geriatr Psychiatry* 16, 384-388.
- Realini, C., Jensen, C. C., Zhang, Z., Johnston, S. C., Knowlton, J. R., Hill, C. P., and Rechsteiner, M. (1997). Characterization of recombinant REGalpha, REGbeta, and REGgamma proteasome activators. *J Biol Chem* 272, 25483-25492.
- Rhoades, E., Ramlall, T. F., Webb, W. W., and Eliezer, D. (2006). Quantification of alpha-synuclein binding to lipid vesicles using fluorescence correlation spectroscopy. *Biophys J* 90, 4692-4700.
- Rochet, J. C. (2007). Novel therapeutic strategies for the treatment of protein-misfolding diseases. *Expert Rev Mol Med* 9, 1-34.
- Rosenzweig, R., Osmulski, P. A., Gaczynska, M., and Glickman, M. H. (2008). The central unit within the 19S regulatory particle of the proteasome. *Nat Struct Mol Biol* 15, 573-580.
- Rothbard, J. B., and Taylor, W. R. (1988). A sequence pattern common to T cell epitopes. *Embo J* 7, 93-100.
- Sampathu, D. M., Giasson, B. I., Pawlyk, A. C., Trojanowski, J. Q., and Lee, V. M. (2003). Ubiquitination of alpha-synuclein is not required for formation of pathological inclusions in alpha-synucleinopathies. *Am J Pathol* 163, 91-100.

- Schafer, K. A. (1998). The cell cycle: a review. *Vet Pathol* 35, 461-478.
- Sevlever, D., Jiang, P., and Yen, S. H. (2008). Cathepsin D is the main lysosomal enzyme involved in the degradation of alpha-synuclein and generation of its carboxy-terminally truncated species. *Biochemistry* 47, 9678-9687.
- Shringarpure, R., Grune, T., and Davies, K. J. (2001). Protein oxidation and 20S proteasome-dependent proteolysis in mammalian cells. *Cell Mol Life Sci* 58, 1442-1450.
- Shringarpure, R., Grune, T., Mehlhase, J., and Davies, K. J. (2003). Ubiquitin conjugation is not required for the degradation of oxidized proteins by proteasome. *J Biol Chem* 278, 311-318.
- Shtilerman, M. D., Ding, T. T., and Lansbury, P. T., Jr. (2002). Molecular crowding accelerates fibrillization of alpha-synuclein: could an increase in the cytoplasmic protein concentration induce Parkinson's disease? *Biochemistry* 41, 3855-3860.
- Sickmeier, M., Hamilton, J. A., LeGall, T., Vacic, V., Cortese, M. S., Tantos, A., Szabo, B., Tompa, P., Chen, J., Uversky, V. N., *et al.* (2007). DisProt: the Database of Disordered Proteins. *Nucleic Acids Res* 35, D786-793.
- Silva Pereira, I., Bey, F., Coux, O., and Scherrer, K. (1992). Two mRNAs exist for the Hs PROS-30 gene encoding a component of human prosomes. *Gene* 120, 235-242.
- Singleton, A. B., Farrer, M., Johnson, J., Singleton, A., Hague, S., Kachergus, J., Hulihan, M., Peuralinna, T., Dutra, A., Nussbaum, R., *et al.* (2003). alpha-Synuclein locus triplication causes Parkinson's disease. *Science* 302, 841.
- Smith, D. M., Chang, S. C., Park, S., Finley, D., Cheng, Y., and Goldberg, A. L. (2007). Docking of the proteasomal ATPases' carboxyl termini in the 20S proteasome's alpha ring opens the gate for substrate entry. *Mol Cell* 27, 731-744.
- Smith, D. M., Kafri, G., Cheng, Y., Ng, D., Walz, T., and Goldberg, A. L. (2005). ATP binding to PAN or the 26S ATPases causes association with the 20S proteasome, gate opening, and translocation of unfolded proteins. *Mol Cell* 20, 687-698.
- Smith, M. A., Rottkamp, C. A., Nunomura, A., Raina, A. K., and Perry, G. (2000). Oxidative stress in Alzheimer's disease. *Biochim Biophys Acta* 1502, 139-144.
- Soto, C. (2003). Unfolding the role of protein misfolding in neurodegenerative diseases. *Nat Rev Neurosci* 4, 49-60.
- Soto, C., and Estrada, L. D. (2008). Protein misfolding and neurodegeneration. *Arch Neurol* 65, 184-189.
- Sprangers, R., and Kay, L. E. (2007). Quantitative dynamics and binding studies of the 20S proteasome by NMR. *Nature* 445, 618-622.

- Stathopoulos, P. B., Scholz, G. A., Hwang, Y. M., Rumfeldt, J. A., Lepock, J. R., and Meiering, E. M. (2004). Sonication of proteins causes formation of aggregates that resemble amyloid. *Protein Sci* 13, 3017-3027.
- Stockl, M., Fischer, P., Wanker, E., and Herrmann, A. (2008). Alpha-synuclein selectively binds to anionic phospholipids embedded in liquid-disordered domains. *J Mol Biol* 375, 1394-1404.
- Sun, F., Anantharam, V., Latchoumycandane, C., Kanthasamy, A., and Kanthasamy, A. G. (2005). Dieldrin induces ubiquitin-proteasome dysfunction in alpha-synuclein overexpressing dopaminergic neuronal cells and enhances susceptibility to apoptotic cell death. *J Pharmacol Exp Ther* 315, 69-79.
- Sun, F., Anantharam, V., Zhang, D., Latchoumycandane, C., Kanthasamy, A., and Kanthasamy, A. G. (2006). Proteasome inhibitor MG-132 induces dopaminergic degeneration in cell culture and animal models. *Neurotoxicology* 27, 807-815.
- Sun, F., Kanthasamy, A., Anantharam, V., and Kanthasamy, A. G. (2007). Environmental neurotoxic chemicals-induced ubiquitin proteasome system dysfunction in the pathogenesis and progression of Parkinson's disease. *Pharmacol Ther* 114, 327-344.
- Sung, Y. H., and Eliezer, D. (2007). Residual structure, backbone dynamics, and interactions within the synuclein family. *J Mol Biol* 372, 689-707.
- Tai, H. C., and Schuman, E. M. (2008). Ubiquitin, the proteasome and protein degradation in neuronal function and dysfunction. *Nat Rev Neurosci* 9, 826-838.
- Tamura, T., Nagy, I., Lupas, A., Lottspeich, F., Cejka, Z., Schoofs, G., Tanaka, K., De Mot, R., and Baumeister, W. (1995). The first characterization of a eubacterial proteasome: the 20S complex of *Rhodococcus*. *Curr Biol* 5, 766-774.
- Tanahashi, N., Murakami, Y., Minami, Y., Shimbara, N., Hendil, K. B., and Tanaka, K. (2000). Hybrid proteasomes. Induction by interferon-gamma and contribution to ATP-dependent proteolysis. *J Biol Chem* 275, 14336-14345.
- Tanaka, K., Yoshimura, T., and Ichihara, A. (1989). Role of substrate in reversible activation of proteasomes (multi-protease complexes) by sodium dodecyl sulfate. *J Biochem* 106, 495-500.
- Tanaka, K., Yoshimura, T., Kumatori, A., Ichihara, A., Ikai, A., Nishigai, M., Kameyama, K., and Takagi, T. (1988). Proteasomes (multi-protease complexes) as 20 S ring-shaped particles in a variety of eukaryotic cells. *J Biol Chem* 263, 16209-16217.
- Tanaka, T., Slamon, D. J., and Cline, M. J. (1985). Efficient generation of antibodies to oncoproteins by using synthetic peptide antigens. *Proc Natl Acad Sci U S A* 82, 3400-3404.
- Tarawneh, R., and Galvin, J. E. (2007). Distinguishing Lewy body dementias from Alzheimer's disease. *Expert Rev Neurother* 7, 1499-1516.
- Tartaglia, G. G., Pawar, A. P., Campioni, S., Dobson, C. M., Chiti, F., and Vendruscolo, M. (2008). Prediction of aggregation-prone regions in structured proteins. *J Mol Biol* 380, 425-436.

- Thomas, P. J., Qu, B. H., and Pedersen, P. L. (1995). Defective protein folding as a basis of human disease. *Trends Biochem Sci* *20*, 456-459.
- Tofaris, G. K., Garcia Reitböck, P., Humby, T., Lambourne, S. L., O'Connell, M., Ghetti, B., Gossage, H., Emson, P. C., Wilkinson, L. S., Goedert, M., and Spillantini, M. G. (2006). Pathological changes in dopaminergic nerve cells of the substantia nigra and olfactory bulb in mice transgenic for truncated human alpha-synuclein(1-120): implications for Lewy body disorders. *J Neurosci* *26*, 3942-3950.
- Tofaris, G. K., Layfield, R., and Spillantini, M. G. (2001). alpha-synuclein metabolism and aggregation is linked to ubiquitin-independent degradation by the proteasome. *FEBS Lett* *509*, 22-26.
- Tokunaga, F., Aruga, R., Iwanaga, S., Tanaka, K., Ichihara, A., Takao, T., and Shimonishi, Y. (1990). The NH₂-terminal residues of rat liver proteasome (multicatalytic proteinase complex) subunits, C2, C3 and C8, are N alpha-acetylated. *FEBS Lett* *263*, 373-375.
- Tompa, P., Prilusky, J., Silman, I., and Sussman, J. L. (2008). Structural disorder serves as a weak signal for intracellular protein degradation. *Proteins* *71*, 903-909.
- Toutou, R., O'Nions, J., Heaney, J., and Allday, M. J. (2005). Epstein-Barr virus EBNA3 proteins bind to the C8/alpha7 subunit of the 20S proteasome and are degraded by 20S proteasomes in vitro, but are very stable in latently infected B cells. *J Gen Virol* *86*, 1269-1277.
- Toutou, R., Richardson, J., Bose, S., Nakanishi, M., Rivett, J., and Allday, M. J. (2001). A degradation signal located in the C-terminus of p21WAF1/CIP1 is a binding site for the C8 alpha-subunit of the 20S proteasome. *Embo J* *20*, 2367-2375.
- Tsvetkov, P., Asher, G., Paz, A., Reuven, N., Sussman, J. L., Silman, I., and Shaul, Y. (2008). Operational definition of intrinsically unstructured protein sequences based on susceptibility to the 20S proteasome. *Proteins* *70*, 1357-1366.
- Ulmer, T. S., and Bax, A. (2005). Comparison of structure and dynamics of micelle-bound human alpha-synuclein and Parkinson disease variants. *J Biol Chem* *280*, 43179-43187.
- Ulmer, T. S., Bax, A., Cole, N. B., and Nussbaum, R. L. (2005). Structure and dynamics of micelle-bound human alpha-synuclein. *J Biol Chem* *280*, 9595-9603.
- Unno, M., Mizushima, T., Morimoto, Y., Tomisugi, Y., Tanaka, K., Yasuoka, N., and Tsukihara, T. (2002). The structure of the mammalian 20S proteasome at 2.75 Å resolution. *Structure* *10*, 609-618.
- Ustrell, V., Hoffman, L., Pratt, G., and Rechsteiner, M. (2002). PA200, a nuclear proteasome activator involved in DNA repair. *Embo J* *21*, 3516-3525.
- Uttenweiler-Joseph, S., Claverol, S., Sylvius, L., Bousquet-Dubouch, M. P., Burlet-Schiltz, O., and Monsarrat, B. (2008). Toward a Full Characterization of the Human 20S Proteasome Subunits and Their Isoforms by a Combination of Proteomic Approaches. *Methods Mol Biol* *484*, 111-130.

Uversky, V. N. (2002). Natively unfolded proteins: a point where biology waits for physics. *Protein Sci* 11, 739-756.

Uversky, V. N., and Fink, A. L. (2004). Conformational constraints for amyloid fibrillation: the importance of being unfolded. *Biochim Biophys Acta* 1698, 131-153.

Uversky, V. N., Gillespie, J. R., and Fink, A. L. (2000). Why are "natively unfolded" proteins unstructured under physiologic conditions? *Proteins* 41, 415-427.

Uversky, V. N., Li, J., Bower, K., and Fink, A. L. (2002a). Synergistic effects of pesticides and metals on the fibrillation of alpha-synuclein: implications for Parkinson's disease. *Neurotoxicology* 23, 527-536.

Uversky, V. N., Li, J., and Fink, A. L. (2001a). Evidence for a partially folded intermediate in alpha-synuclein fibril formation. *J Biol Chem* 276, 10737-10744.

Uversky, V. N., Li, J., and Fink, A. L. (2001b). Metal-triggered structural transformations, aggregation, and fibrillation of human alpha-synuclein. A possible molecular link between Parkinson's disease and heavy metal exposure. *J Biol Chem* 276, 44284-44296.

Uversky, V. N., Li, J., and Fink, A. L. (2001c). Pesticides directly accelerate the rate of alpha-synuclein fibril formation: a possible factor in Parkinson's disease. *FEBS Lett* 500, 105-108.

Uversky, V. N., Yamin, G., Souillac, P. O., Goers, J., Glaser, C. B., and Fink, A. L. (2002b). Methionine oxidation inhibits fibrillation of human alpha-synuclein in vitro. *FEBS Lett* 517, 239-244.

Vucetic, S., Obradovic, Z., Vacic, V., Radivojac, P., Peng, K., Iakoucheva, L. M., Cortese, M. S., Lawson, J. D., Brown, C. J., Sikes, J. G., *et al.* (2005). DisProt: a database of protein disorder. *Bioinformatics* 21, 137-140.

Vucetic, S., Xie, H., Iakoucheva, L. M., Oldfield, C. J., Dunker, A. K., Obradovic, Z., and Uversky, V. N. (2007). Functional anthology of intrinsic disorder. 2. Cellular components, domains, technical terms, developmental processes, and coding sequence diversities correlated with long disordered regions. *J Proteome Res* 6, 1899-1916.

Wakamatsu, M., Ishii, A., Iwata, S., Sakagami, J., Ukai, Y., Ono, M., Kanbe, D., Muramatsu, S. I., Kobayashi, K., Iwatsubo, T., and Yoshimoto, M. (2006). Selective loss of nigral dopamine neurons induced by overexpression of truncated human alpha-synuclein in mice. *Neurobiol Aging*.

Webb, J. L., Ravikumar, B., Atkins, J., Skepper, J. N., and Rubinsztein, D. C. (2003). Alpha-Synuclein is degraded by both autophagy and the proteasome. *J Biol Chem* 278, 25009-25013.

Weinreb, P. H., Zhen, W., Poon, A. W., Conway, K. A., and Lansbury, P. T., Jr. (1996). NACP, a protein implicated in Alzheimer's disease and learning, is natively unfolded. *Biochemistry* 35, 13709-13715.

- Whitby, F. G., Masters, E. I., Kramer, L., Knowlton, J. R., Yao, Y., Wang, C. C., and Hill, C. P. (2000). Structural basis for the activation of 20S proteasomes by 11S regulators. *Nature* *408*, 115-120.
- Wolf, D. H., and Hilt, W. (2004). The proteasome: a proteolytic nanomachine of cell regulation and waste disposal. *Biochim Biophys Acta* *1695*, 19-31.
- Wright, P. E., and Dyson, H. J. (1999). Intrinsically unstructured proteins: re-assessing the protein structure-function paradigm. *J Mol Biol* *293*, 321-331.
- Xia, Y., Rohan de Silva, H. A., Rosi, B. L., Yamaoka, L. H., Rimmler, J. B., Pericak-Vance, M. A., Roses, A. D., Chen, X., Masliah, E., DeTeresa, R., *et al.* (1996). Genetic studies in Alzheimer's disease with an NACP/alpha-synuclein polymorphism. *Ann Neurol* *40*, 207-215.
- Xie, H., Vucetic, S., Iakoucheva, L. M., Oldfield, C. J., Dunker, A. K., Obradovic, Z., and Uversky, V. N. (2007a). Functional anthology of intrinsic disorder. 3. Ligands, post-translational modifications, and diseases associated with intrinsically disordered proteins. *J Proteome Res* *6*, 1917-1932.
- Xie, H., Vucetic, S., Iakoucheva, L. M., Oldfield, C. J., Dunker, A. K., Uversky, V. N., and Obradovic, Z. (2007b). Functional anthology of intrinsic disorder. 1. Biological processes and functions of proteins with long disordered regions. *J Proteome Res* *6*, 1882-1898.
- Yamin, G., Uversky, V. N., and Fink, A. L. (2003). Nitration inhibits fibrillation of human alpha-synuclein in vitro by formation of soluble oligomers. *FEBS Lett* *542*, 147-152.
- Yang, Y., Fruh, K., Ahn, K., and Peterson, P. A. (1995). In vivo assembly of the proteasomal complexes, implications for antigen processing. *J Biol Chem* *270*, 27687-27694.
- Yang, Y. X., Wood, N. W., and Latchman, D. S. (2009). Molecular basis of Parkinson's disease. *Neuroreport* *20*, 150-156.
- Yao, Y., Huang, L., Krutchinsky, A., Wong, M. L., Standing, K. G., Burlingame, A. L., and Wang, C. C. (1999). Structural and functional characterizations of the proteasome-activating protein PA26 from *Trypanosoma brucei*. *J Biol Chem* *274*, 33921-33930.
- Yokota, O., Tsuchiya, K., Uchihara, T., Ujike, H., Terada, S., Takahashi, M., Kimura, Y., Ishizu, H., Akiyama, H., and Kuroda, S. (2007). Lewy body variant of Alzheimer's disease or cerebral type lewy body disease? Two autopsy cases of presenile onset with minimal involvement of the brainstem. *Neuropathology* *27*, 21-35.
- Yoshimura, T., Kameyama, K., Takagi, T., Ikai, A., Tokunaga, F., Koide, T., Tanahashi, N., Tamura, T., Cejka, Z., Baumeister, W., and *et al.* (1993). Molecular characterization of the "26S" proteasome complex from rat liver. *J Struct Biol* *111*, 200-211.
- Yu, J., Malkova, S., and Lyubchenko, Y. L. (2008). alpha-Synuclein misfolding: single molecule AFM force spectroscopy study. *J Mol Biol* *384*, 992-1001.

Zarranz, J. J., Alegre, J., Gomez-Esteban, J. C., Lezcano, E., Ros, R., Ampuero, I., Vidal, L., Hoenicka, J., Rodriguez, O., Atares, B., *et al.* (2004). The new mutation, E46K, of alpha-synuclein causes Parkinson and Lewy body dementia. *Ann Neurol* 55, 164-173.

Zhang, N. Y., Tang, Z., and Liu, C. W. (2008). alpha-Synuclein protofibrils inhibit 26 S proteasome-mediated protein degradation: understanding the cytotoxicity of protein protofibrils in neurodegenerative disease pathogenesis. *J Biol Chem* 283, 20288-20298.

Zhu, M., Li, J., and Fink, A. L. (2003). The association of alpha-synuclein with membranes affects bilayer structure, stability, and fibril formation. *J Biol Chem* 278, 40186-40197.

Zong, C., Young, G. W., Wang, Y., Lu, H., Deng, N., Drews, O., and Ping, P. (2008). Two-dimensional electrophoresis-based characterization of post-translational modifications of mammalian 20S proteasome complexes. *Proteomics* 8, 5025-5037.

Zwickl, P., Kleinz, J., and Baumeister, W. (1994). Critical elements in proteasome assembly. *Nat Struct Biol* 1, 765-770.